Supporting Information

Mapping and Exploiting the Promiscuity of OxyB toward Biocatalytic Production of Vancomycin Aglycone Variants

Clarissa C. Forneris[†,&], Andy K. L. Nguy[†,&], Mohammad R. Seyedsayamdost[†,‡,]*

Departments of Chemistry[†] and Molecular Biology[‡], Princeton University,
Princeton, NJ 08544

[&]These authors contributed equally
*Email: mrseyed@princeton.edu

Materials and strains.

Amycolatopsis orientalis DSM40040 was obtained from the DSMZ. LB broth, Terrific Broth and LB agar were purchased from Becton Dickinson. All antibiotics, IPTG, PMSF, lysozyme, βME, Sephadex G-25, COMU, NEt_3, DIPEA, TIS, DBU, TFA, *N*-methylmorpholine, hydrazine monohydrate, $NaNO_2$, coenzyme A trilithium salt, glucose-6-phosphate dehydrogenase, glucose-6-phosphate, and other components necessary for biochemical assays were obtained from Sigma-Aldrich. Nickel affinity resin and DNase I were purchased from Clontech. Restriction enzymes, T4 DNA ligase, proofreading Q5 DNA polymerase, and the corresponding buffers were purchased from New England Biolabs. PCR reactions were routinely carried out in Failsafe buffer G (Epicentre). Commercially available Fmoc- and side chain-protected amino acids, 2-chlorotrityl chloride resin and other components for solid-phase peptide synthesis were purchased from Novabiochem/EMD Millipore, Sigma-Aldrich and ChemImpex.

Reactions were monitored by thin layer chromatography (TLC) carried out on 250 μm Merck silica gel plates (60 F254) containing a fluorescent indicator (254 nm). Visualization of the developed TLC plate was performed by irradiation with UV light. Standard NMR spectra were acquired at the Princeton University Department of Chemistry Core Facilities. ^{1}H spectra were recorded in the TCI cryoprobe of a Bruker Avance III 500 MHz spectrometer. Data for ^{1}H spectra are reported as follows: chemical shift (δ ppm), multiplicity (s = singlet, d = doublet, t = triplet, q = quartet, m = multiplet, b = broad), integration, coupling constant (Hz) and assignment. ^{13}C NMR spectra were also recorded in a Bruker Avance III 500 MHz (126 MHz) spectrometer. Reported below are ^{13}C chemical shifts.

For structural elucidation of enzymatic reaction products, 1D/2D NMR spectra were acquired at the Princeton University Department of Chemistry NMR Facilities on an A8 Avance III HD 800-MHz NMR spectrometer (Bruker) with a triple resonance cryoprobe. The NMR samples were prepared in $(CD_3)_2SO$.

Expression and purification of OxyB, OxyA, OxyC, PCP7-X, Fd, FdR, Sfp R4-4. OxyB, OxyA, OxyC and PCP7-X from *Amycolatopsis orientalis* DSM 40040 were expressed and purified as previously described. [1,2] Spinach ferredoxin (Fd), *E. coli* ferredoxin reductase (FdR), and Spf R4-4 from *B. subtilis* (codon-optimized, K28E/T44E/C77Y triple mutant of phosphopantetheinyl transferase) were expressed and purified as previously described.[1,3]

***N*-Fmoc-L-3,5-$^{2}H_2$-4-hydroxyphenylglycine**

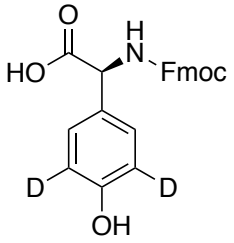

A 50-mL Schlenk flask equipped with a stir bar and rubber septum was charged with L-4-hydroxyphenylglycine (600 mg, 3.60 mmol), potassium tetrachloroplatinate(II) (372 mg, 0.90 mmol, 0.25 equiv.) and DCl-D_2O (1 N, 15 mL). The reaction mixture was evacuated and refilled with N_2 five times to remove oxygen and stirred under reflux for 24 h. After cooling to room temperature, the reaction mixture was concentrated, dissolved in MeOH (45 mL) and filtered through a Buchner funnel to remove the catalyst. The filtrate was concentrated, and the hydrochloride amino acid was obtained as a colorless powder (600 mg, 3.60 mmol, quantitative yield). ^{1}H NMR (500 MHz, $(CD_3)_2SO$): δ 8.73 (d, *J* = 5.2 Hz, 2H), 7.28 (s, 2H), 4.93 (t, *J* = 5.2 Hz, 1H). *N*-Fmoc protection of L-3,5-$^{2}H_2$-4-hydroxyphenylglycine was carried out using the same procedure as previously described. (2) A colorless powder was obtained (1.2 g, 3.24 mmol, 90% yield). ^{1}H NMR (500 MHz, $(CD_3)_2SO$) δ 12.69 (s, 1H), 9.47 (s, 1H), 8.06 (d, *J* = 7.7 Hz, 1H), 7.89 (d, *J* = 7.5 Hz, 2H), 7.75 (d, *J* = 7.5 Hz, 2H), 7.41 (t, *J* = 7.4 Hz, 2H), 7.31 (q, *J* = 7.9 Hz, 2H), 7.21 (s, 2H), 5.01 (d, *J* = 7.8 Hz, 1H), 4.24 (m, 4H).

***N*-Fmoc-L-3,5-$^{2}H_2$-homotyrosine**

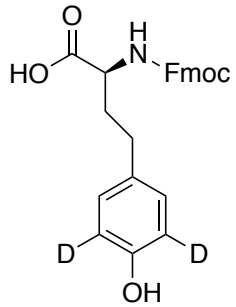

L-3,5-$^{2}H_2$-homotyrosine was prepared from L-homotyrosine by the same procedure outlined for the synthesis of L-3,5-$^{2}H_2$-4-hydroxyphenylglycine and isolated as a colorless powder. ^{1}H NMR (500 MHz, $(CD_3)_2SO$) δ 8.62 (d, 5.5 Hz, 2H), 7.07 (s, 2H), 3.94 – 3.86 (m, 1H), 3.22 (s, 3H), 2.71 (m, 1H), 2.08 (m, 1H) (other β-protons are obscured by solvent peaks). *N*-Fmoc protection was carried out without intermediate purification and following previously described

procedure.[2] A colorless powder was obtained (1.05 g, 2.5 mmol, 69% yield over two steps). ^{1}H NMR (500 MHz, $(CD_3)_2SO$) δ 12.56 (s, 1H), 9.15 (s, 1H), 7.91 (d, *J* = 7.6 Hz, 2H), 7.78 – 7.71 (m, 2H), 7.43 (t, *J* = 7.5 Hz, 2H), 7.34 (td, *J* = 7.4, 3.2 Hz, 2H), 6.97 (s, 2H), 4.36 – 4.23 (m, 4H), 3.87 (m, 1H), 2.56 (m, 1H), 1.88 (m, 2H). ^{13}C NMR (126 MHz, $(CD_3)_2SO$) δ 174.52, 156.67, 155.85, 144.35, 144.28, 141.22, 131.42, 129.60, 128.12, 127.55, 125.77, 125.74, 120.60, 66.02, 60.24, 47.15, 33.35, 31.18.

_N_-Boc-4-CD_3-L-phenylalanine methyl ester

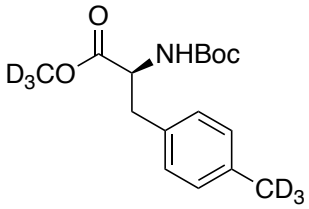

A 100-mL round bottom flask equipped with a stir bar, reflux condenser, rubber septum and N_2 inlet was charged with *N*-Boc-4-BPin-L-phenylalanine (1 g, 2.56 mmol), potassium carbonate (1.77 g, 12.8 mmol, 5.0 equivalents), iodomethane-d3 (2.2 g, 15.3 mmol, 6.0 equivalents), 1,4-dioxane (44.8 mL) and water (6.4 mL). The resulting mixture was degassed and $Pd(dppf)_2Cl_2$ (93 mg, 0.128 mmol, 5 mol%) was added. After stirring under reflux overnight, the reaction mixture was cooled to room temperature and diluted with 7.7 mL of methanol. 1,4-dioxane was removed by rotatory evaporation and the resulting solution was extracted into EtOAc (3 x 20 mL). The organic layers were combined, dried over Na_2SO_4, filtered and concentrated to yield a brown oil. The desired product was purified by preparative HPLC in a Phenomenex Luna C18 (5 μ, 250 x 21.2 mm) equilibrated with 15% MeCN; product was eluted with a gradient of 60-100% MeCN over 15 min. A colorless oil was isolated (243 mg, 0.81 mmol, 32% yield). ^{1} NMR (500 MHz, methanol-d_4) δ 7.14 – 7.04 (m, 4H), 4.31 (m, 1H), 3.04 (dd, *J* = 13.8, 5.7 Hz, 1H), 2.85 (dd, *J* = 13.9, 8.8 Hz, 1H), 1.38 (s, 9H). ^{13}C NMR (126 MHz, methanol-d_4) δ 174.30, 157.8, 137.3, 135.2, 130.1, 130.0 80.6, 56.6, 38.3, 28.6.

4-CD_3-L-phenylalanine

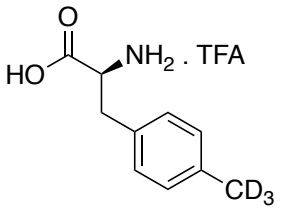

N-Boc-4-CD_3-L-phenylalanine methyl ester (250 mg, 0.83 mmol) was dissolved in a 1:1 water/THF mixture (8 mL) and cooled in an ice/water bath. LiOH (105 mg, 2.5 mmol, 3.0 equivalents) was added to the solution and the reaction mixture was stirred for 5 hours. Subsequently, the mixture's pH was adjusted to 2 with 1 N HCl and THF was removed by rotatory evaporation. The resulting solution was extracted with EtOAc (3 x 10 mL) and the combined organic layers were dried over Na_2SO_4, filtered and concentrated. The resulting colorless solid was dissolved in DCM (5.4 mL), cooled in an ice/water bath, charged with TFA (5.4 mL) and stirred for 3 hours. DCM and TFA were removed by rotatory evaporation and a clear oil was obtained (208 mg, 0.74 mmol, 91% yield). ^{1}H NMR (500 MHz, Methanol-d_4) δ 7.18 (m, 4H), 4.21 (dd, J = 7.9, 5.3 Hz, 1H), 3.27 (dd, J = 14.5, 5.3 Hz, 1H), 3.10 (dd, J = 14.6, 7.9 Hz, 1H). ^{13}C NMR (126 MHz, methanol-d_4) δ 171.3 138.7, 132.4, 130.8, 130.3, 55.2, 37.0, 27.7.

***N*-Fmoc-4-CD_3-L-phenylalanine**

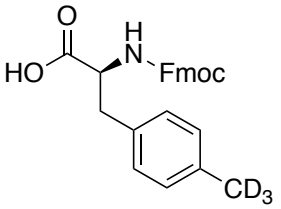

N-Fmoc protection of 4-CD_3-L-phenylalanine was performed as outlined previously. A colorless powder was isolated (286 mg, 0.71 mmol, 86% yield). ^{1}H NMR (500 MHz, Methanol-d_4) δ 7.79 (d, J = 7.5 Hz, 2H), 7.59 (t, J = 7.0 Hz, 2H), 7.41 – 7.35 (m, 2H), 7.29 (ddd, J = 9.1, 7.5, 1.2 Hz, 2H), 7.12 (d, J = 8.1 Hz, 2H), 7.07 (d, J = 8.1 Hz, 2H), 4.40 (dd, J = 9.6, 4.8 Hz, 1H), 4.30 (dd, J = 10.5, 7.0 Hz, 1H), 4.20 (dd, J = 10.3, 7.2 Hz, 1H), 4.15 (t, J = 7.1 Hz, 1H), 3.17 (dd, J = 14.0, 4.8 Hz, 1H), 2.89 (dd, J = 13.9, 9.6 Hz, 1H). ^{13}C NMR (126 MHz, methanol-d_4) δ 173.82, 156.98, 143.82, 141.14, 134.13, 128.79, 128.66, 127.34, 126.73, 124.96, 124.84, 119.48, 119.45, 66.60, 55.46, 36.76, 24.88.

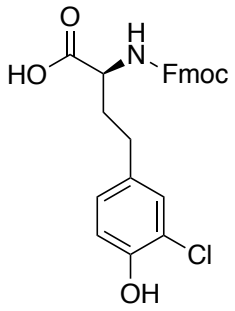

***N*-Fmoc-3-Cl-L-homotyrosine**

A 25-mL round bottom flask was charged with homotyrosine (200 mg, 0.72 mmol), AcOH (1 mL) and SO_2Cl_2 (106 mg, 0.79 mmmol, 1.10 equivalents). The resulting slurry was stirred at room temperature for 3 hours, filtered, washed with AcOH and purified via preparative HPLC. Multiple injections on a Phenomenex Luna C18 (5 μ, 250 x 21.2 mm) equilibrated with 5% MeCN were performed and the product was eluted with a gradient of 5-42% MeCN over 20 min. A colorless solid was isolated (107 mg, 0.39 mmol, 54% yield) ^{1}H NMR (500 MHz, $(CD_3)_2SO$) δ 10.02 (s, 1H), 7.56 (s, 2H), 7.31 (s, 1H), 7.01 (d, *J* = 8.1 Hz, 1H), 6.87 (d, *J* = 8.2 Hz, 1H), 3.07 (s, 1H), 1.93 (d, *J* = 12.7 Hz, 1H), 1.77 (s, 1H). *N*-Fmoc protection of 3-Cl-L-homotyrosine was performed without intermediate purification and as outlined previously. A colorless powder was isolated (106 mg, 0.23 mmol, 60% yield). ^{1}H NMR (500 MHz, $(CD_3)_2SO$) δ 12.63 (s, 1H), 10.02 (s, 1H), 7.93 – 7.88 (m, 2H), 7.75 (dd, *J* = 7.7, 2.4 Hz, 2H), 7.68 (d, *J* = 7.5 Hz, 1H), 7.43 (t, *J* = 7.5 Hz, 2H), 7.37 – 7.31 (m, 2H), 7.31 (d, *J* = 2.1 Hz, 1H), 6.98 (dd, *J* = 8.3, 2.1 Hz, 1H), 6.86 (d, *J* = 8.2 Hz, 1H), 4.71 (d, *J* = 6.1 Hz, 1H), 4.36 – 4.22 (m, 3H), 2.66 – 2.63 (m, 1H), 2.39 – 2.35 (m, 1H).

Synthesis and purification of 7mer substrates by Fmoc SPPS. The synthesis of 7mer hydrazine substrates followed the method described previously.[1,2] Pure peptides were verified by HPLC-MS and average yields of synthesis were 80-85%.

Synthesis and purification of coenzyme A adducts of 7mer peptides. The preparation of coenzyme A adducts of 7mer hydrazine substrates followed the procedure outlined previously.[1,2] The purified peptides were verified by HPLC-MS, aliquoted and lyophilized. Yields for generation of heptapeptides varied between 80-95%.

Synthesis and purification of 7mer peptides and coenzyme A adducts of 43, 46 and substrate for product 45 using Dawson resin SPPS. Synthesis of oxidation-prone peptides was

adapted from previously described procedure.[4] Dawson resin (130 mg) was added to an Econo-Pac (Bio-Rad) column, swelled in DMF for 30 minutes and deprotected with a cocktail of 1% DBU in DMF (3 x 2 mL). Amino acids were coupled as previously described.[1] Resin activation was carried out by adding a solution of *p*-nitrochloroformate (66 mg, 5.0 equivalents) in DCM (6.6 mL), gently agitating with N_2 bubbling at room temperature for 40 minutes and finally washing the resin with DCM (3 x 2mL) and DMF (3 x 2mL). Subsequently, a solution of DIPEA (58 uL, 5.0 equivalents) in DMF (3.9 mL) was added to the resin, which was allowed to agitate at room temperature for 15 minutes. After thorough washing with DMF (3 x 2mL) and DCM (3 x 2mL), the resin was dried under vacuum and transferred to a 25-mL pear-shaped flask equipped with a stir bar, rubber septum and N_2 inlet. DMF (3.3 mL) was added to the resin, which was allowed to swell with stirring for 20 minutes. For peptide cleavage, the resin suspension was degassed by bubbling N_2 for 20 minutes and charged with a degassed solution of 4-mercaptophenylacetic acid (4-MPAA, 110 mg, 10 equivalents) in DMF (0.65 mL). Tributylphosphine (262 uL, 0.96 mmol, 24 equivalents) was added to the resin suspension via syringe and the cleavage reaction was allowed to proceed at room temperature for 24 h, under inert gas. The resin residue was then filtered, and the filtrate was concentrated by rotatory evaporation. To remove side-chain protecting groups, a cocktail of TFA:TIS:H_2O (95 : 2.5 : 2.5, 6 mL) was added to the 4-MPAA-peptide adduct, stirred for 90 minutes at room temperature and subsequently removed under a stream of N_2. The resulting peptide was precipitated by adding cold Et_2O, which was then decanted. The crude 4-MPAA-peptide adduct was verified by HPLC-MS. A portion of the crude material (2.65 mg, corresponding to approximately 2.25 μmol of peptide, as quantified by UV-Vis spectroscopy), was dissolved in 50 mM phosphate buffer pH 8.3 (0.9 mL) and MeCN (0.45 mL). A final concentration of 20 mM TCEP was added to the thioester exchange reaction from a 500 mM stock solution at pH 7.0. Finally, the exchange reaction was charged with coenzyme A (7 mg, 9 umol, 4.0 equivalents) and adjusted to pH 8.3. The reaction was allowed to stir at room temperature for 2 hours and the peptide-coenzyme A adducts were purified via repeated injections onto an analytical Phenomenex Luna C18 column (5 μm, 250 x 4.6 mm) that had been equilibrated with 10% MeCN in H_2O (+ 0.1% FA). The peptide-CoA adducts were eluted with a gradient of 10–55% MeCN in H_2O (+ 0.1% FA) over 17 minutes. The purified material was verified by HPLC-MS, aliquoted, and lyophilized. Yields for this synthetic procedure were on average 2%.

Enzymatic reactions with OxyB. A typical analytical-scale reaction with OxyB was carried out on a 100 μL scale. Loading buffer (50 mM HEPES, 20 mM KCl, 10 mM $MgCl_2$, pH 7.0) was added to an Eppendorf tube containing 20 nmol of lyophilized peptide-CoA adduct, to a final peptide concentration of 400 μM. Subsequently, final concentrations of 400 μM PCP-X and 80 μM of Sfp R4-4 were added to the reaction mixture, which was placed in a 30°C incubator for one hour. In standard reactions, final concentrations of the following reagents were added to the reaction mixture, in this order: 4 mM glucose-6-phosphate, 0.04U/μL glucose-6-phosphate dehydrogenase, 20 μM spinach ferredoxin, 8 μM *E. coli* ferredoxin reductase, 20 μM OxyB. The oxidative crosslinking reaction was initiated by the addition of 2 mM NADPH. We tested several re-reducing systems with substrates **6**, **15**, **25**, and **32**, and found that the spinach ferredoxin/*E. coli* ferredoxin reductase yielded the highest conversion rates; this pair was previously also shown to be most effective in $OxyB_{van}$ crosslinking reactions.[5,6] Alternative reduction systems, such as the ferredoxin/ferredoxin reductase pair from *Rhodopseudomonas palustris*, led to identical product outcomes, though at lower rates, when compared to spinach ferredoxin/*E. coli* ferredoxin reductase.[3] Typical assays were carried out at room temperature for 3 hours in the dark, at which point the reactions were complete; we previously showed that product formation plateaus by 50 min even with poor substrates.[1] In order to remove the peptide from the carrier domain, 20,000 equivalents of propylamine were added and the reaction mixture incubated for 15 minutes. Proteins were precipitated by adding 15 μL of formic acid and 50 μL of MeCN (+ 0.1% FA). Denatured proteins were pelleted, and the supernatant was analyzed by HR-HPLC-MS and HR-MS/MS.

Enzymatic reaction of 4 (AA2 = L-Hpg; AA4 = D-Hpg) with OxyB and purification of product 5. This reaction was carried out on a 10.6 mL scale. Loading buffer (50 mM HEPES, 20 mM KCl, 10 mM $MgCl_2$, pH 7.0) was added to 2.14 μmol of lyophilized 7mer-CoA adduct, to a final peptide concentration of 400 μM. PCP-X and Sfp R4-4 were added to final concentrations of 400 μM and 80 μM, respectively, and loading reaction was placed in an incubator at 30 °C. Final concentrations of the following components were then added to the reaction, in this order: 4mM G6P, 0.04 U/μL G6P-DH, 20 μM spinach ferredoxin, 8μM ferredoxin reductase, 7.5 μM OxyB and 4 mM NADPH. The reaction proceeded for 3 h, at room temperature, shielded from light. The peptide was cleaved from PCP-X through the addition of 20,000 equivalents of propyl amine and the reaction was incubated for 15 min. Proteins were then precipitated by adding formic

acid (15% v/v) and MeCN (50% v/v). Purification of the resulting product was carried out through repeated injections onto a Phenomenex Luna C18 column (5μm, 250mm x 10mm), initially equilibrated with 5% MeCN. **5** (0.4 mg) was eluted with a gradient of 5-44% over 20 min and dried *in vacuo*.

Enzymatic reaction of 6 (AA2 = L-Tyr; AA4 = D-Tyr) with OxyB and purification of product 7. This reaction was carried out on a 5.0 mL scale. Loading buffer (50 mM HEPES, 20 mM KCl, 10 mM $MgCl_2$, pH 7.0) was added to 1.00 μmol of lyophilized 7mer-CoA adduct, to a final peptide concentration of 400 μM. PCP-X and Sfp R4-4 were added to final concentrations of 400 μM and 80 μM, respectively, and loading reaction was placed in an incubator at 30 °C. Final concentrations of the following components were then added to the reaction, in this order: 4mM G6P, 0.04 U/μL G6P-DH, 20 μM spinach ferredoxin, 8μM ferredoxin reductase, 20 μM OxyB and 4 mM NADPH. The reaction proceeded for 3 h, at room temperature, shielded from light. The peptide was cleaved from PCP-X through the addition of 20,000 equivalents of propyl amine and the reaction was incubated for 15 min. Proteins were then precipitated by adding formic acid (15% v/v) and MeCN (50% v/v). Purification of the resulting product was carried out through repeated injections onto a Supelco Discovery RP Amide C16 column (5μm, 250mm x 10mm), initially equilibrated with 10% MeCN. **7** (0.3 mg) was eluted with a gradient of 10-44% over 30 min and dried *in vacuo*.

Enzymatic reaction of 15 (AA2 = L-Tyr; AA4 = L-Hpg) with OxyB and purification of product 16. This reaction was carried out on a 26.3 mL scale. Loading buffer (50 mM HEPES, 20 mM KCl, 10 mM $MgCl_2$, pH 7.0) was added to 5.26 μmol of lyophilized 7mer-CoA adduct, to a final peptide concentration of 400 μM. PCP-X and Sfp R4-4 were added to final concentrations of 400 μM and 80 μM, respectively, and loading reaction was placed in an incubator at 30 °C. Final concentrations of the following components were then added to the reaction, in this order: 4mM G6P, 0.04 U/μL G6P-DH, 20 μM spinach ferredoxin, 8μM ferredoxin reductase, 8 μM OxyB and 4 mM NADPH. The reaction proceeded for 3 h, at room temperature, shielded from light. The peptide was cleaved from PCP-X through the addition of 20,000 equivalents of propyl amine and the reaction was incubated for 15 min. Proteins were then precipitated by adding formic acid (15% v/v) and MeCN (50% v/v). Purification of the resulting product was carried out through

repeated injections onto a Phenomenex Luna C18 column (5μm, 250mm x 10mm), initially equilibrated with 5% MeCN. **16** (0.3 mg) was eluted with a gradient of 5-44% over 20 min and dried *in vacuo*.

Enzymatic reaction of 25 (AA2 = L-Tyr; AA4 = D-PhGly) with OxyB and purification of product 26. This reaction was carried out on a 14.5 mL scale. Loading buffer (50 mM HEPES, 20 mM KCl, 10 mM $MgCl_2$, pH 7.0) was added to 2.9 μmol of lyophilized 7mer-CoA adduct, to a final peptide concentration of 400 μM. PCP-X and Sfp R4-4 were added to final concentrations of 400 μM and 80 μM, respectively, and loading reaction was placed in an incubator at 30 °C. Final concentrations of the following components were then added to the reaction, in this order: 4mM G6P, 0.04 U/μL G6P-DH, 20 μM spinach ferredoxin, 8 μM ferredoxin reductase, 30 μM OxyB and 4 mM NADPH. The reaction proceeded for 3 h, at room temperature, shielded from light. The peptide was cleaved from PCP-X through the addition of 20,000 equivalents of propyl amine and the reaction was incubated for 15 min. Proteins were then precipitated by adding formic acid (15% v/v) and MeCN (50% v/v). Purification of the resulting product was carried out through repeated injections onto a Phenomenex Luna C18 column (5μm, 250mm x 10mm), initially equilibrated with 5% MeCN. **26** (0.9 mg) was eluted with a gradient of 5-49% over 20 min and dried *in vacuo*.

Large-scale enzymatic reaction of 32 (AA2 = L-Phe; AA4 = D-PhGly) with OxyB and purification of product 33. This reaction was carried out on a 24 mL scale. Loading buffer (50 mM HEPES, 20 mM KCl, 10 mM $MgCl_2$, pH 7.0) was added to 4.8 μmol of lyophilized 7mer-CoA adduct, to a final peptide concentration of 400 μM. PCP-X and Sfp R4-4 were added to final concentrations of 200 μM and 80 μM, respectively, and loading reaction was placed in an incubator at 30 °C. Final concentrations of the following components were then added to the reaction, in this order: 4mM G6P, 0.04 U/μL G6P-DH, 20 μM spinach ferredoxin, 8μM ferredoxin reductase, 60 μM OxyB and 4 mM NADPH. The reaction proceeded for 3 h, at room temperature, shielded from light. The peptide was cleaved from PCP-X through the addition of 20,000 equivalents of propyl amine and the reaction was incubated for 15 min. Proteins were then precipitated by adding formic acid (15% v/v) and MeCN (50% v/v). Purification of the resulting

product was carried out through repeated injections onto a Phenomenex Luna C18 column (5μm, 250mm x 10mm), initially equilibrated with 10% MeCN. **33** (0.3 mg) was eluted with a gradient of 10-55% over 20 min and dried *in vacuo*.

Fluorescence Assays for products 44, 47. A typical enzymatic reaction with OxyB was carried out as previously described above. Purification of OxyB product was achieved by repeated injections onto an analytical Phenomenex Luna C18 column (5 μm, 250 x 4.6 mm) that had been equilibrated with 10% MeCN in H_2O (+0.1% FA). The OxyB product was eluted with a gradient of 10-55% MeCN in H_2O (+0.1% FA) over 20 minutes. The purified material was verified by HPLC-MS, aliquoted and lyophilized. After lyophilization, 20 to 50 μL of DMSO was added to the purified OxyB product and subsequently transferred to a 96-well plate in the Synergy H1 Microplate Reader. Fluorescence experiments were performed at λ_{excite} = 288 nm and λ_{excite} = 310 nm, which correspond to the λ_{max} of diphenylamine and 2-aminobiphenyl, respectively.

Antibiotic Activity Assays. *E. coli* K12 (wt, Kolter lab collection), *Enterococcus faecalis* OG1RF (ATCC), *Staphylococcus aureus* Newman (wt, Muir lab collection), *Vibrio cholerae* (wt, Bassler lab collection), and *Saccharomyces cerevisiae* ZSR3385 (wt, Kolter lab collection) were used for antibiotic assays. *E. coli* and *E. faecalis* were cultured in LB broth at 37°C. *S. aureus* was cultured in Brain-Heart Infusion (BHI) medium at 37°C, and *V. cholera* was grown in marine broth at 37°C. *S. cerevisiae* was cultured at 30°C in YPM medium (0.5% yeast extract, 0.3% peptone, 2.5% mannitol). Bioactivity assays were carried out in accordance to the 2003 guidelines of the Clinical and Laboratory Standards Institute (CLSI) using the microtiter method. Microbial seed cultures were initiated by inoculating 5 mL of the specified medium for each strain and by incubating overnight at the indicated temperatures and shaking at 200 rpm. Each culture was then diluted with Mueller-Hinton broth to an initial OD600 nm of 0.02 in 80 μL volume per well in a 96-well plate. The wells contained varying concentrations of the compounds tested: 0, 0.02, 0.04, 0.1, 0.2, 0.4, 1, 3, 8, 20, 40 μM final concentration, in DMSO. Assays were set-up in duplicates, with appropriate controls. The plates were then incubated at the temperatures listed above without shaking and OD600 nm was determined after 2 h, 4 h, 6 h and 8 h. Both replicates gave near-identical IC_{50}s. The reported error is based on systematic error from determination of the concentration of the monocyclic peptides, which we estimate at 15%.

Enzymatic reactions with OxyB, OxyA, OxyC. Analytical-scale reactions with OxyB, OxyA and OxyC were carried out as previously described.[2]

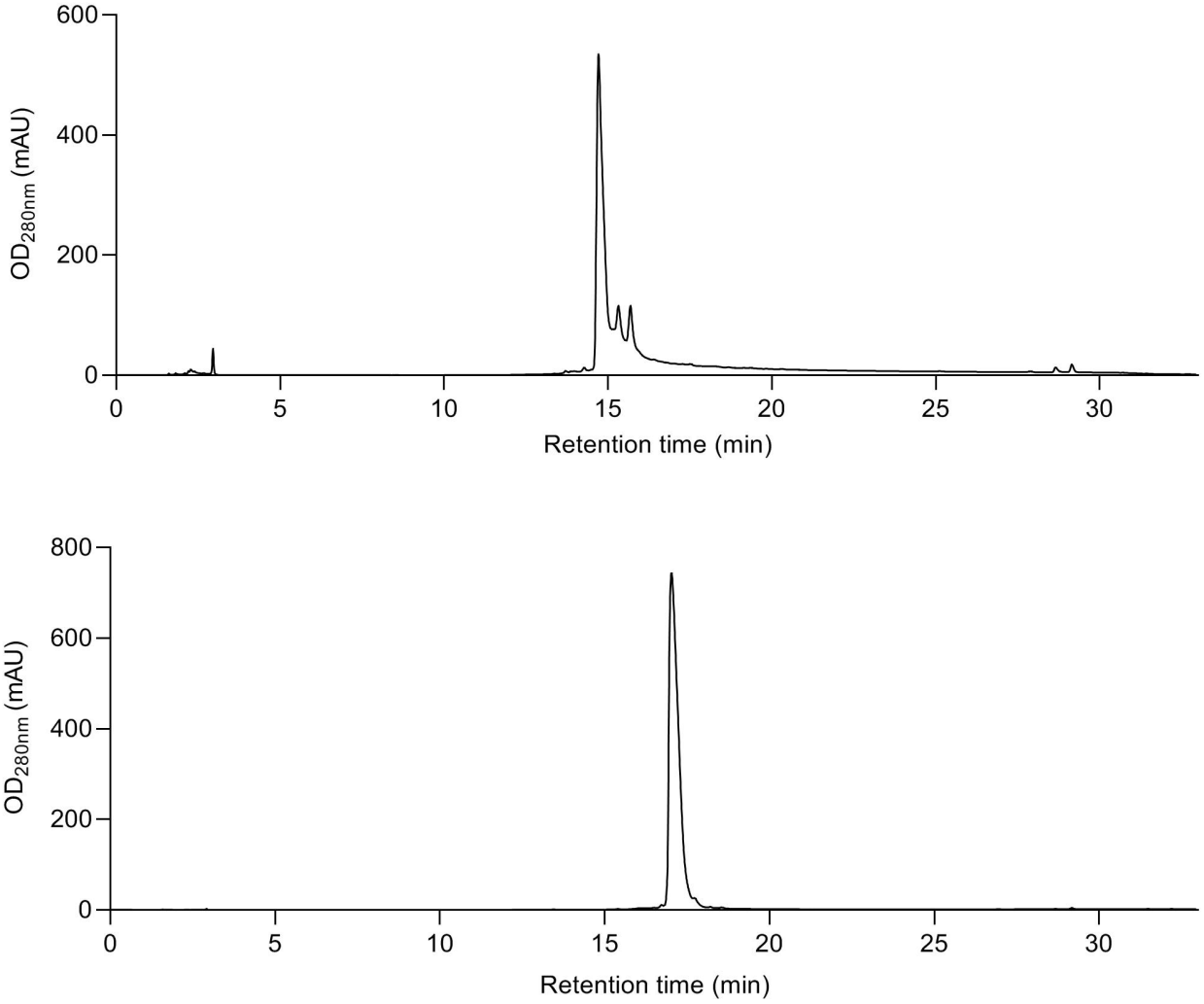

Figure S1. HPLC-MS analysis of pure **4** as a 7mer hydrazide (top) and as a CoA thioester adduct (bottom).

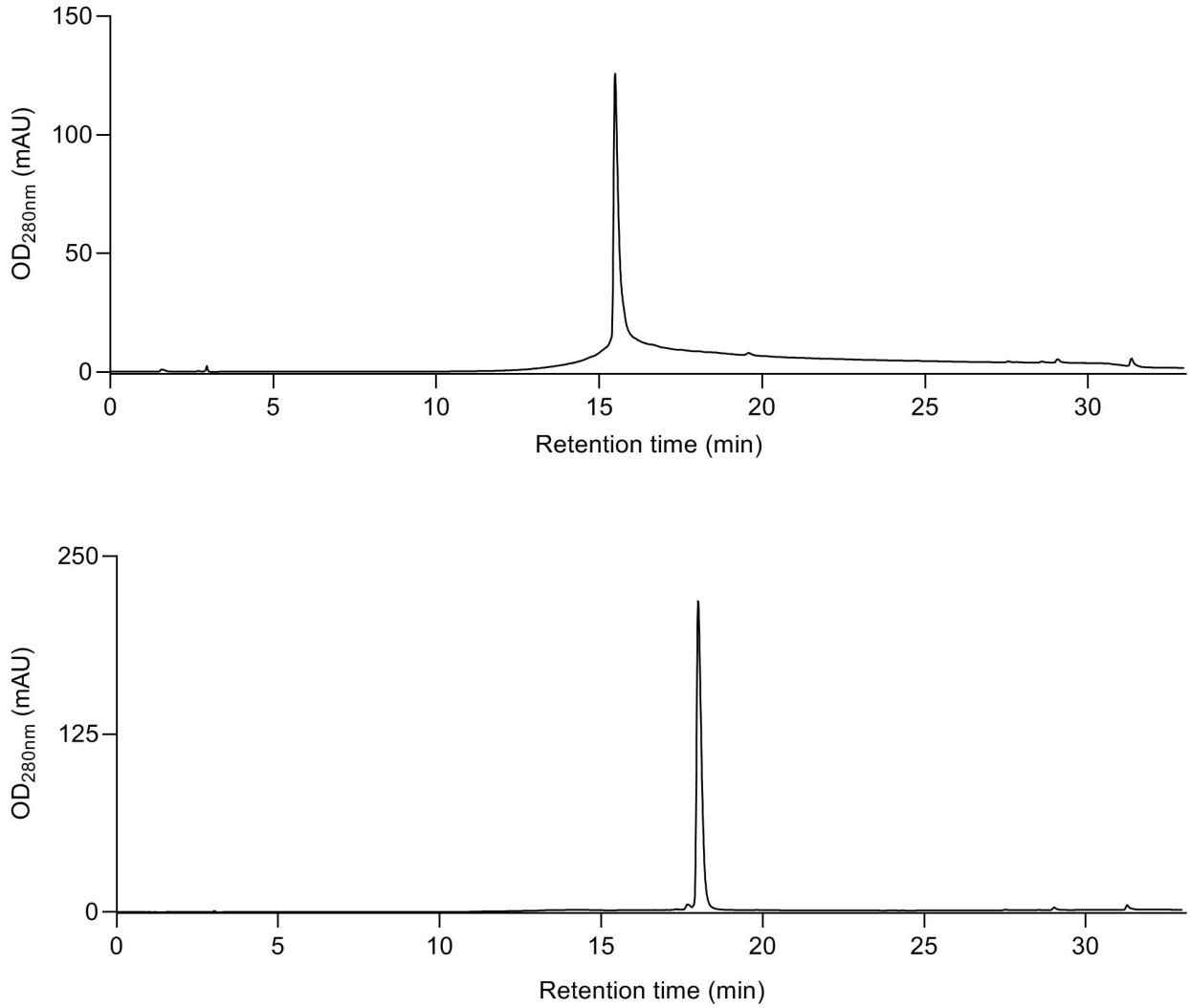

Figure S2. HPLC-MS analysis of pure **6** as a 7mer hydrazide (top) and as a CoA thioester adduct (bottom).

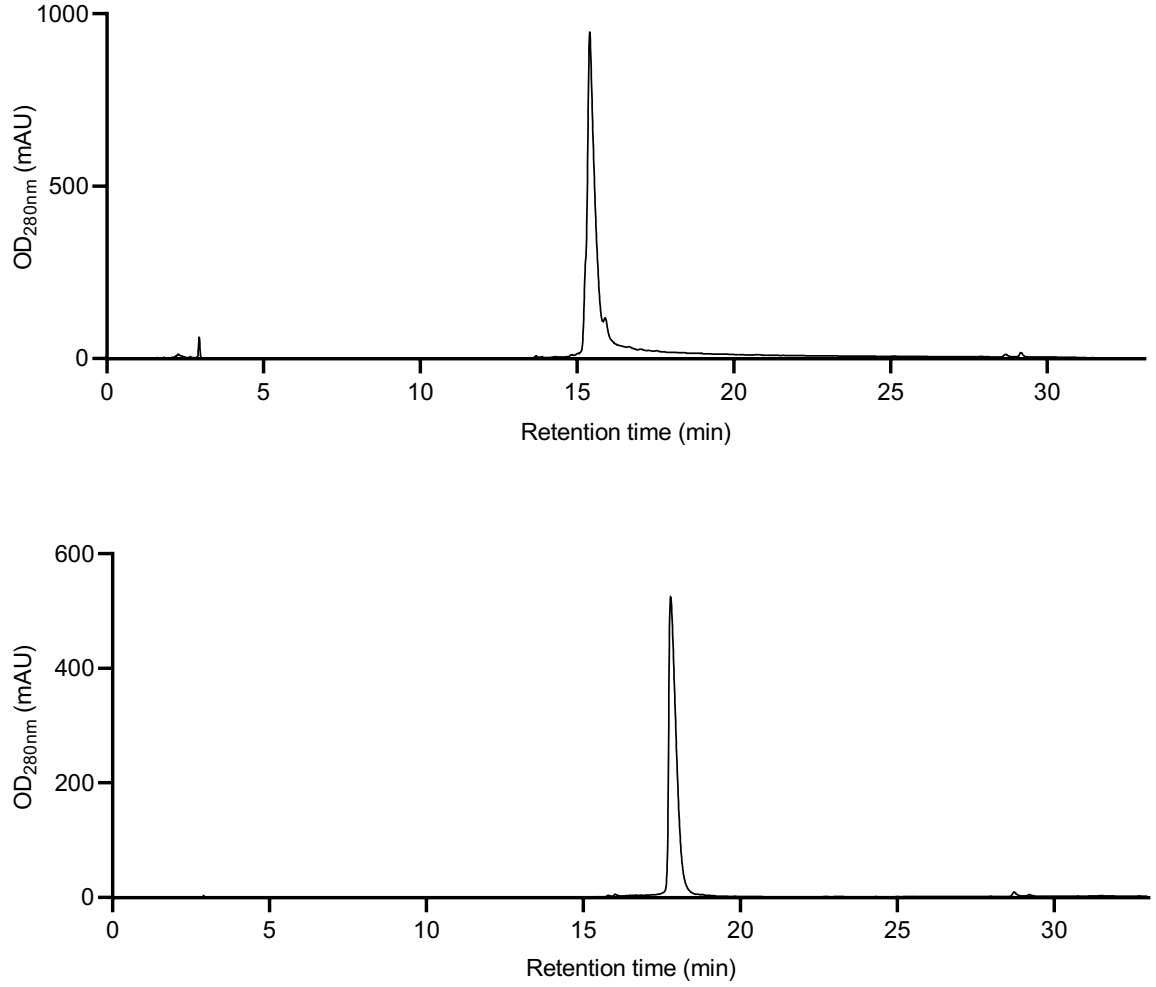

Figure S3. HPLC-MS analysis of pure **8** as a 7mer hydrazide (top) and as a CoA thioester adduct (bottom).

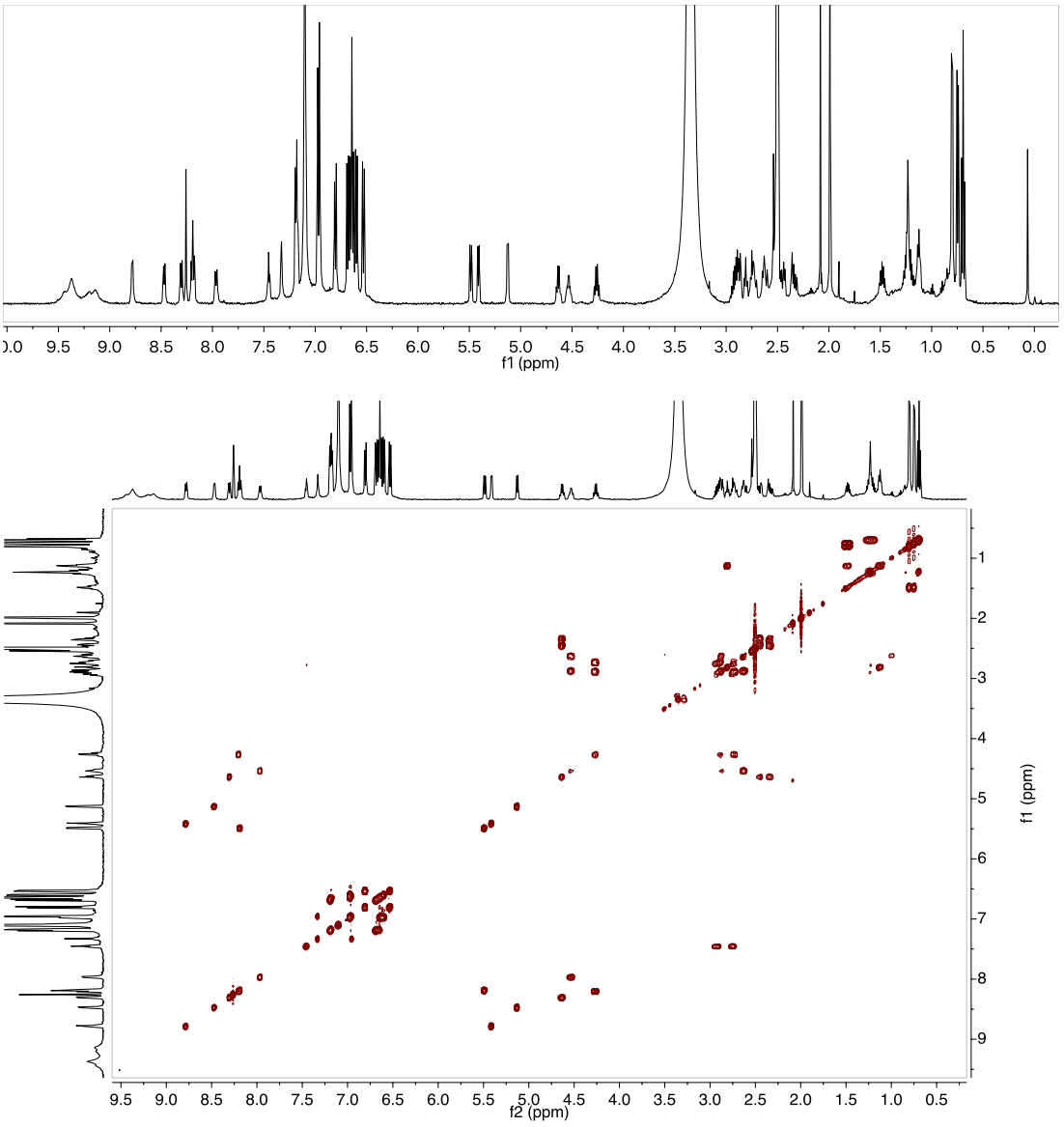

Figure S4. 800 MHz ^{1}H NMR of **4** in $(CD_3)_2SO$ (top). 800 MHz COSY spectra of **4** in $(CD_3)_2SO$ (bottom).

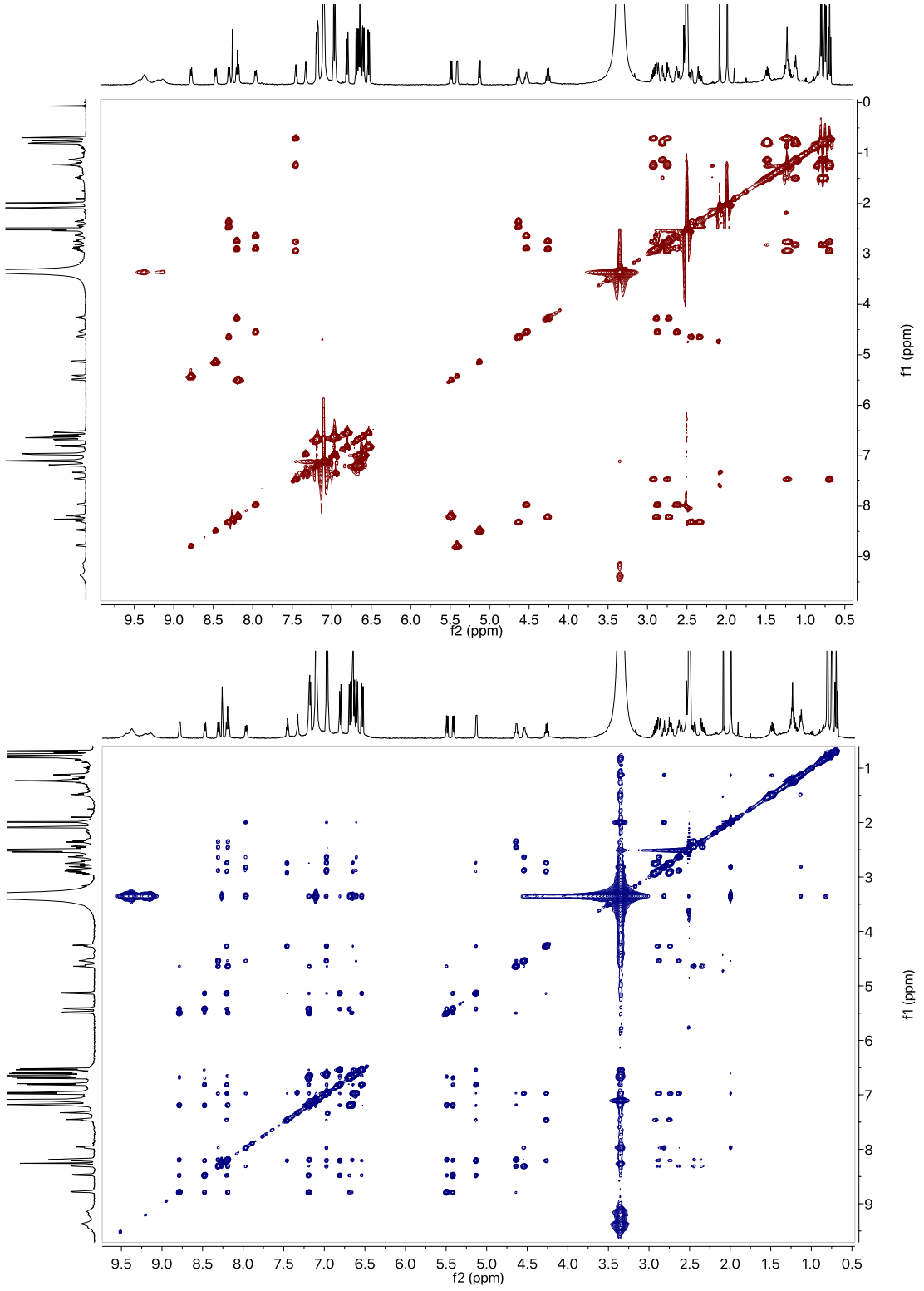

Figure S5. 800 MHz TOCSY spectra of **4** in $(CD_3)_2SO$ (top). 800 MHz NOESY spectra of **4** in $(CD_3)_2SO$ (bottom).

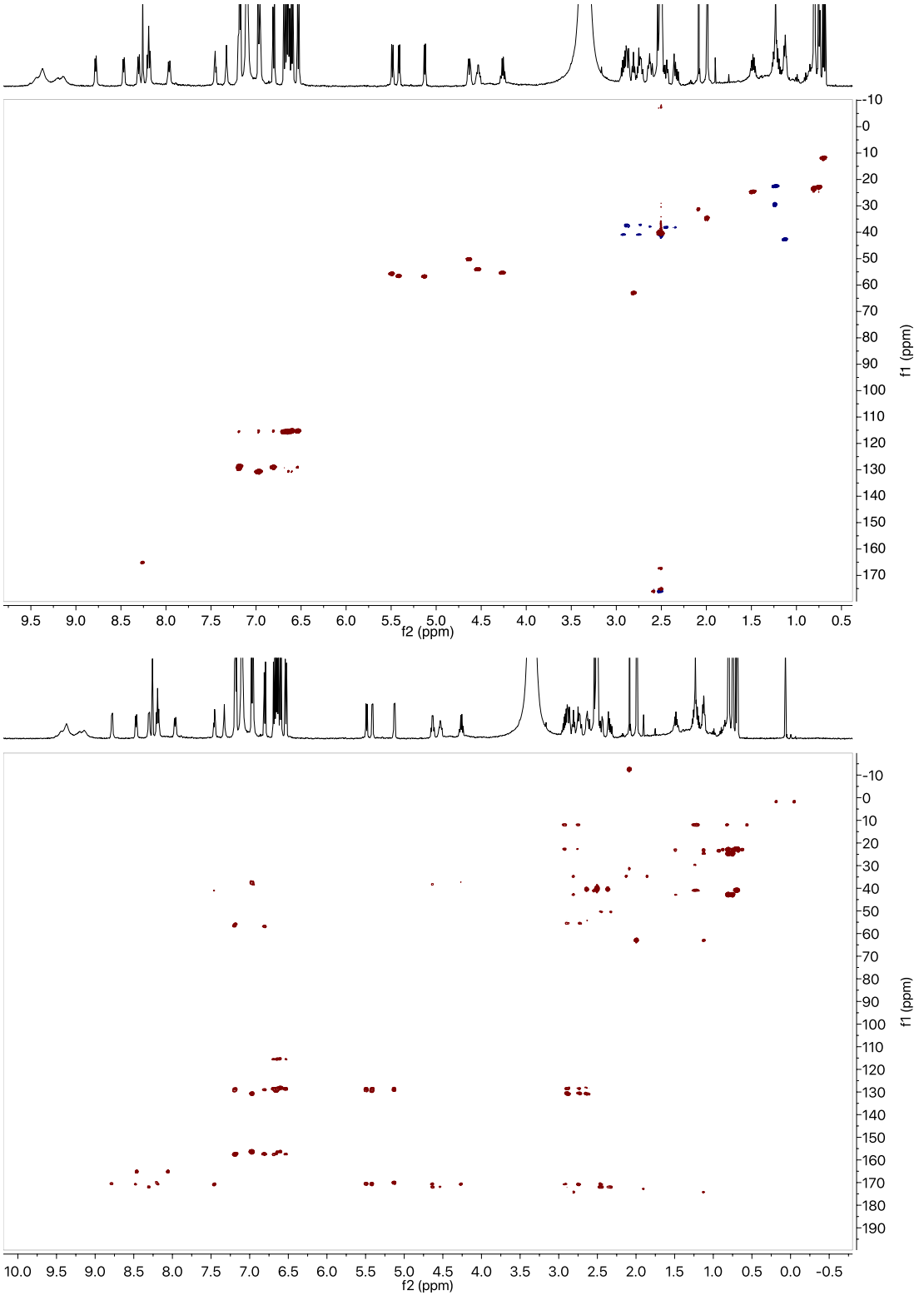

Figure S6. 800 MHz HSQC spectra of **4** in $(CD_3)_2SO$ (top). 800 MHz HMBC spectra of **4** in $(CD_3)_2SO$ (bottom).

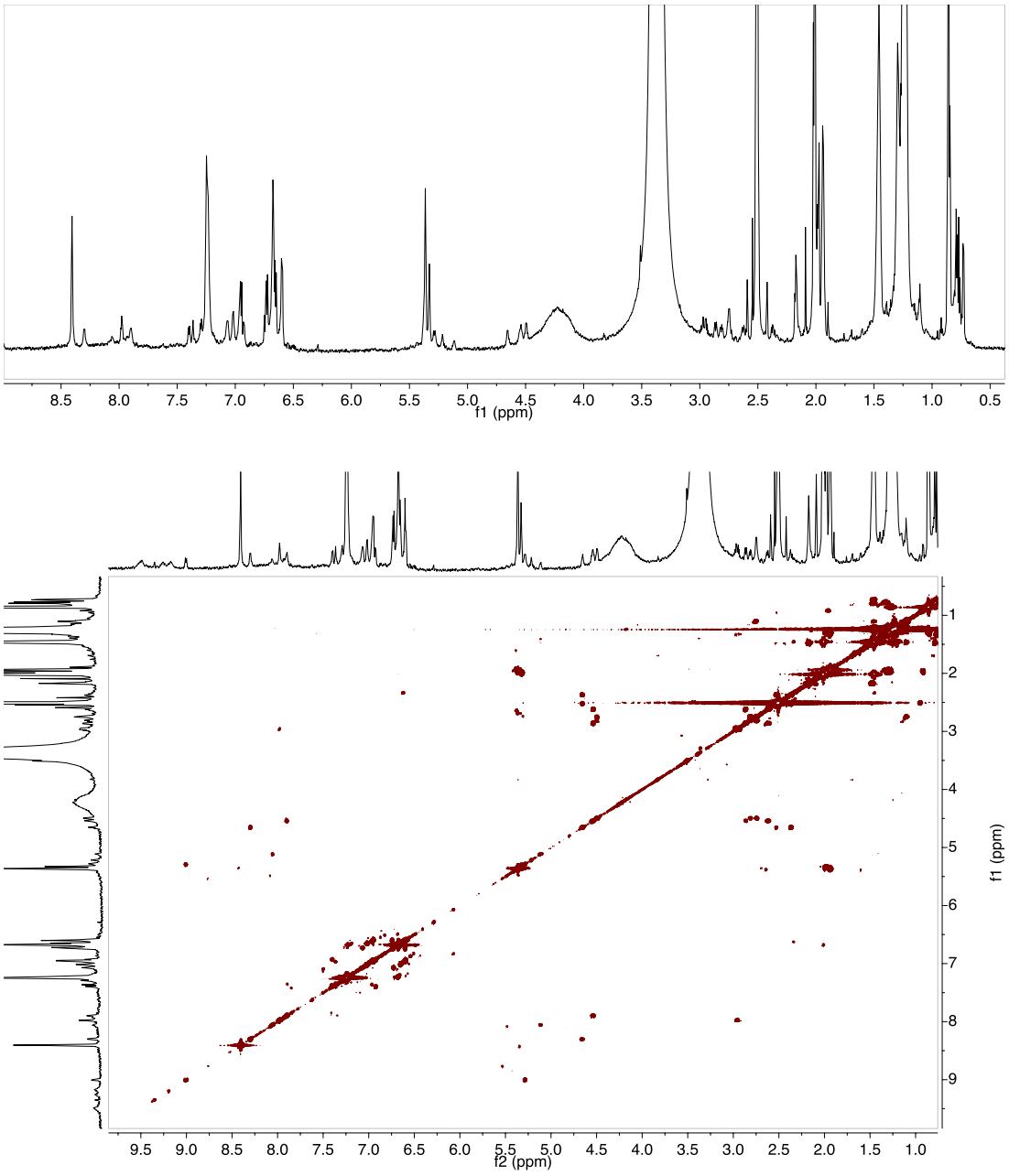

Figure S7. 800 MHz ^{1}H NMR of **5** in $(CD_3)_2SO$ (top). 800 MHz COSY spectra of **5** in $(CD_3)_2SO$ (bottom).

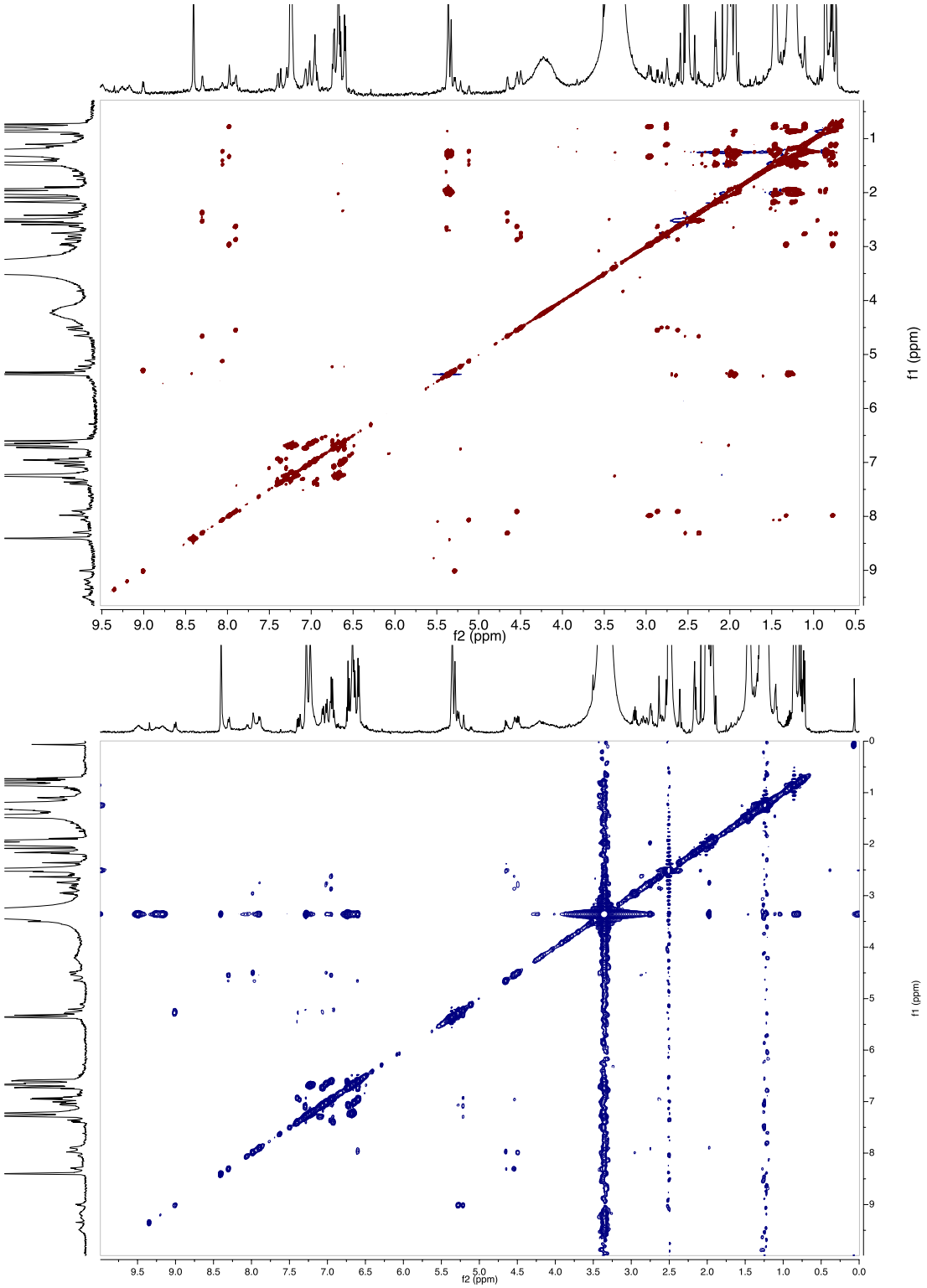

Figure S8. 800 MHz TOCSY spectra of **5** in $(CD_3)_2SO$ (top). 800 MHz NOESY spectra of **5** in $(CD_3)_2SO$ (bottom).

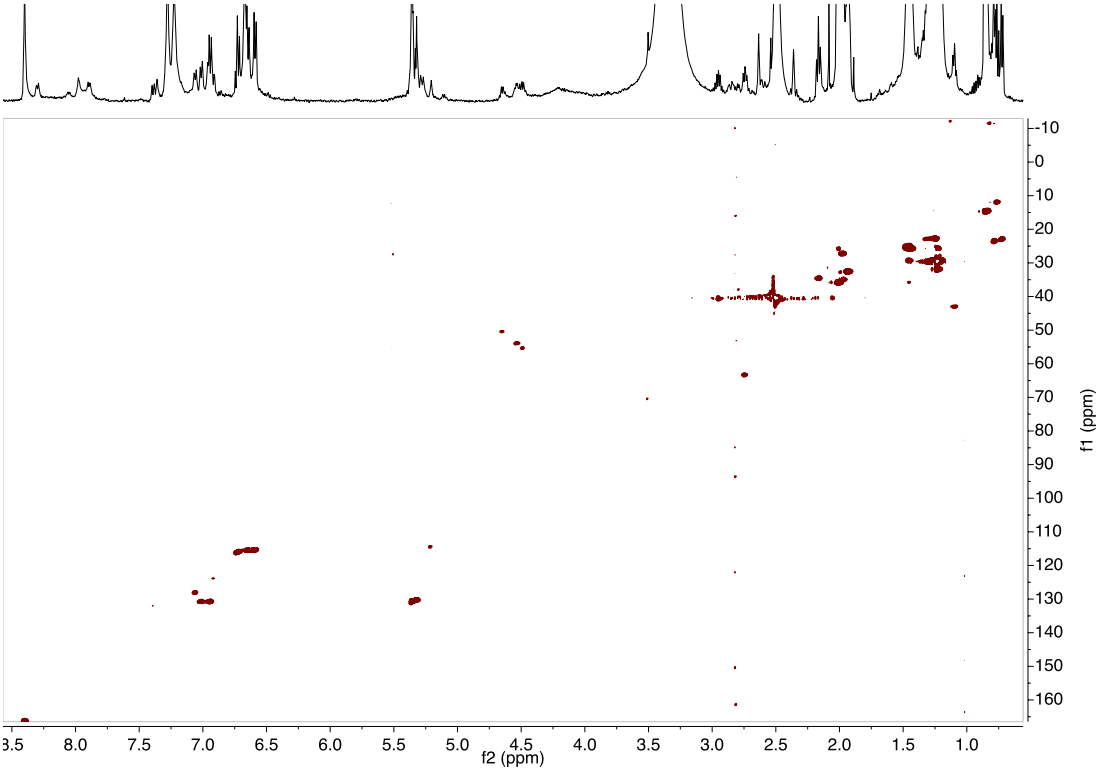

Figure S9. 800 MHz HSQC spectra of **5** in $(CD_3)_2SO$ (top).

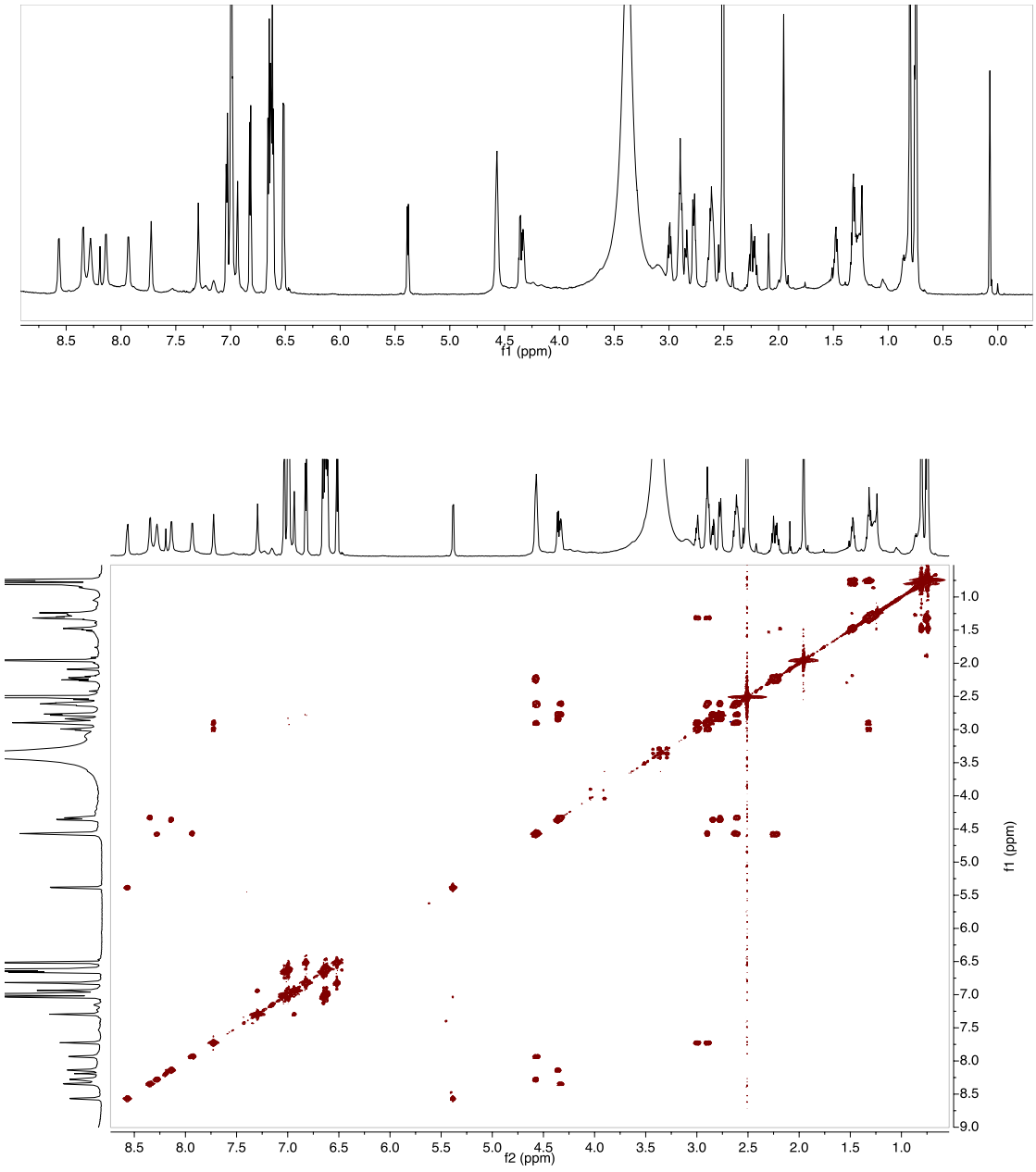

Figure S10. 800 MHz ^{1}H NMR of **6** in $(CD_3)_2SO$ (top). 800 MHz COSY spectra of **6** in $(CD_3)_2SO$ (bottom).

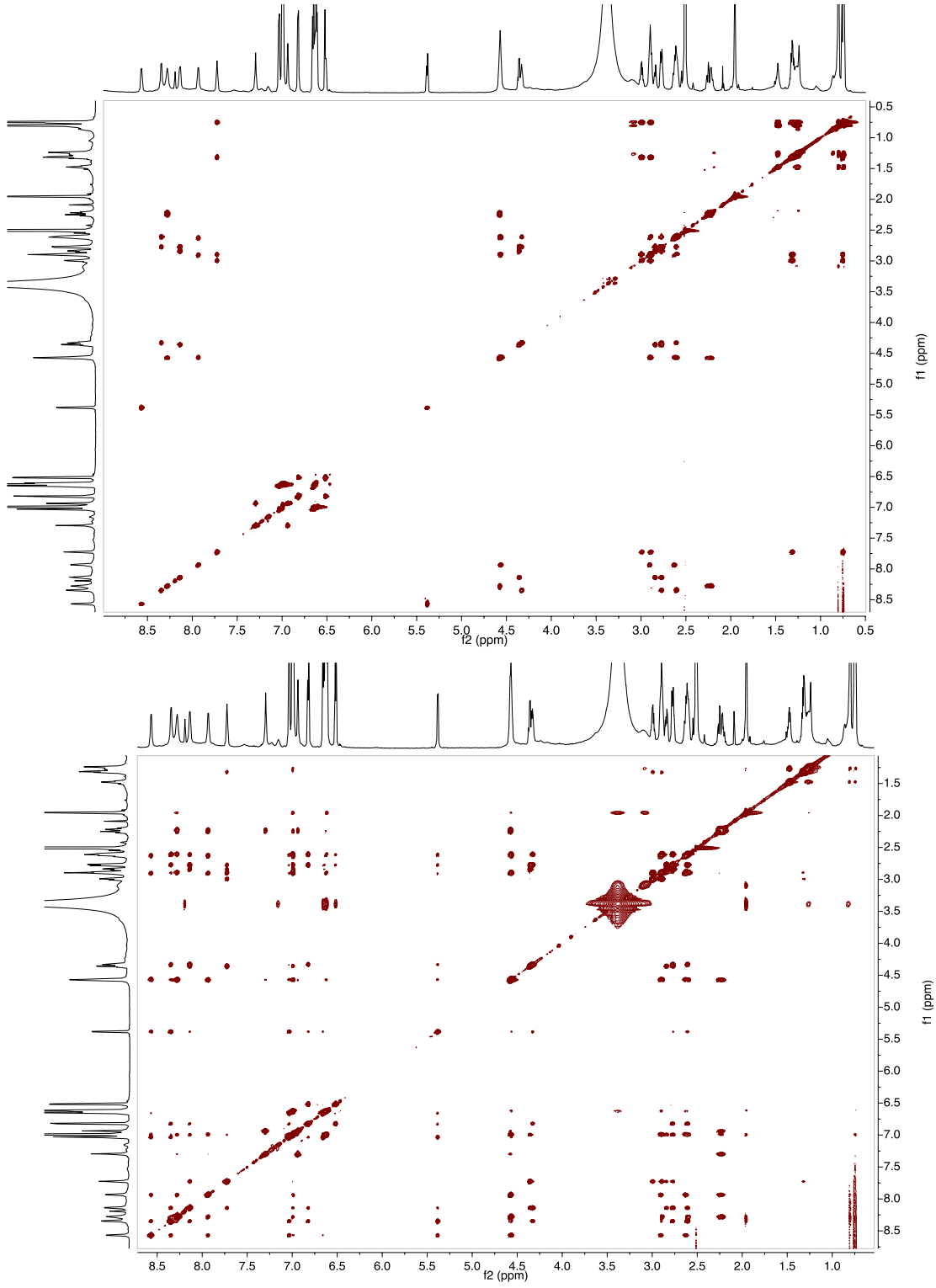

Figure S11. 800 MHz TOCSY spectra of **6** in $(CD_3)_2SO$ (top). 800 MHz NOESY spectra of **6** in $(CD_3)_2SO$ (bottom).

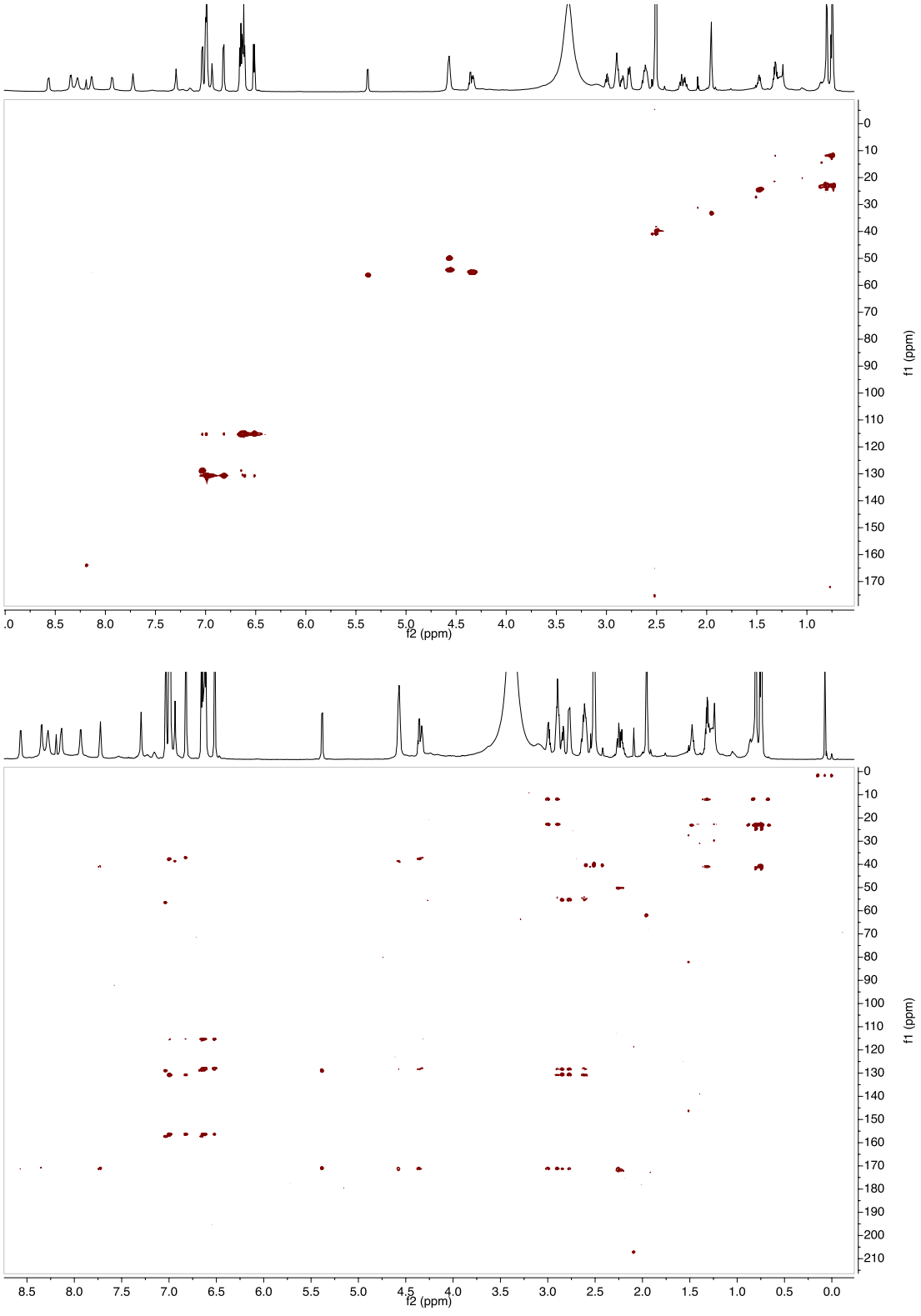

Figure S12. 800 MHz HSQC spectra of **6** in $(CD_3)_2SO$ (top). 800 MHz HMBC spectra of **6** in $(CD_3)_2SO$ (bottom).

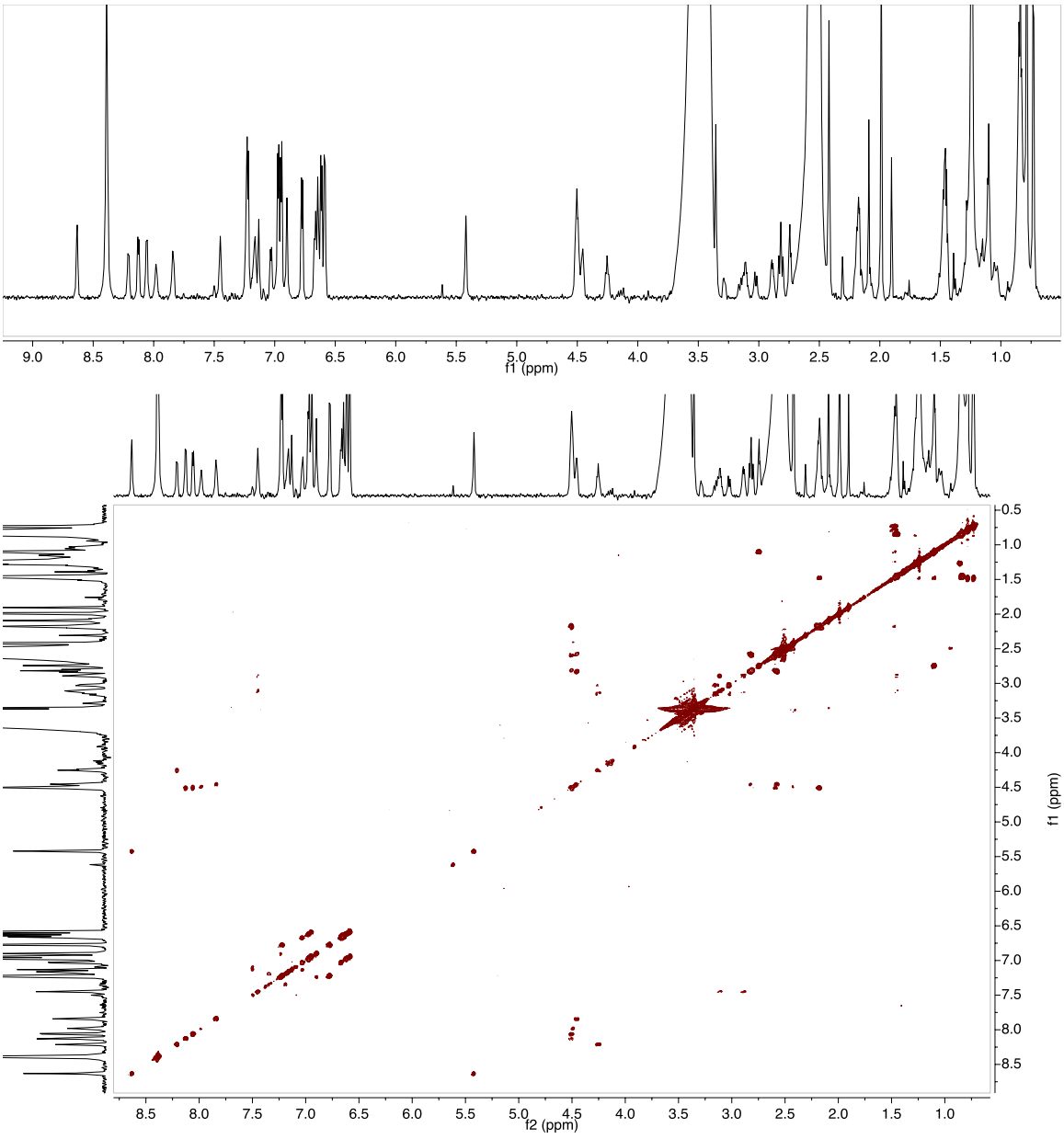

Figure S13. 800 MHz ^{1}H NMR of **7** in $(CD_3)_2SO$ (top). 800 MHz COSY spectra of **7** in $(CD_3)_2SO$ (bottom).

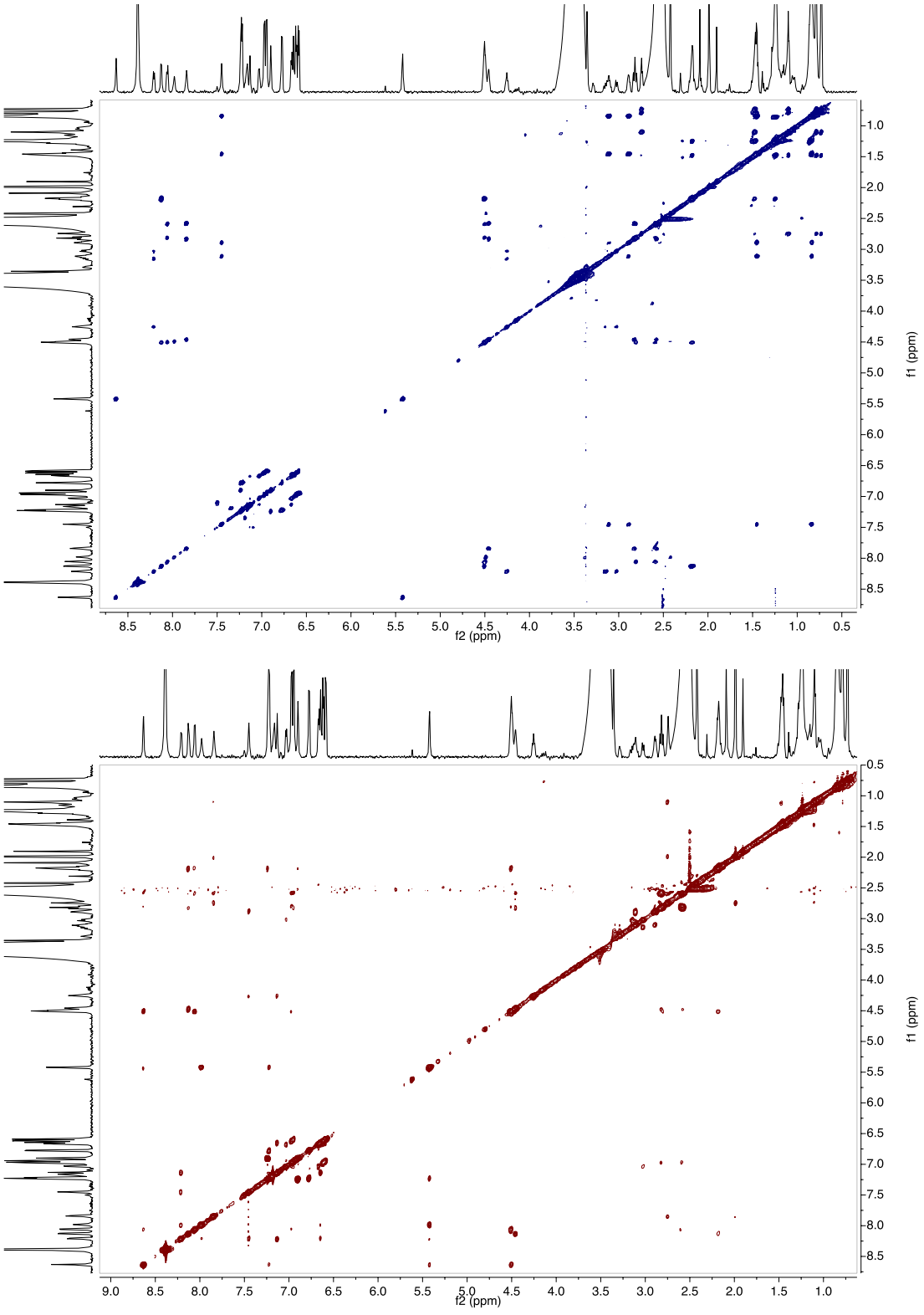

Figure S14. 800 MHz TOCSY spectra of **7** in $(CD_3)_2SO$ (top). 800 MHz NOESY spectra of **7** in $(CD_3)_2SO$ (bottom).

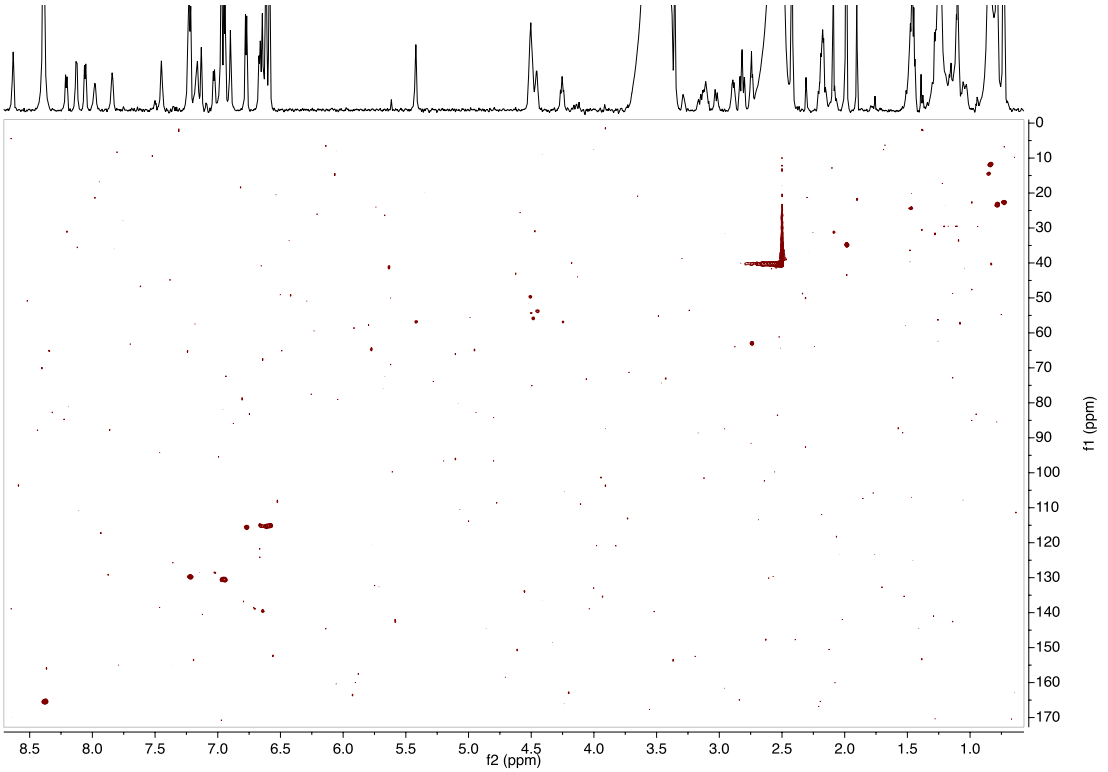

Figure S15. 800 MHz HSQC spectra of **7** in $(CD_3)_2SO$ (top).

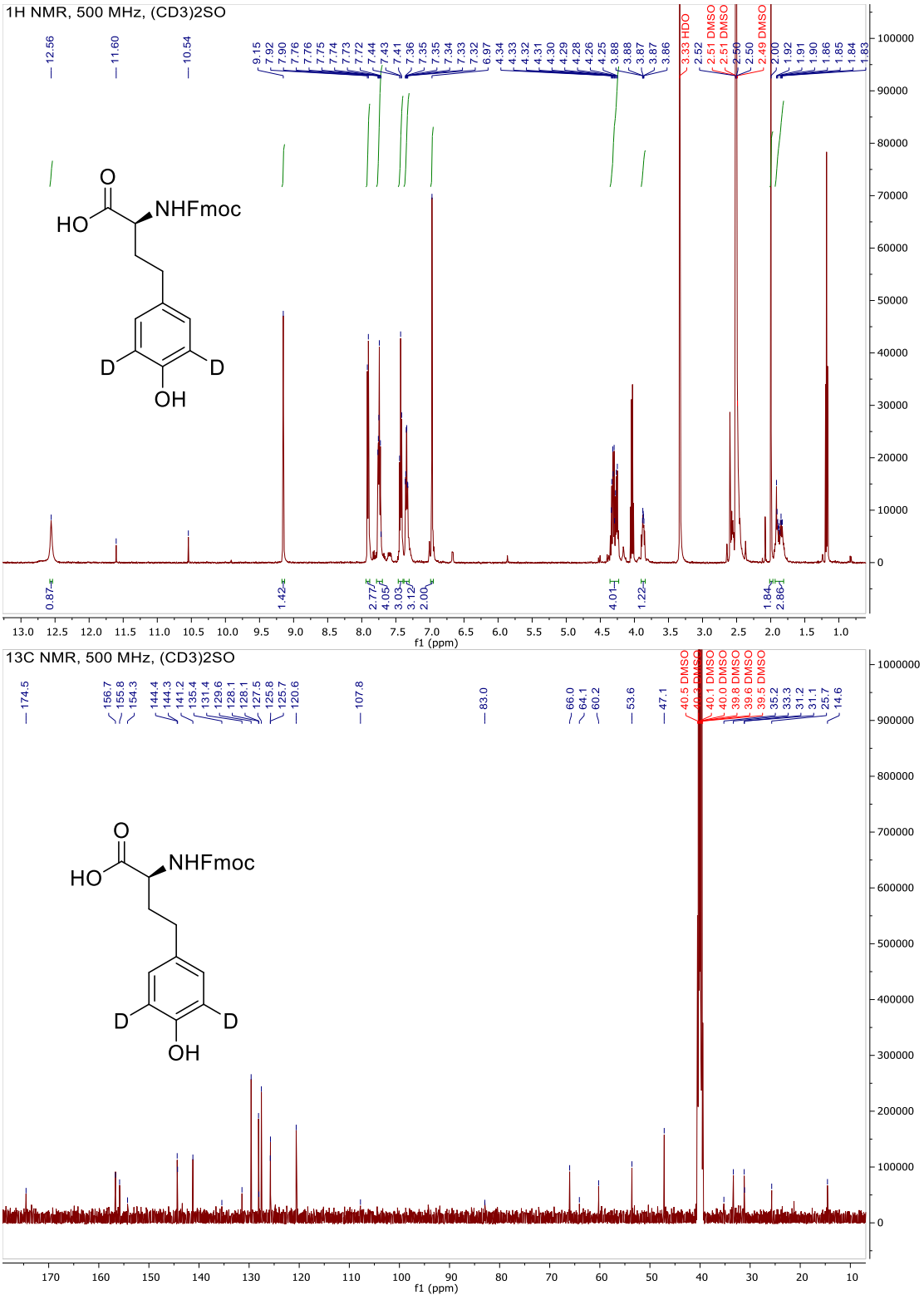

Figure S16. ^{1}H NMR spectrum (top) and ^{13}C NMR spectrum (bottom) of *N*-Fmoc-L-3,5-$^{2}H_2$-homotyrosine.

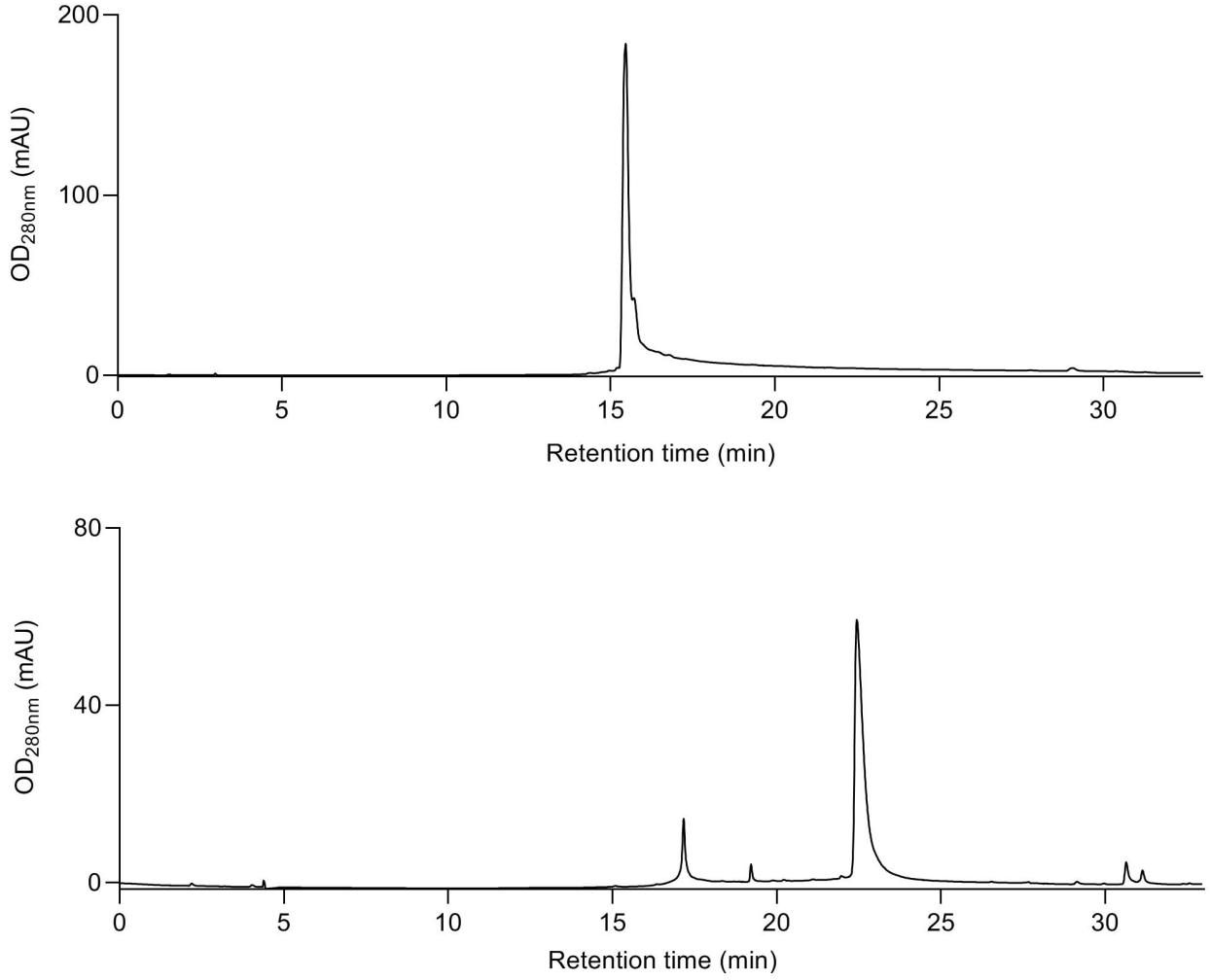

Figure S17. HPLC-MS analysis of pure *ortho*-$^{2}H_2$-homotyrosine as AA2 and D-Hpg as AA4 (precursor to **11**, **12**) as a 7mer hydrazide (top) and as a CoA thioester adduct (bottom).

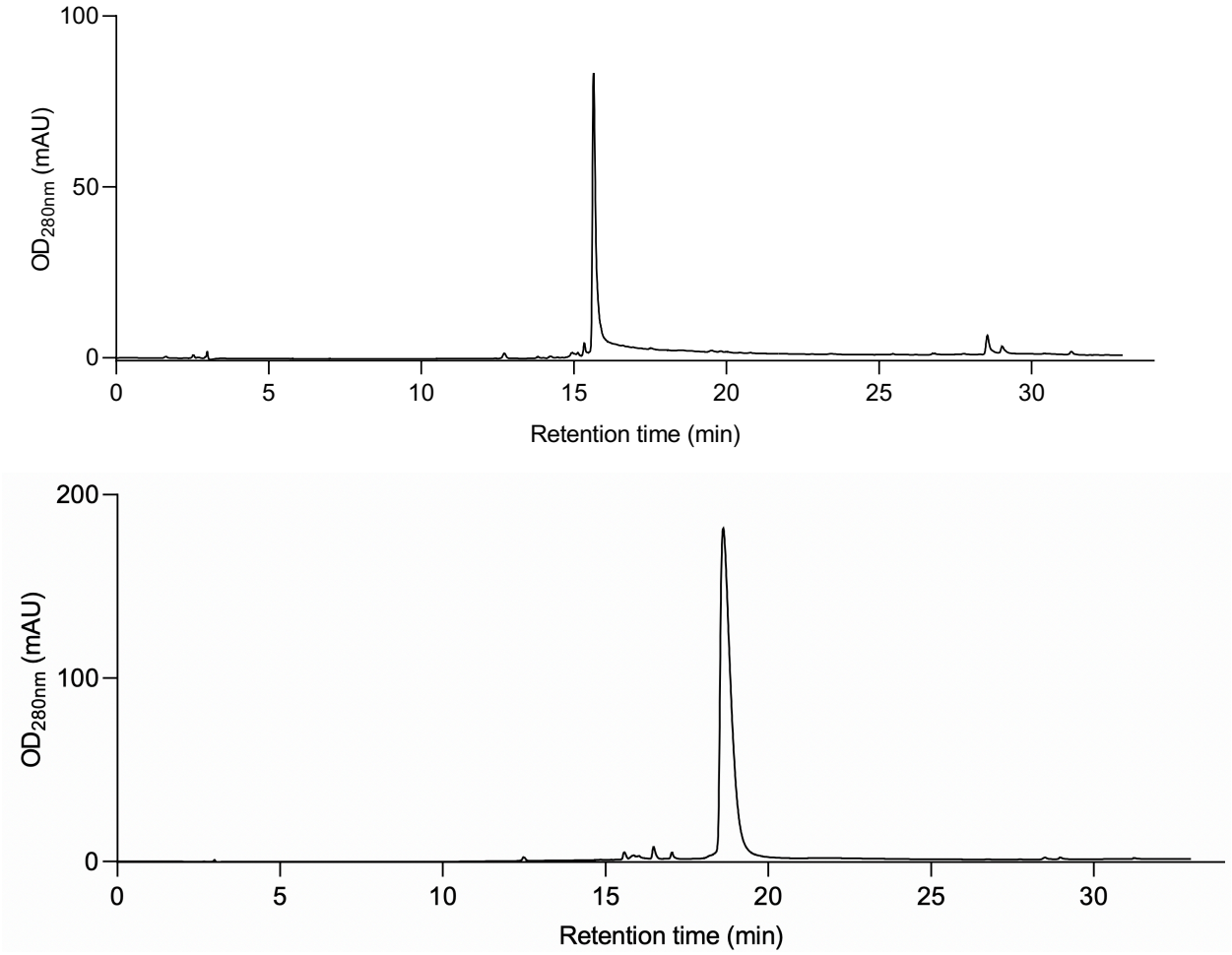

Figure S18. HPLC-MS analysis of pure peptide containing L-homotyrosine as AA2 and *ortho*-$^{2}H_{2}$-D-Hpg as AA4 (precursor to **13**, **14**) as a 7mer hydrazide (top) and as a CoA thioester adduct (bottom).

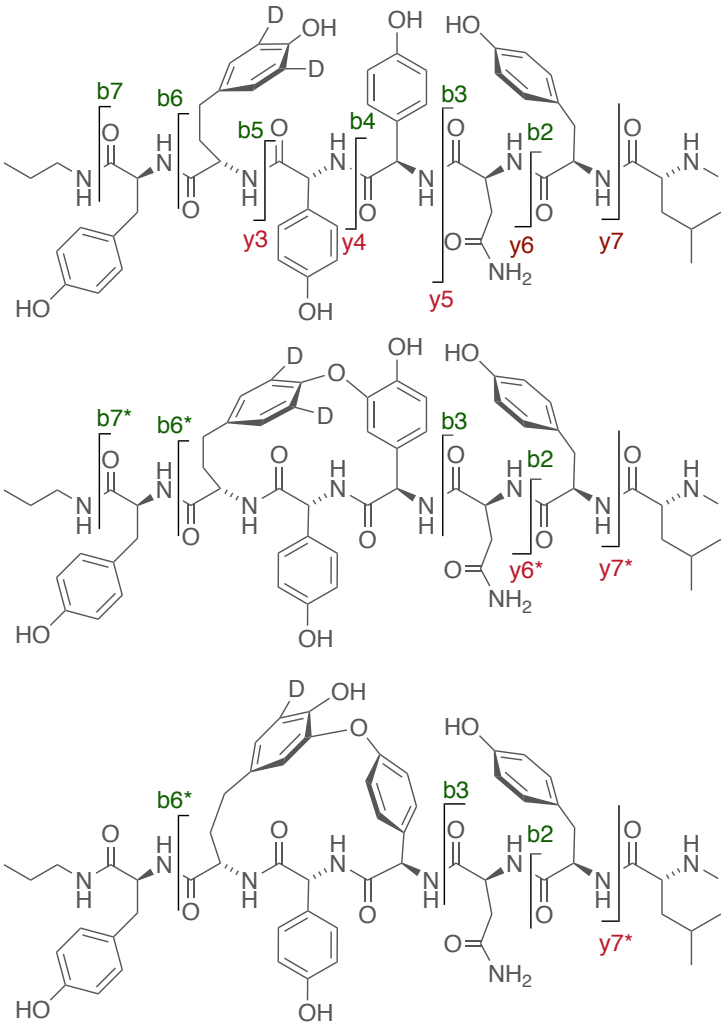

Figure S19. HR-MS/MS for peptide substrate containing *ortho*-$^{2}H_2$-L-homotyrosine as AA2 and D-Hpg as AA4 and its products (**11**, **12**) upon reaction with OxyB.

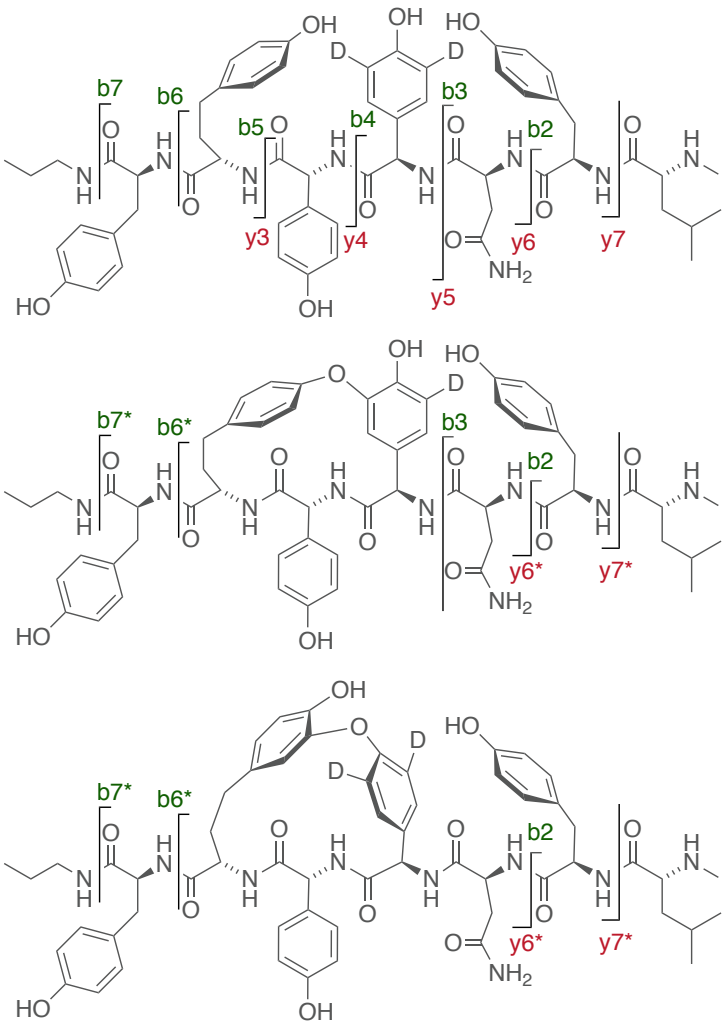

Figure S20. HR-MS/MS for peptide substrate containing L-homotyrosine as AA2 and *ortho*-$^{2}H_2$-D-Hpg as AA4 and its products (**13**, **14**) upon reaction with OxyB.

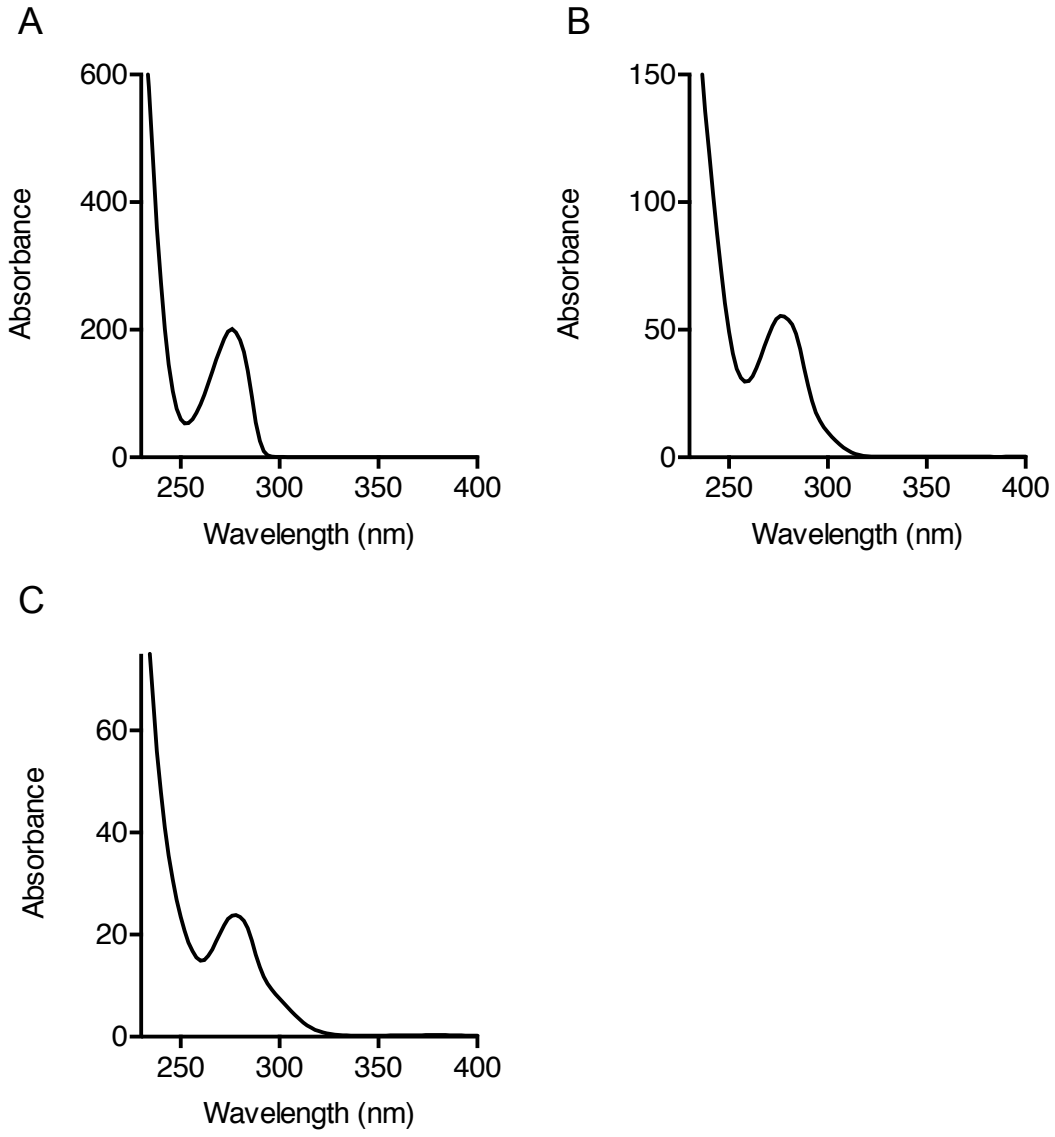

Figure S21. UV-Vis spectra for A) substrate **8**; B) product **11**; C) product **12**.

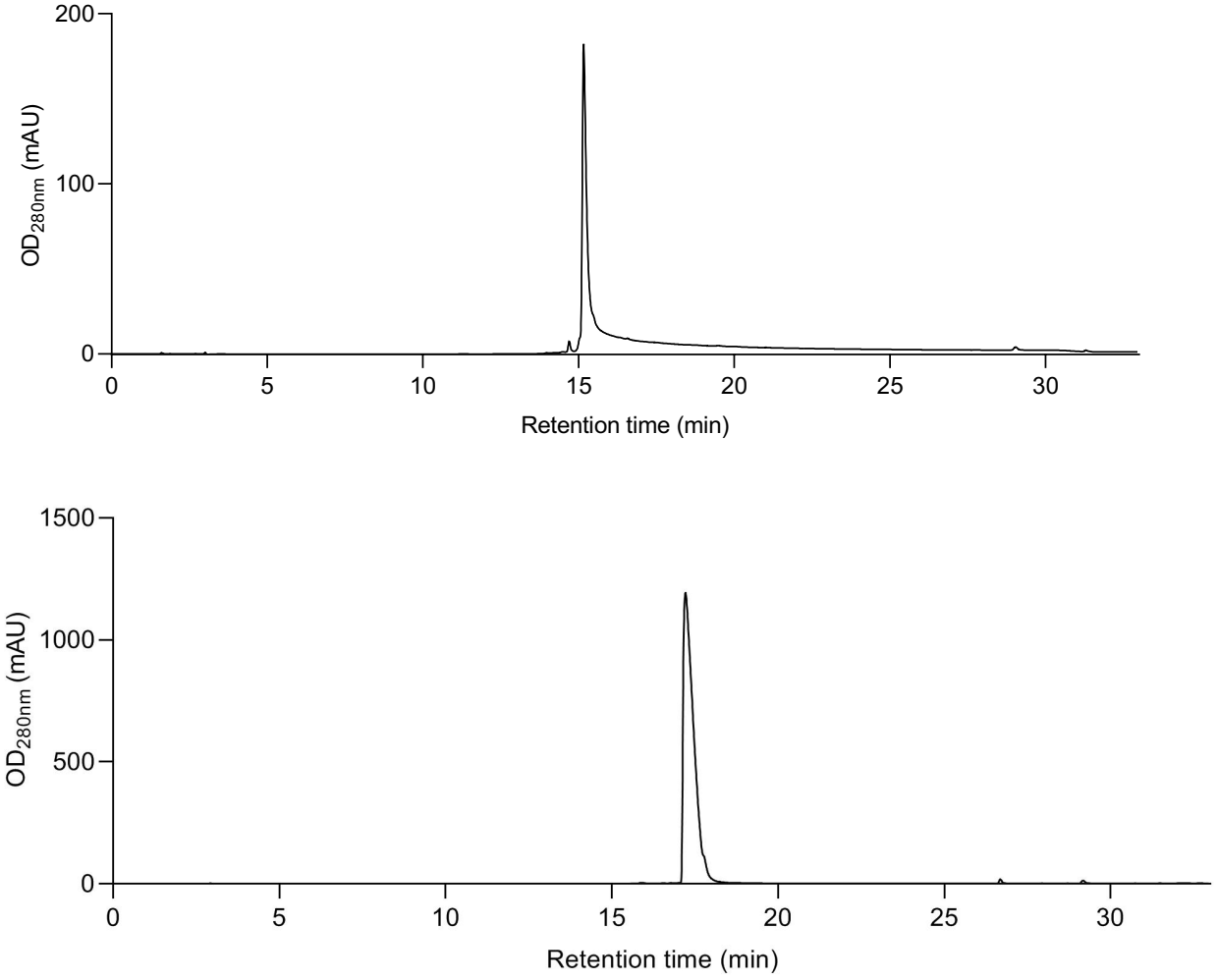

Figure S22. HPLC-MS analysis of pure **15** as a 7mer hydrazide (top) and as a CoA thioester adduct (bottom).

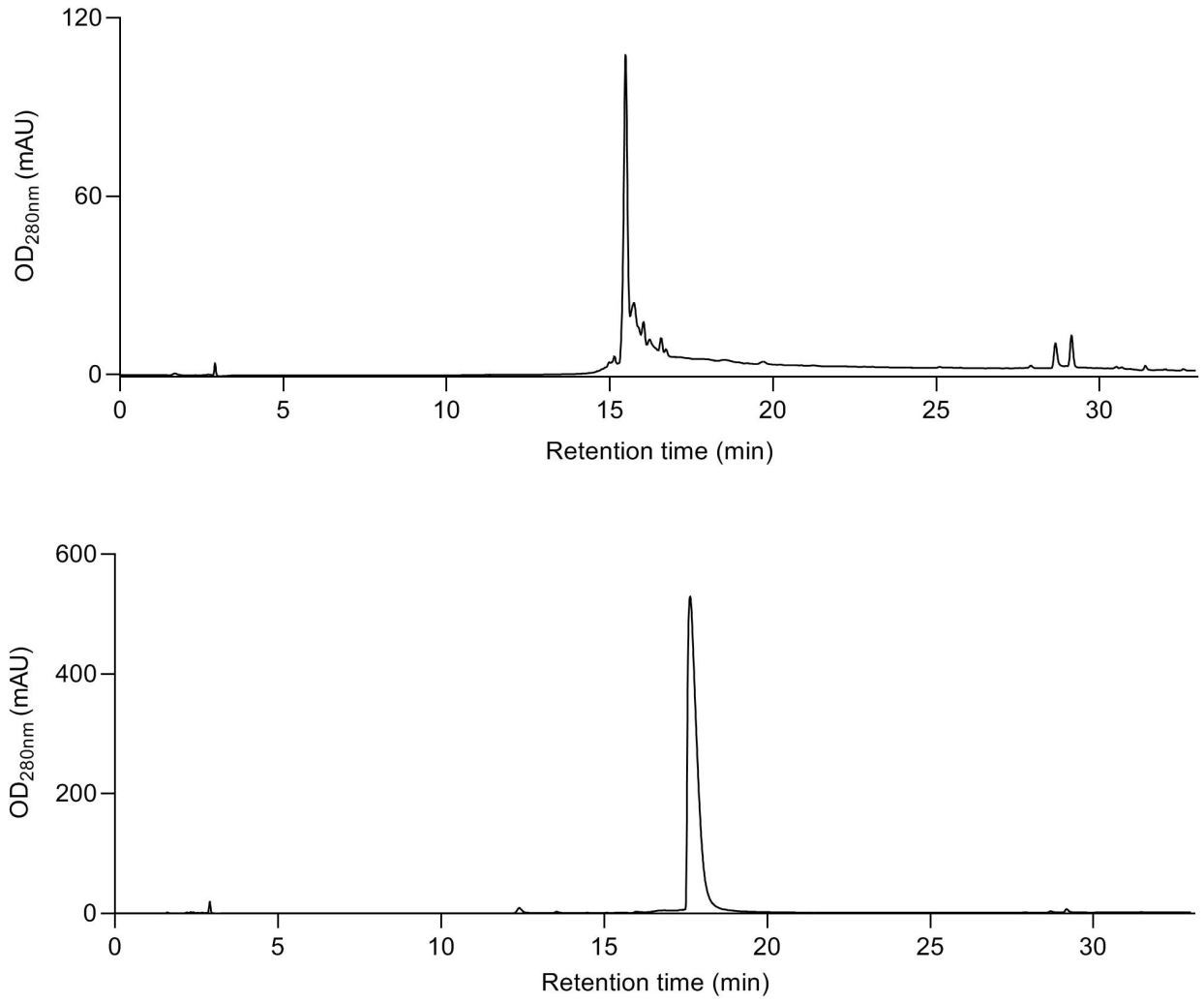

Figure S23. HPLC-MS analysis of pure **17** as a 7mer hydrazide (top) and as a CoA thioester adduct (bottom).

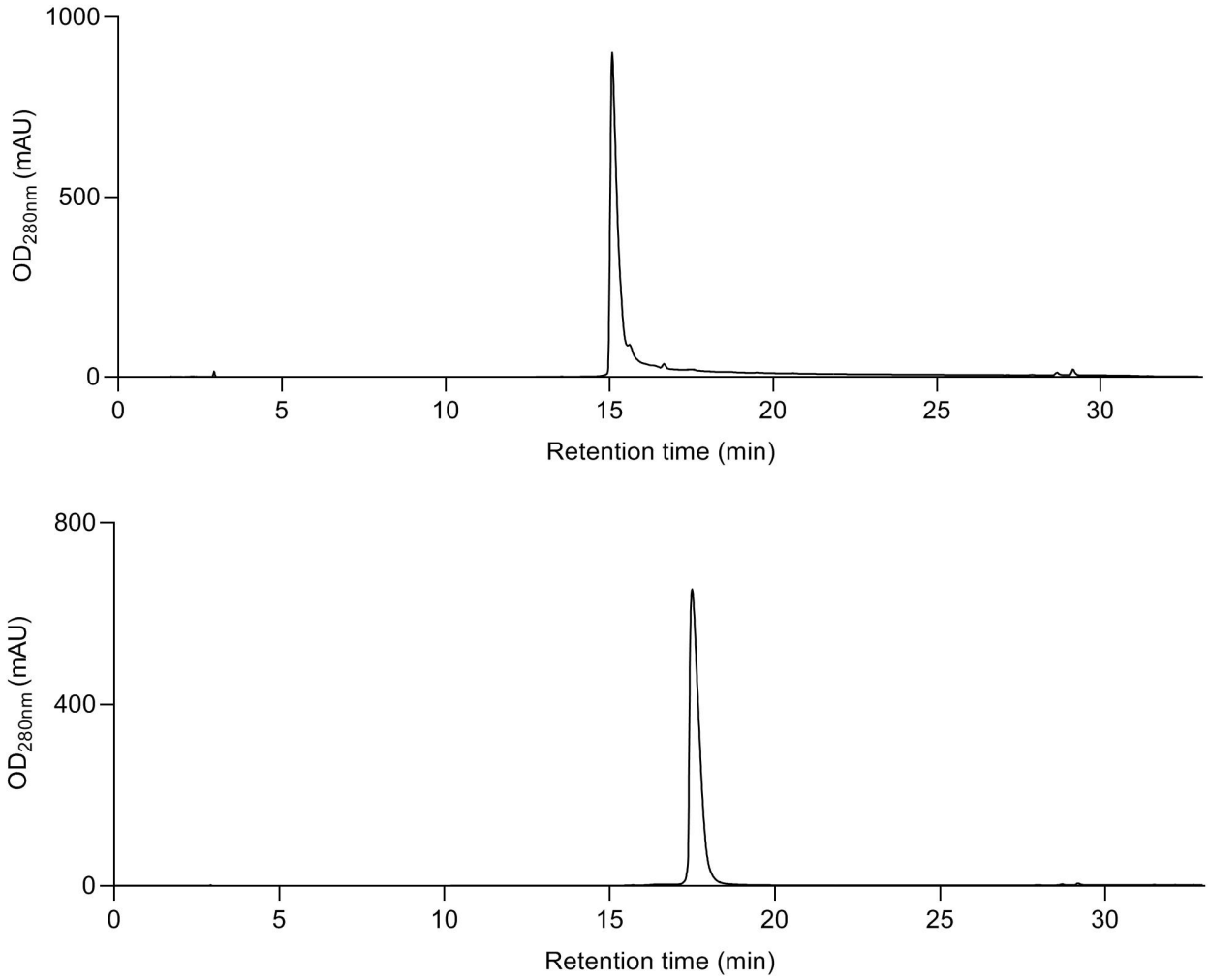

Figure S24. HPLC-MS analysis of pure **20** as a 7mer hydrazide (top) and as a CoA thioester adduct (bottom).

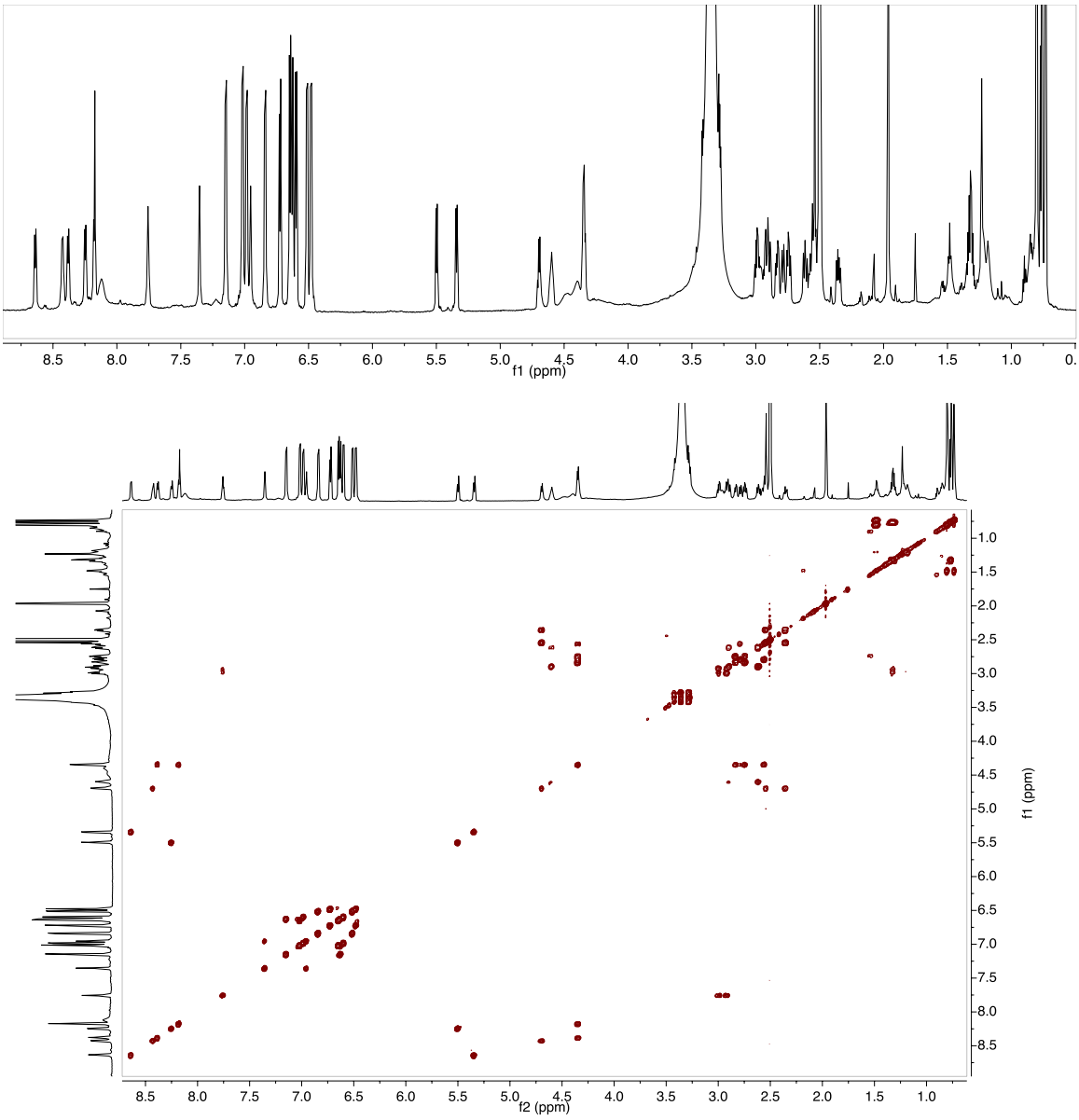

Figure S25. 800 MHz ^{1}H NMR of **15** in $(CD_3)_2SO$ (top). 800 MHz COSY spectra of **15** in $(CD_3)_2SO$ (bottom).

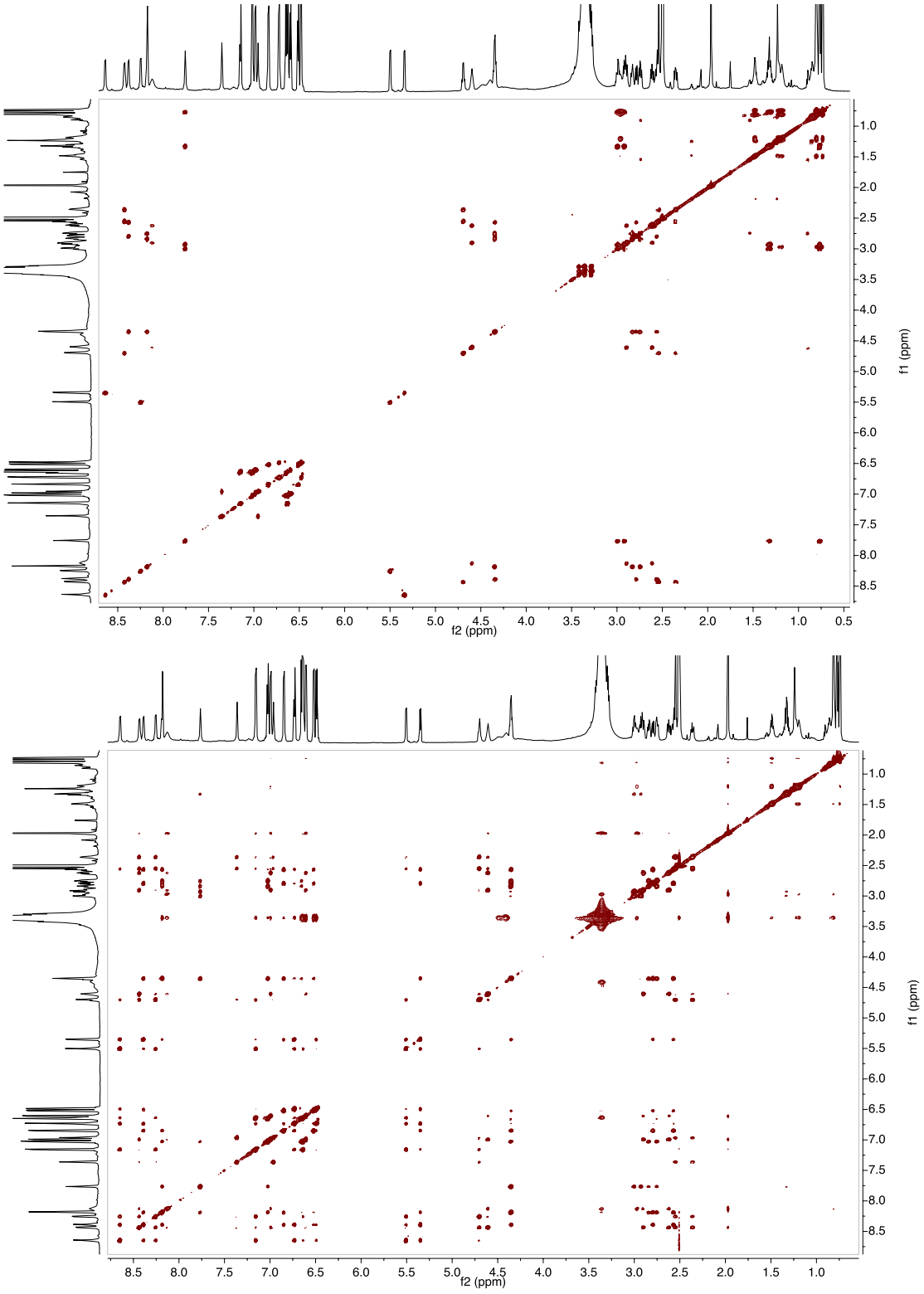

Figure S26. 800 MHz TOCSY spectra of **15** in $(CD_3)_2SO$ (top). 800 MHz NOESY spectra of **15** in $(CD_3)_2SO$ (bottom).

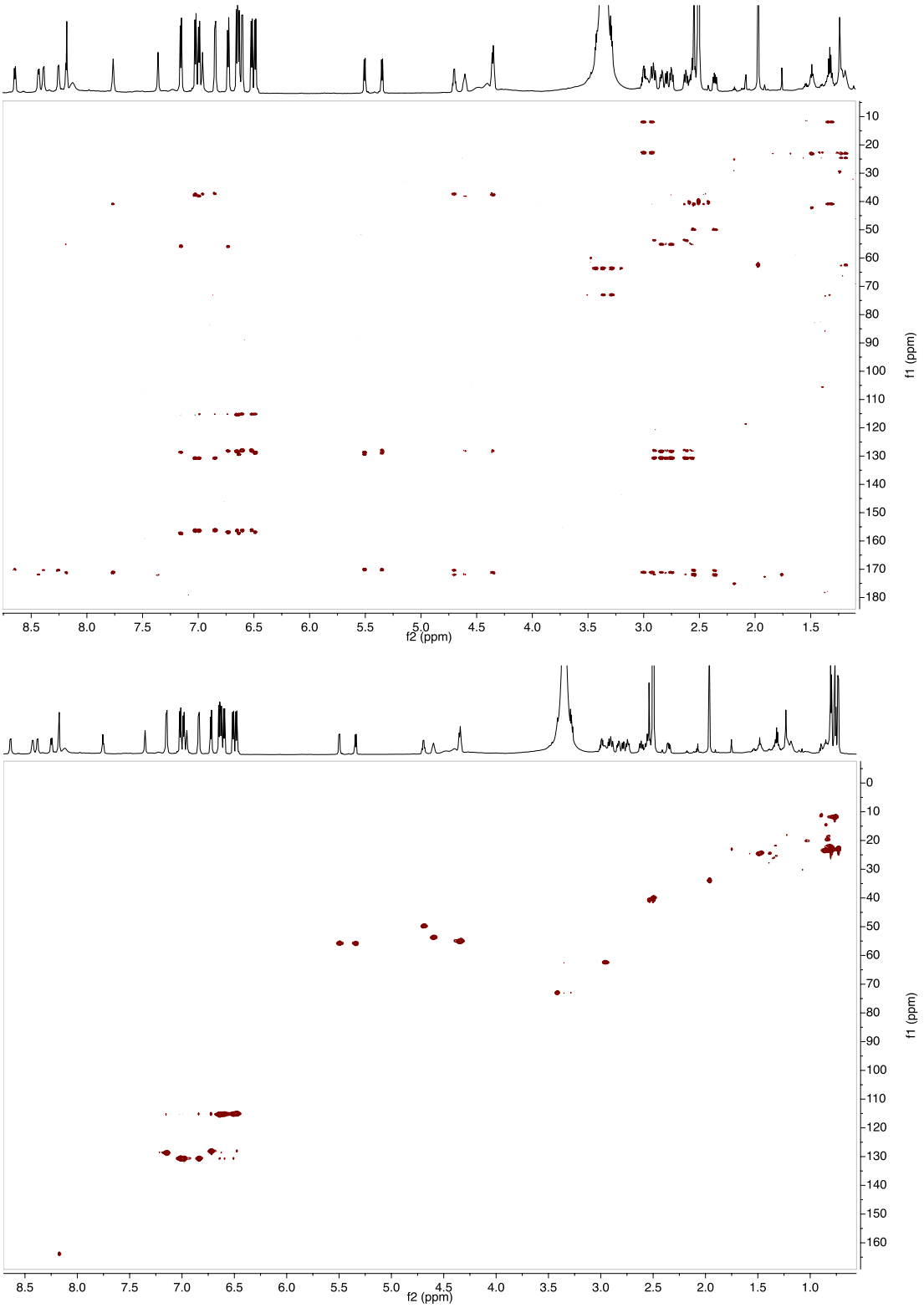

Figure S27. 800 MHz HSQC spectra of **15** in $(CD_3)_2SO$ (top). 800 MHz HMBC spectra of **15** in $(CD_3)_2SO$ (bottom).

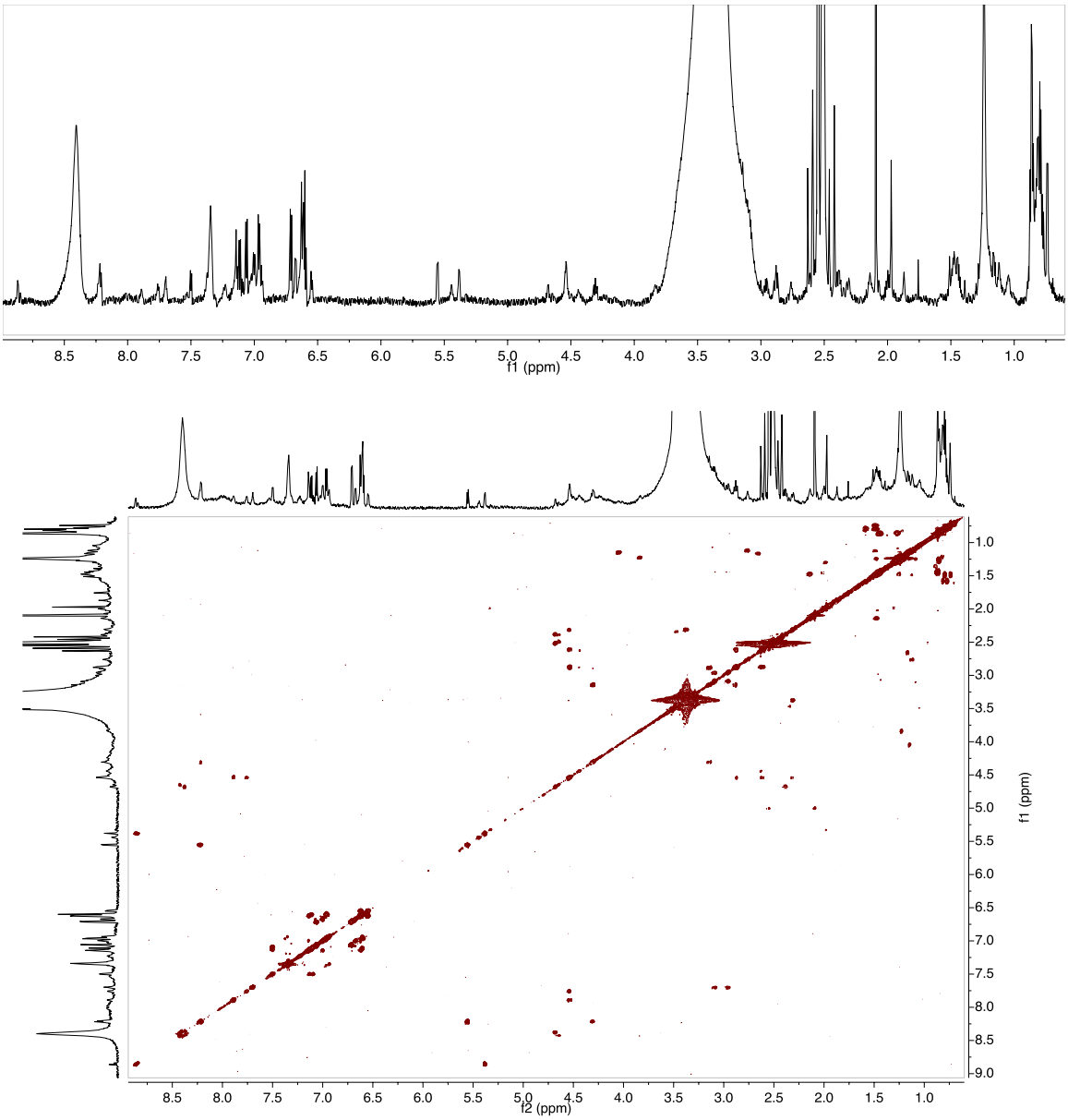

Figure S28. 800 MHz ^{1}H NMR of **16** in $(CD_3)_2SO$ (top). 800 MHz COSY spectra of **16** in $(CD_3)_2SO$ (bottom).

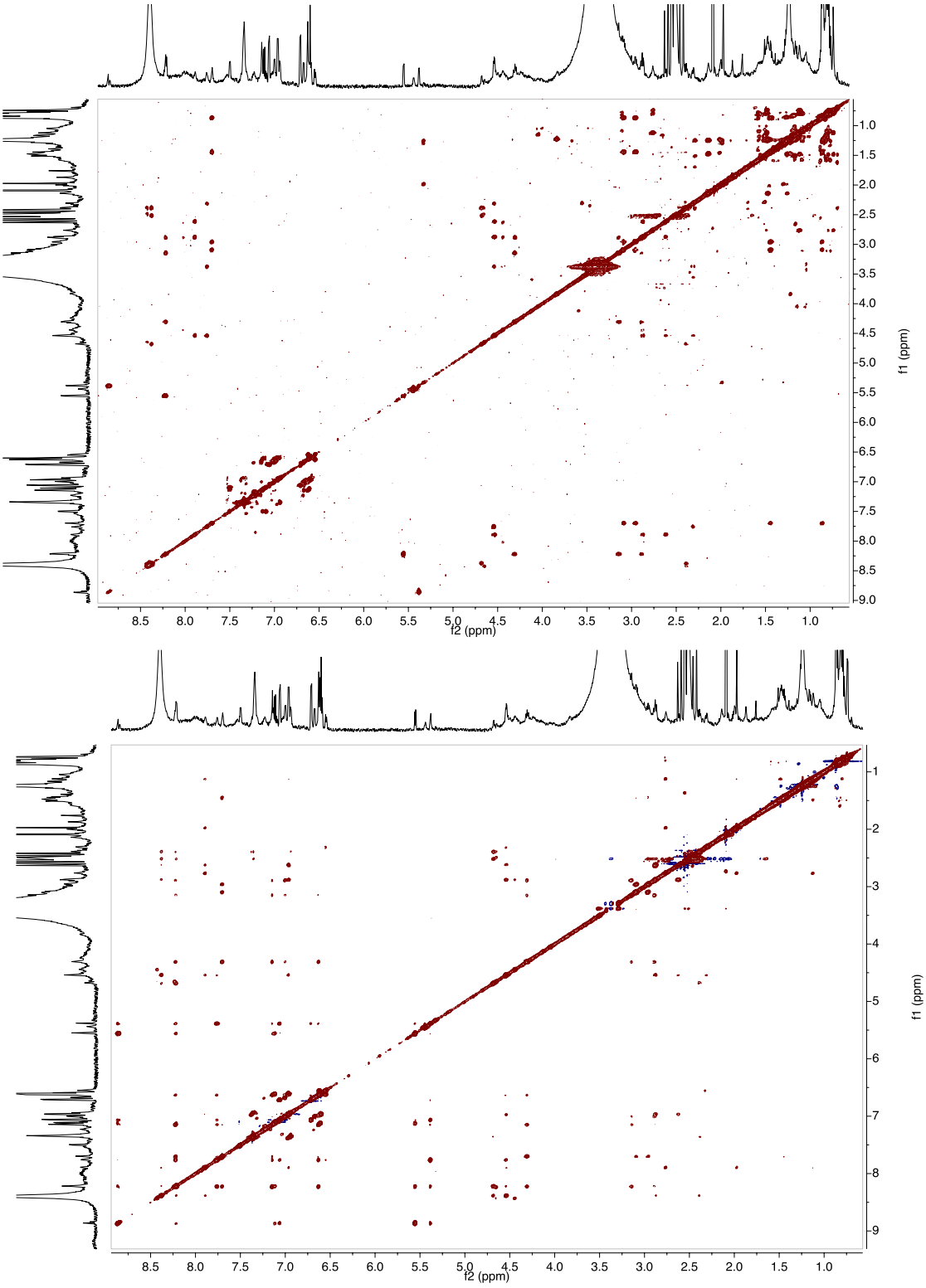

Figure S29. 800 MHz TOCSY spectra of **16** in $(CD_3)_2SO$ (top). 800 MHz NOESY spectra of **16** in $(CD_3)_2SO$ (bottom).

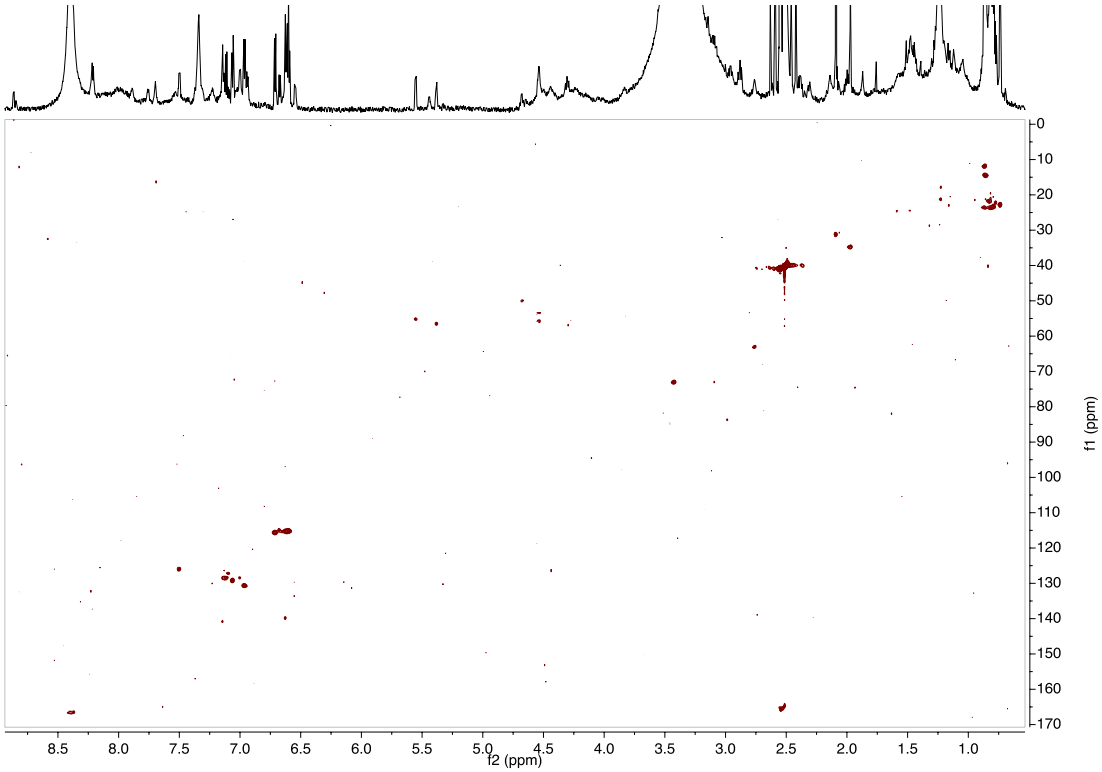

Figure S30. 800 MHz HSQC spectra of **16** in $(CD_3)_2SO$ (top).

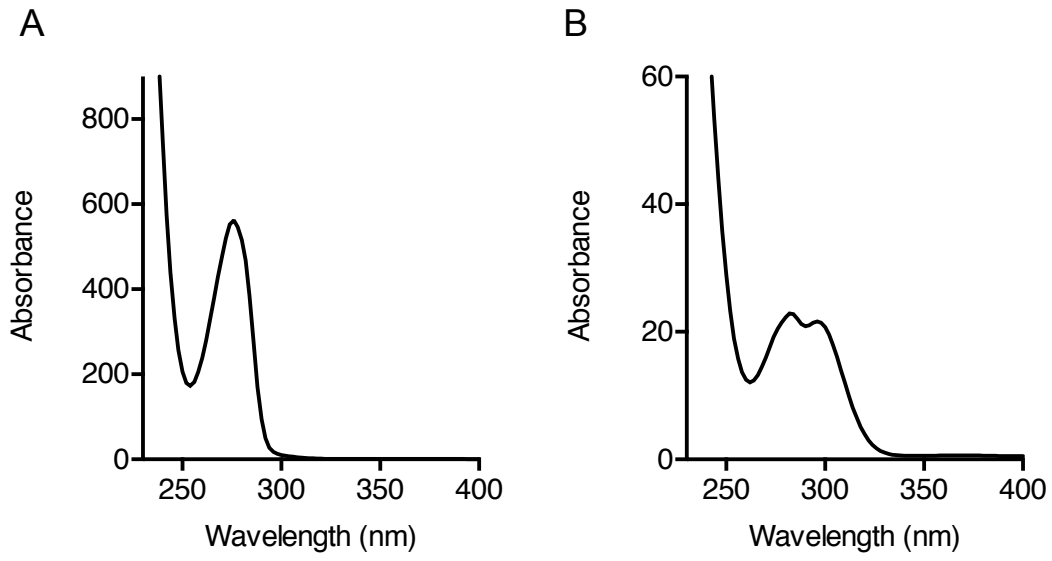

Figure S31. UV-Vis spectra for A) substrate **15**; B) product **16**.

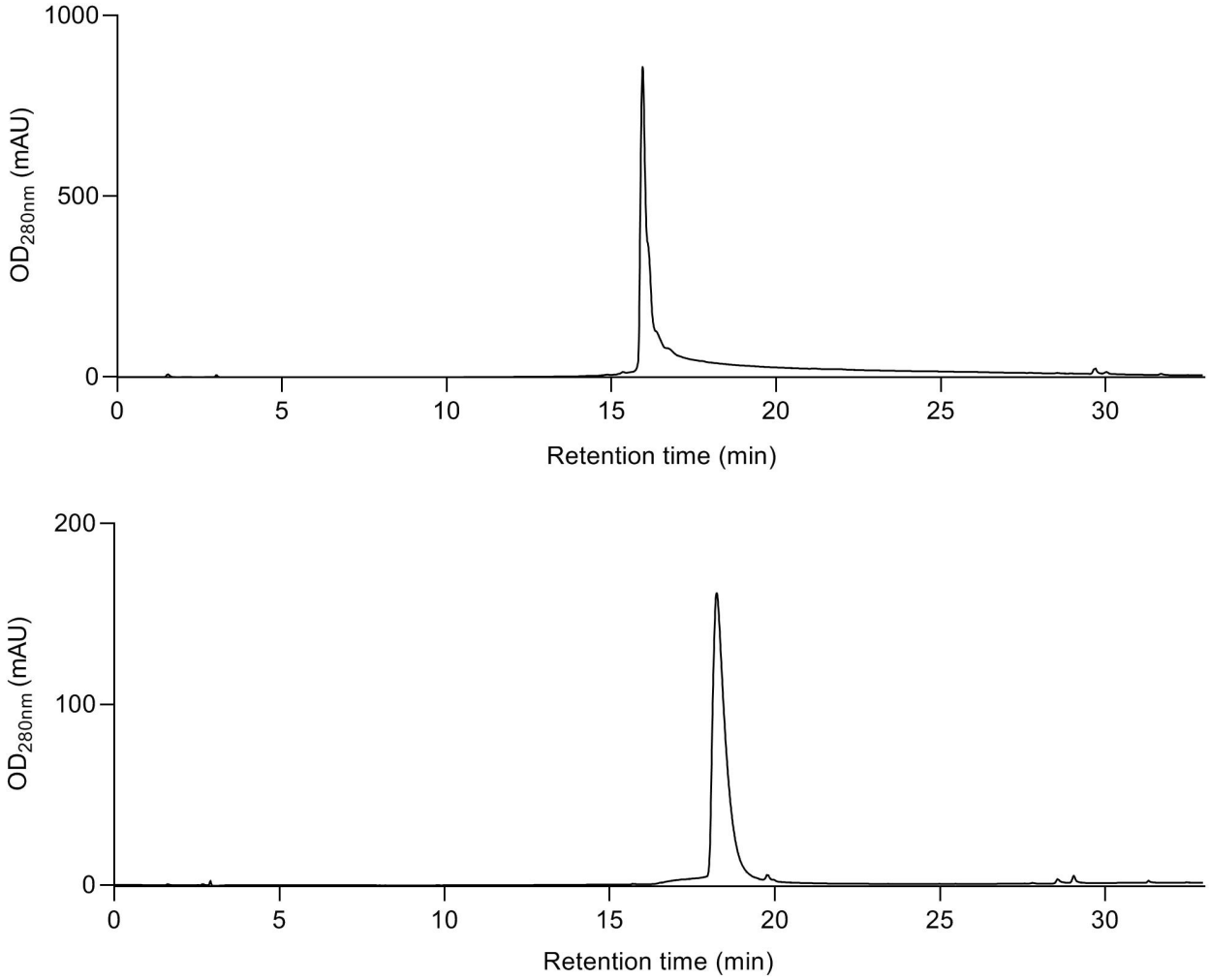

Figure S32. HPLC-MS analysis of pure peptide containing D-tyrosine as AA2 and *ortho*-$^{2}H_2$-D-Hpg as AA4 (precursor to **19**) as a 7mer hydrazide (top) and as a CoA thioester adduct (bottom).

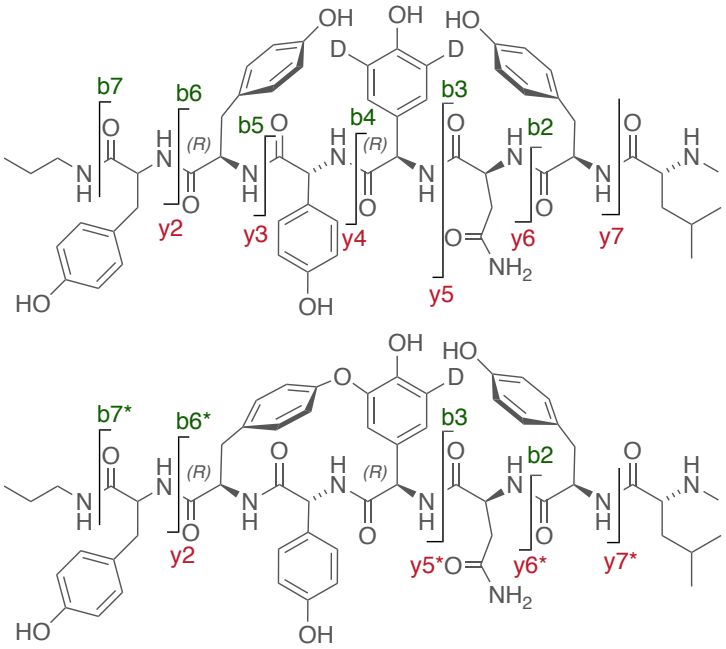

Figure S33. HR-MS/MS for peptide substrate containing D-tyrosine as AA2 and *ortho*-$^{2}H_2$-D-Hpg as AA4 and its product (**19**) upon reaction with OxyB.

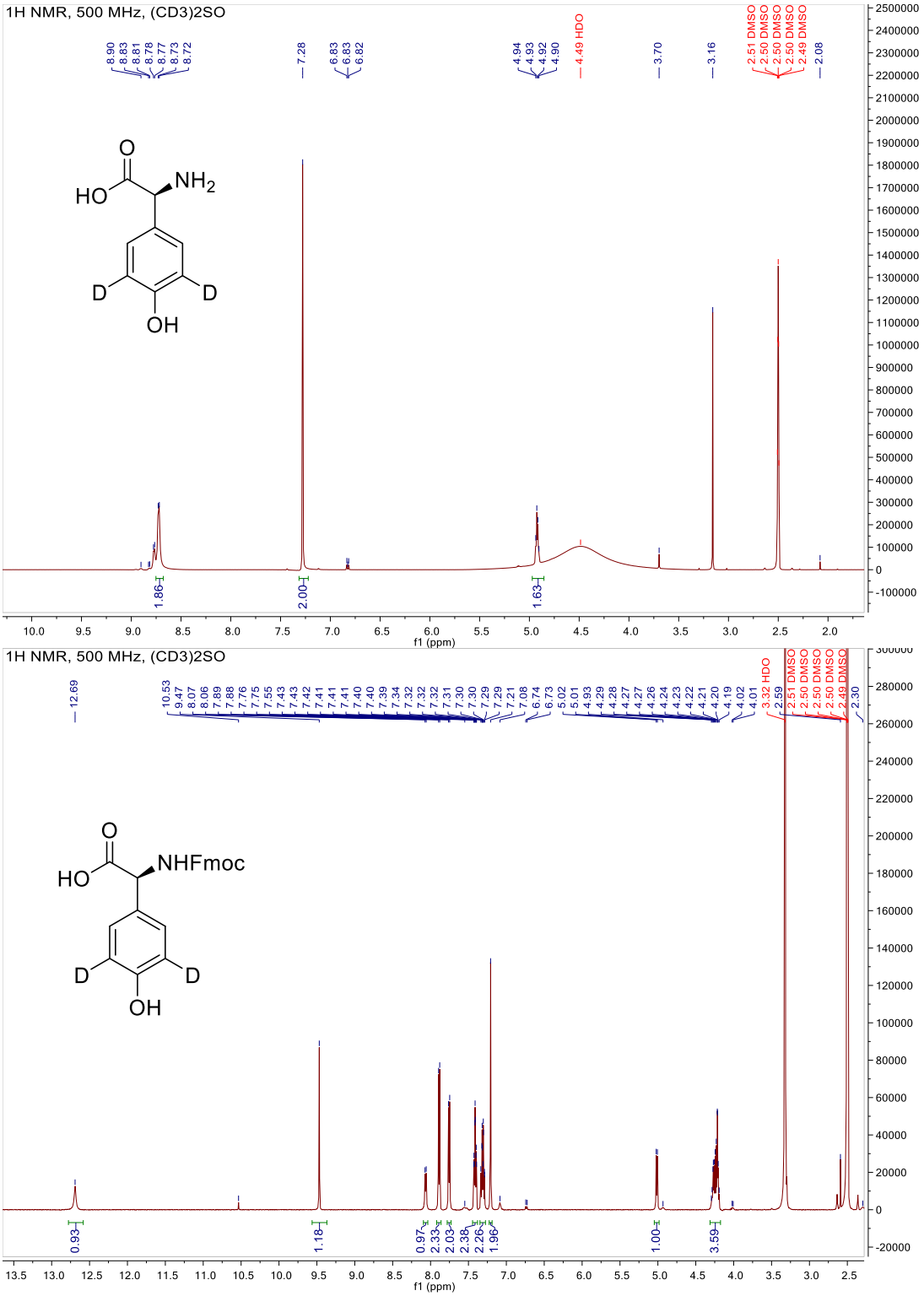

Figure S34. ^{1}H NMR spectrum of L-3,5-$^{2}H_2$-4-hydroxyphenylglycine (top) and *N*-Fmoc- L-3,5-$^{2}H_2$-4-hydroxyphenylglycine (bottom).

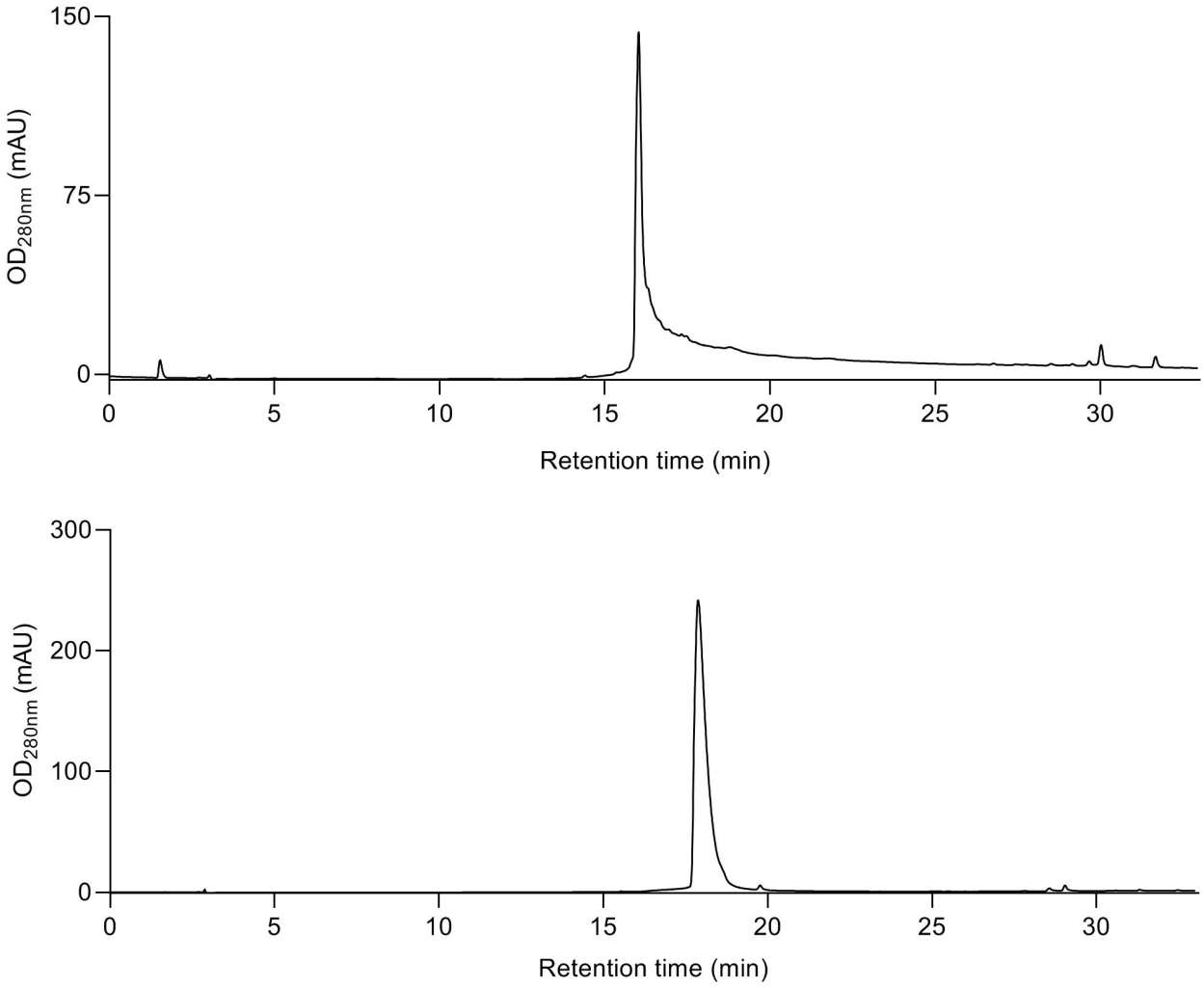

Figure S35. HPLC-MS analysis of pure peptide containing D-Tyr2 as AA2 and *ortho*-$^{2}H_{2}$-L-Hpg4 (precursor to **23**, **24**) as a 7mer hydrazide (top) and as a CoA thioester adduct (bottom).

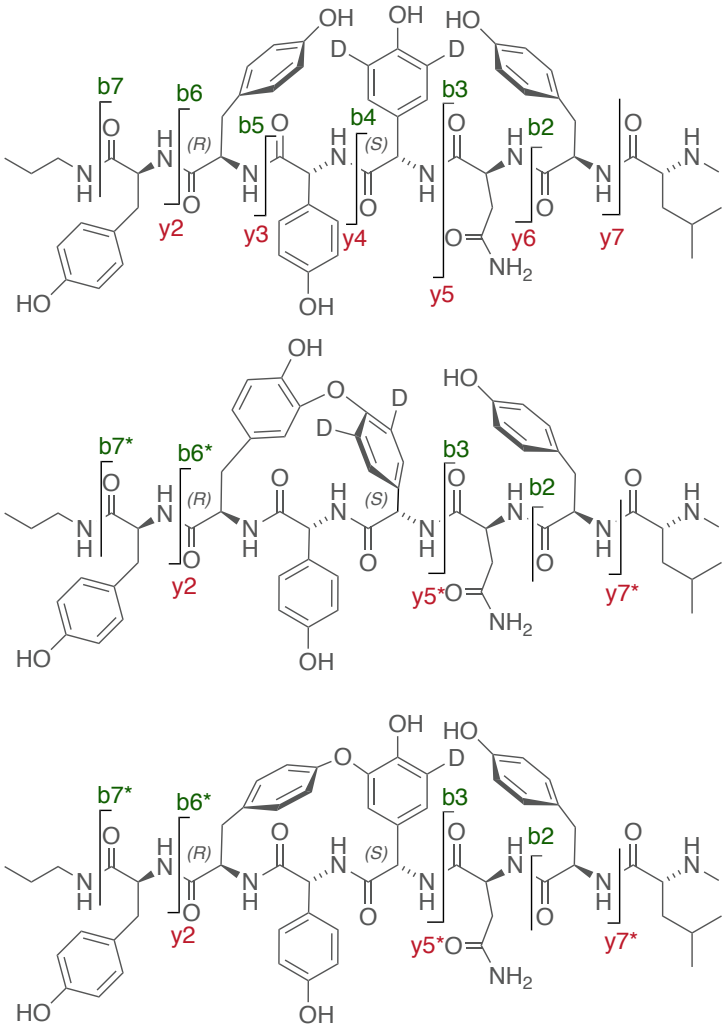

Figure S36. HR-MS/MS data for starting material containing D-Tyr as AA2 and 3,5-$^{2}H_2$-L-Hpg as AA4 and products **23**, **24**.

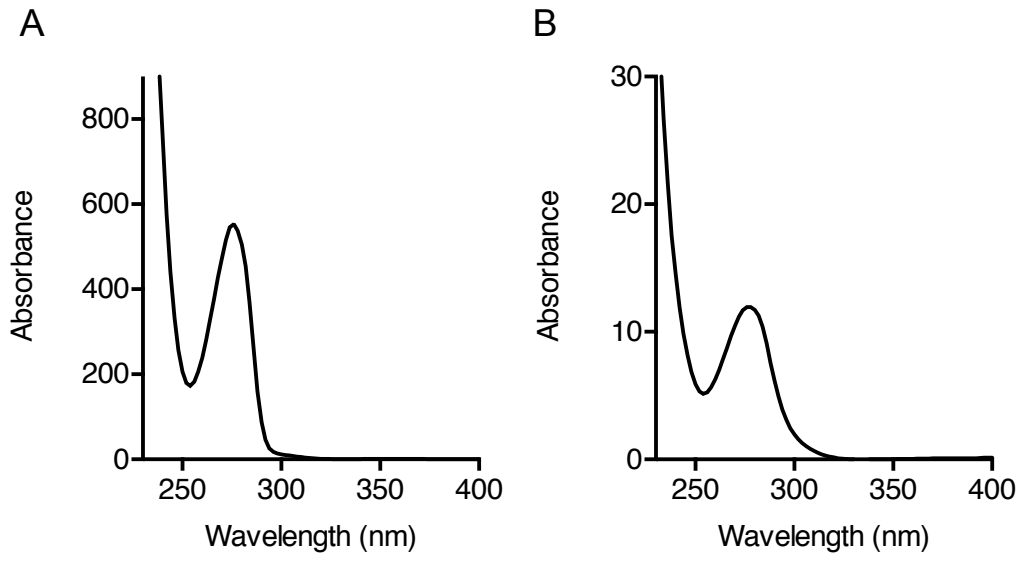

Figure S37. UV-Vis spectrum of A) substrate **20**; B) products **21**, **22**.

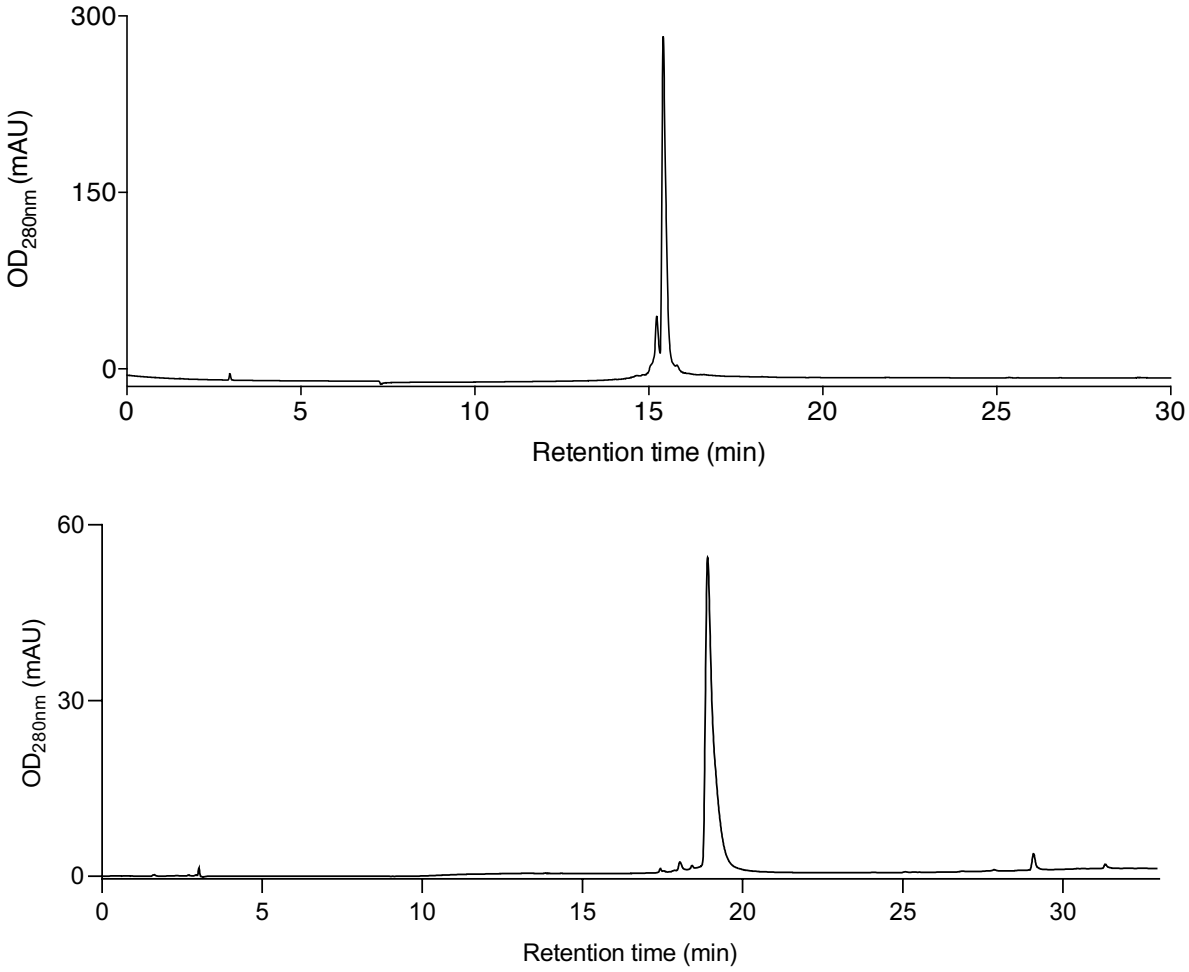

Figure S38. HPLC-MS analysis of pure **25** as a 7mer hydrazide (top) and as a CoA thioester adduct (bottom).

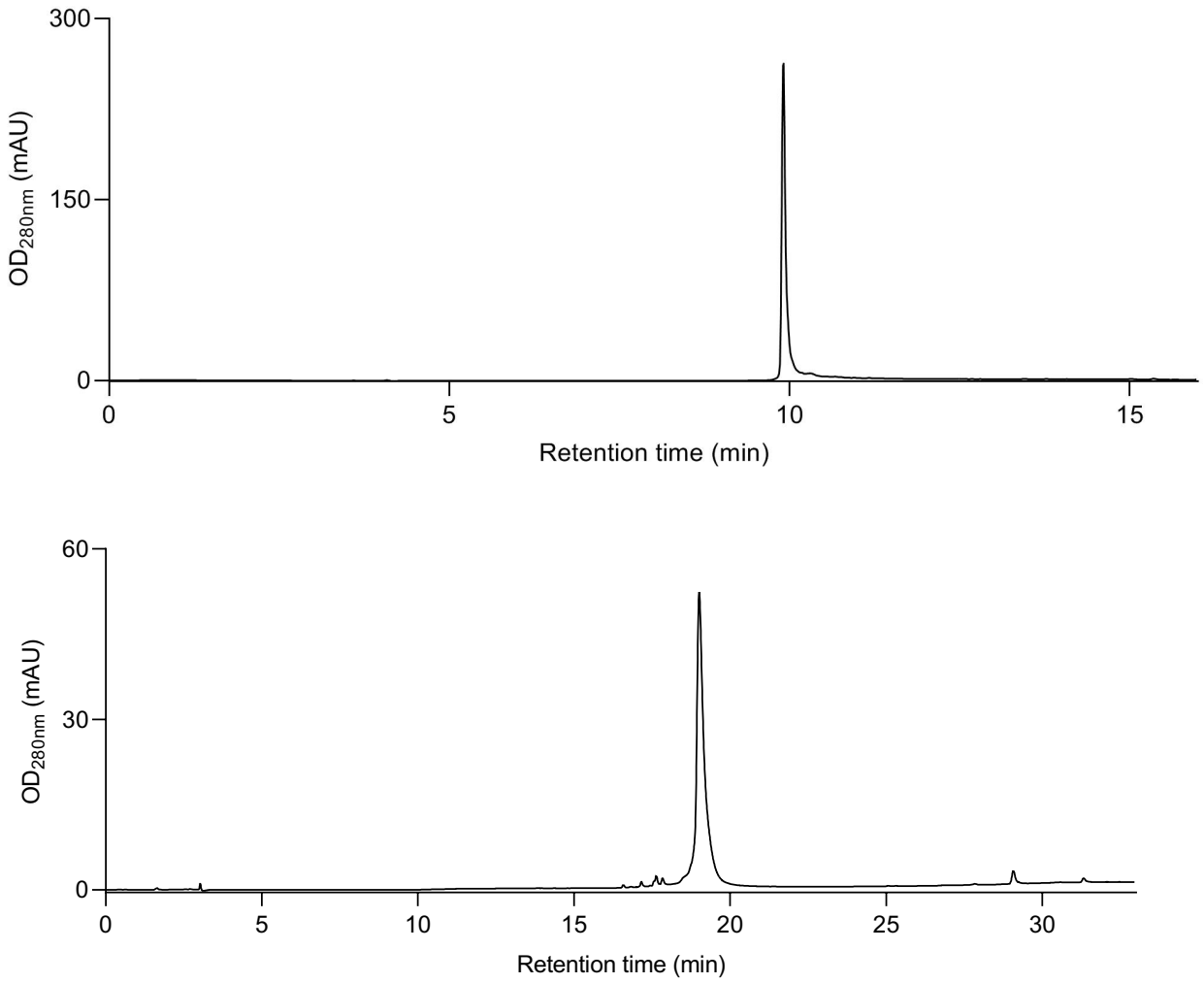

Figure S39. HPLC-MS analysis of pure **27** as a 7mer hydrazide (top) and as a CoA thioester adduct (bottom).

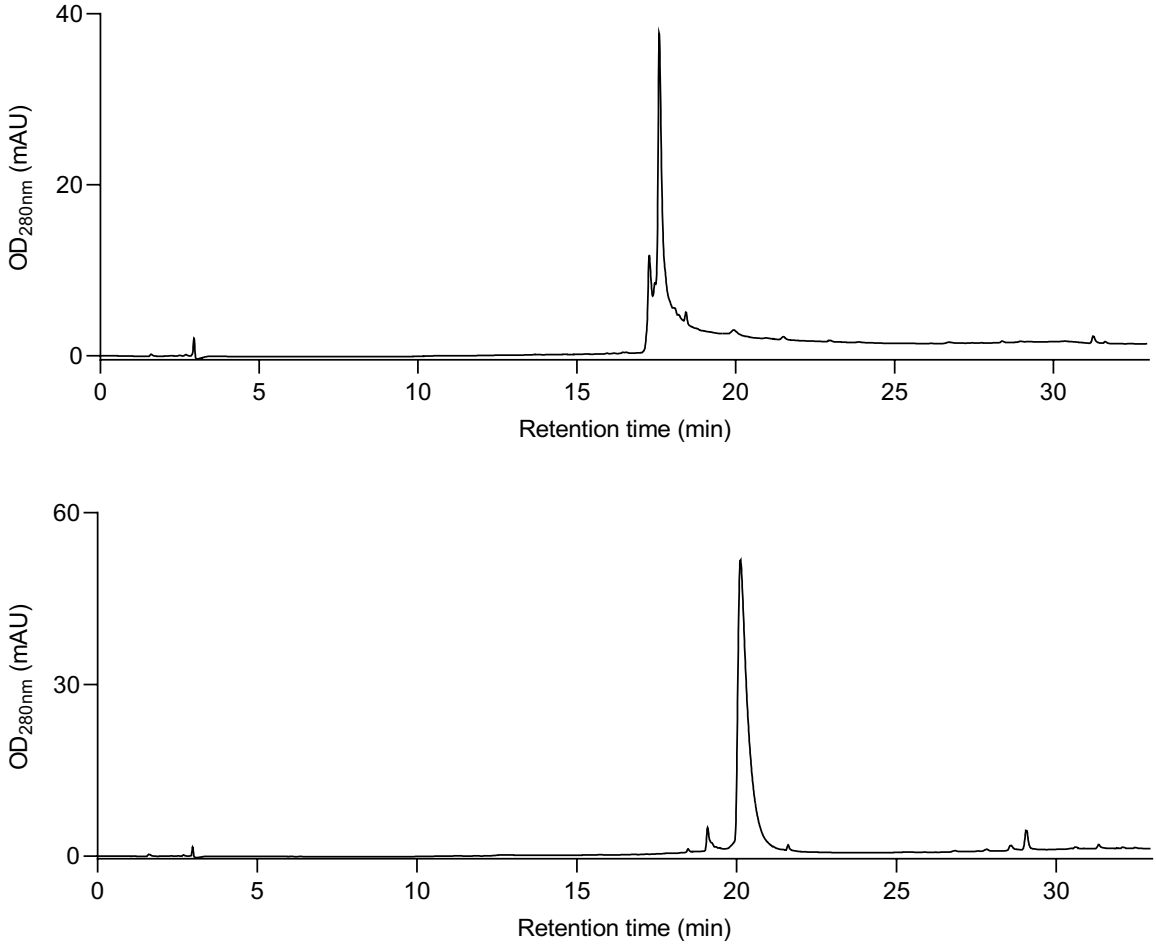

Figure S40. HPLC-MS analysis of pure **32** as a 7mer hydrazide (top) and as a CoA thioester adduct (bottom).

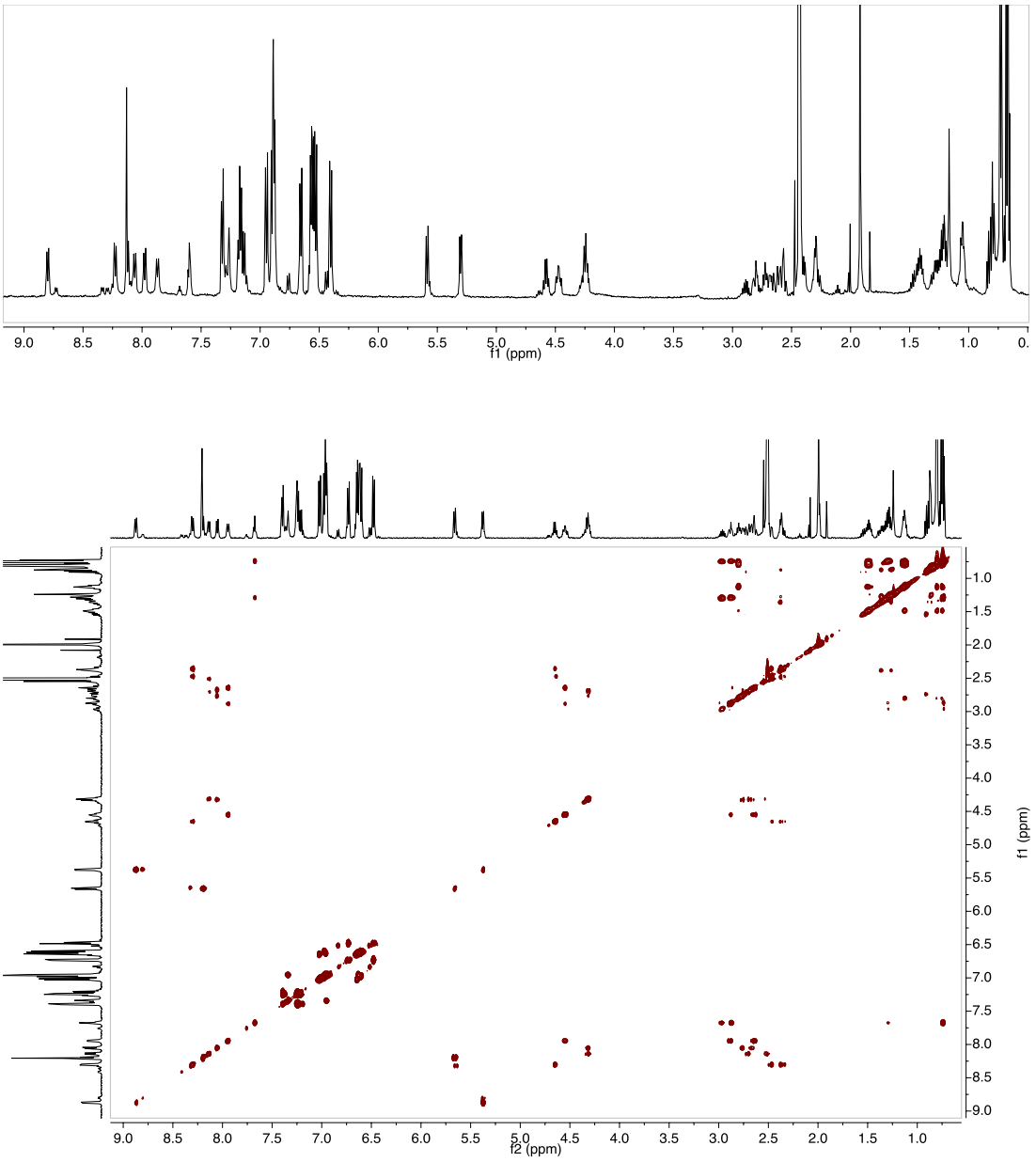

Figure S41. 800 MHz ^{1}H NMR of **25** in $(CD_3)_2SO$ (top). 800 MHz COSY spectra of **25** in $(CD_3)_2SO$ (bottom).

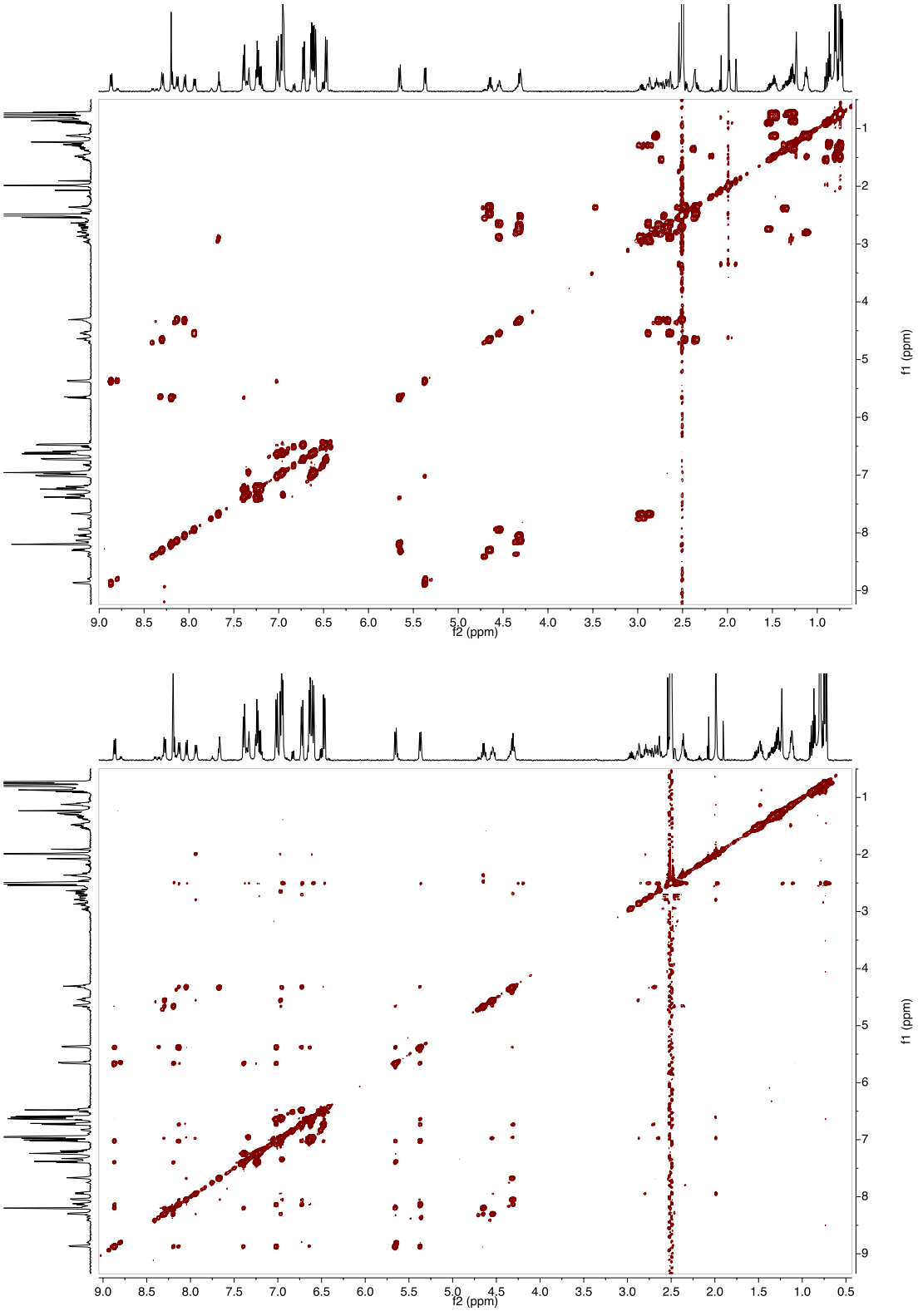

Figure S42. 800 MHz TOCSY spectra of **25** in $(CD_3)_2SO$ (top). 800 MHz NOESY spectra of **25** in $(CD_3)_2SO$ (bottom).

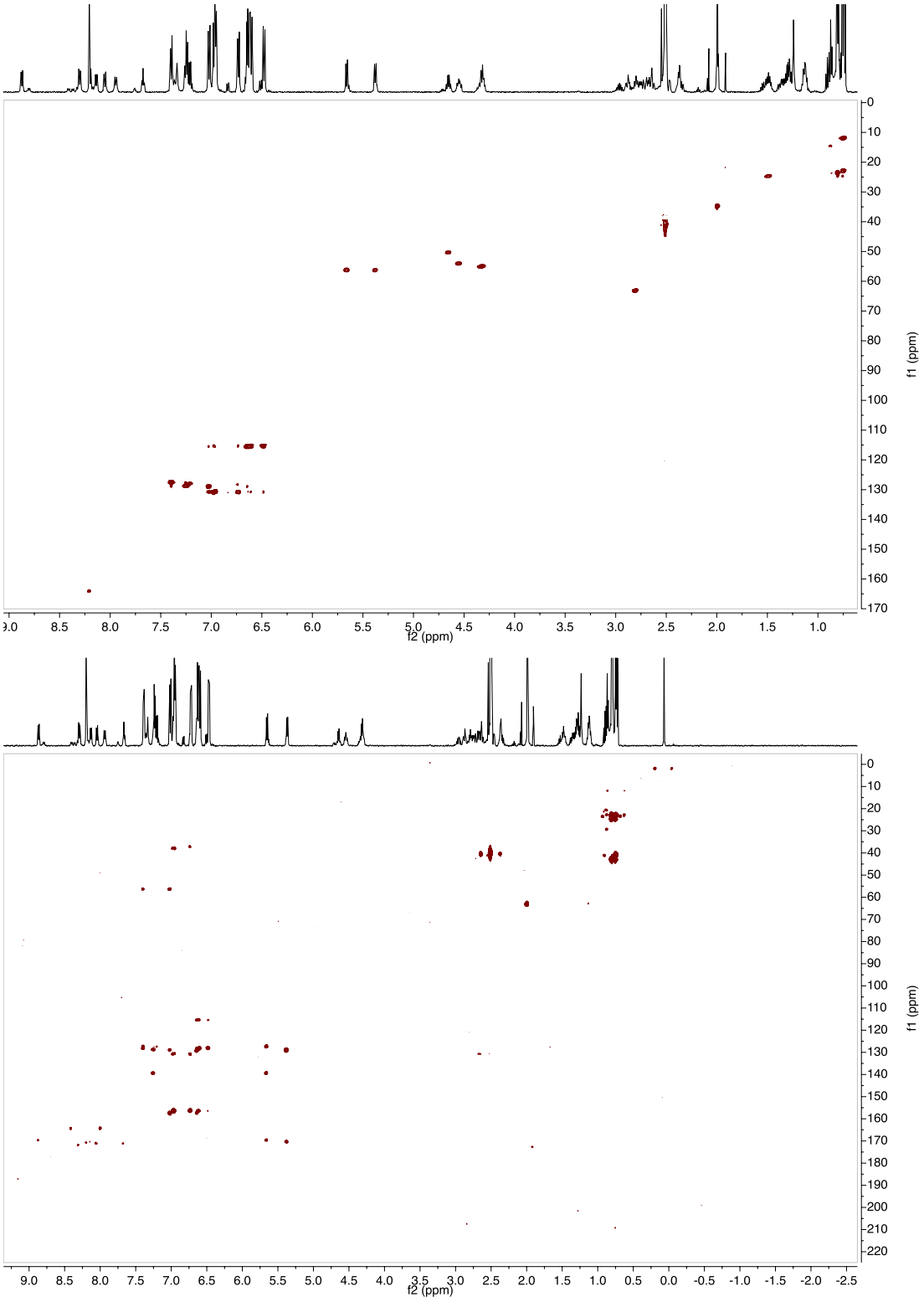

Figure S43. 800 MHz HSQC spectra of **25** in $(CD_3)_2SO$ (top). 800 MHz HMBC spectra of **25** in $(CD_3)_2SO$ (bottom).

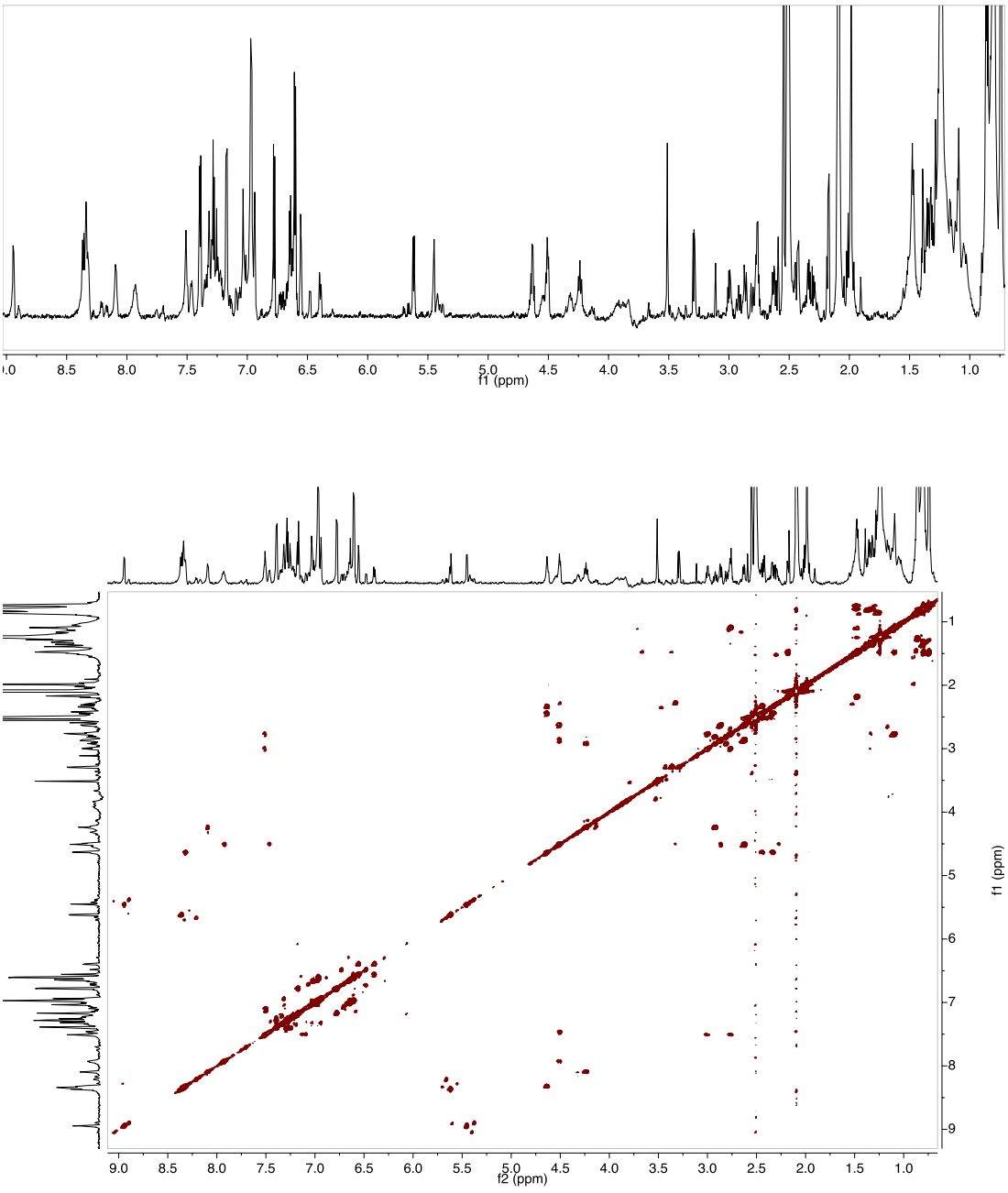

Figure S44. 800 MHz ^{1}H NMR of **26** in $(CD_3)_2SO$ (top). 800 MHz COSY spectra of **26** in $(CD_3)_2SO$ (bottom).

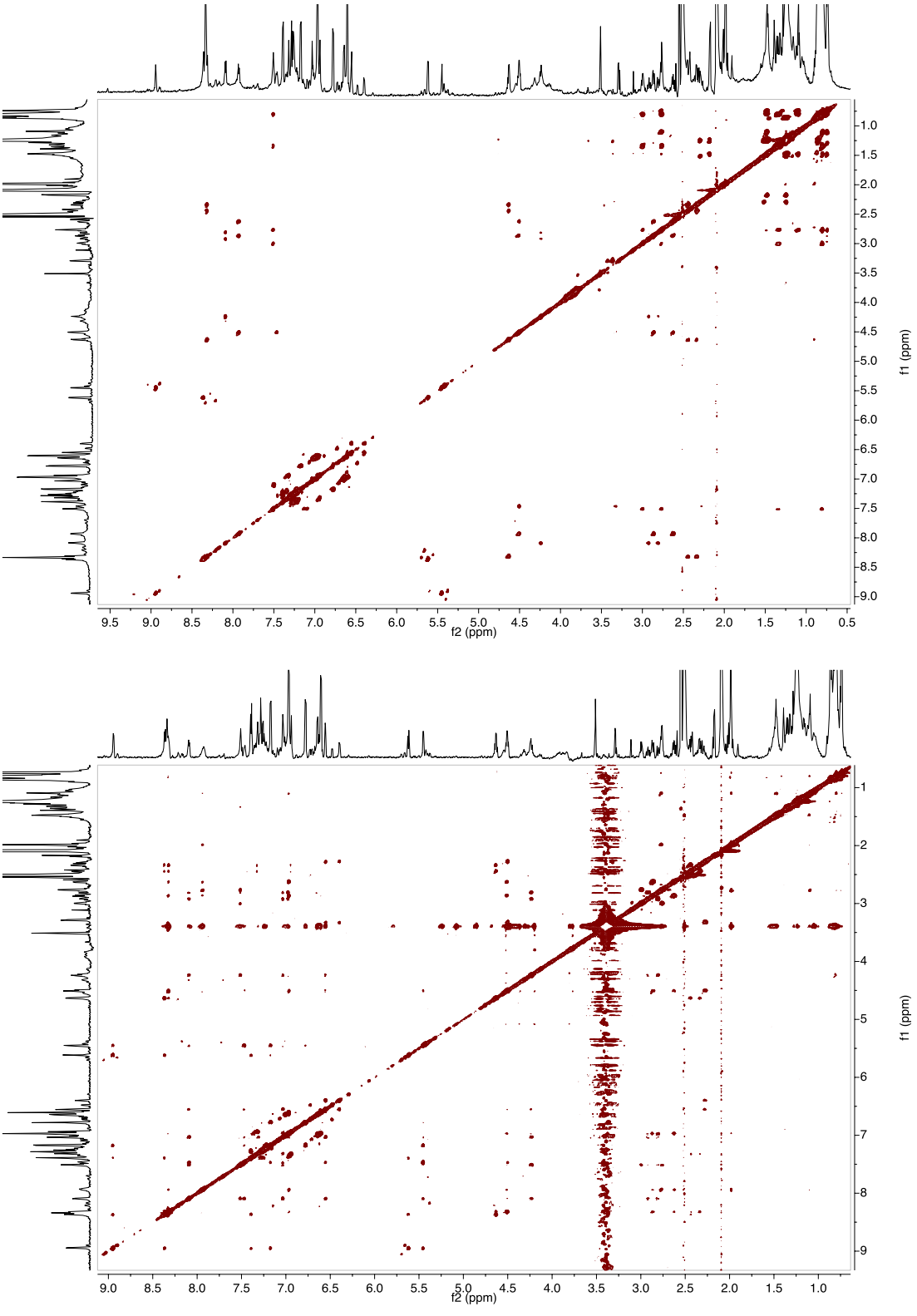

Figure S45. 800 MHz TOCSY of **26** in $(CD_3)_2SO$ (top). 800 MHz NOESY spectra of **26** in $(CD_3)_2SO$ (bottom).

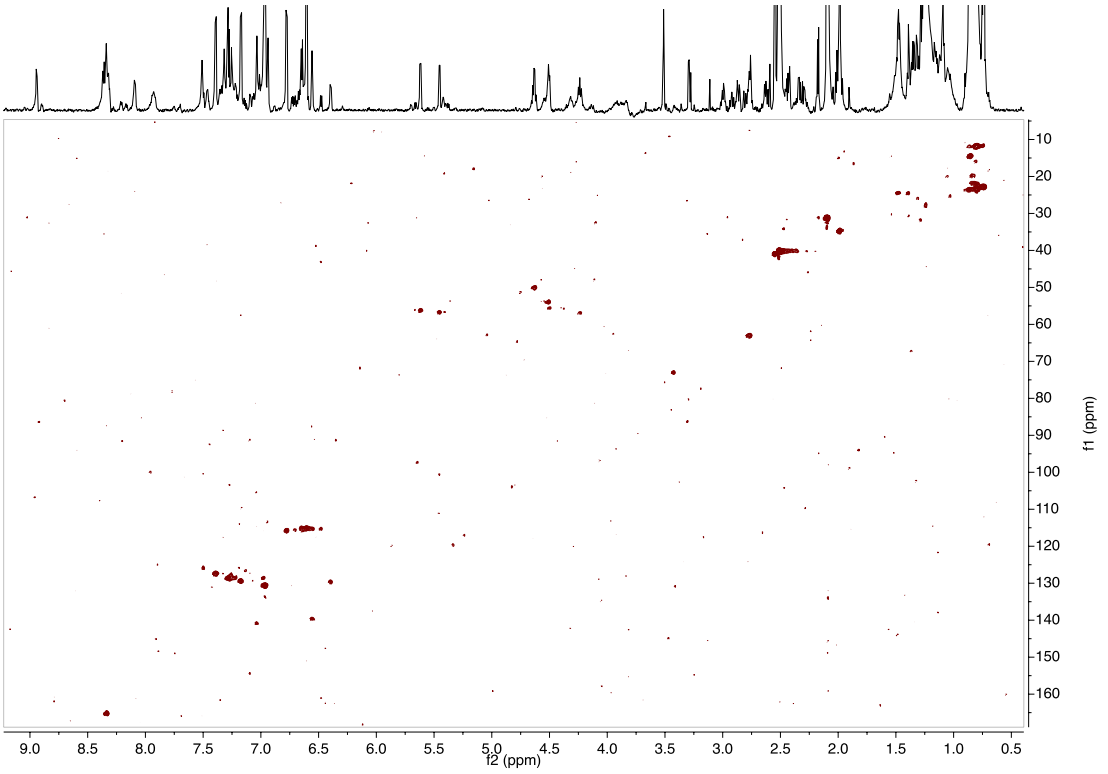

Figure S46. 800 MHz HSQC of **26** in $(CD_3)_2SO$ (top).

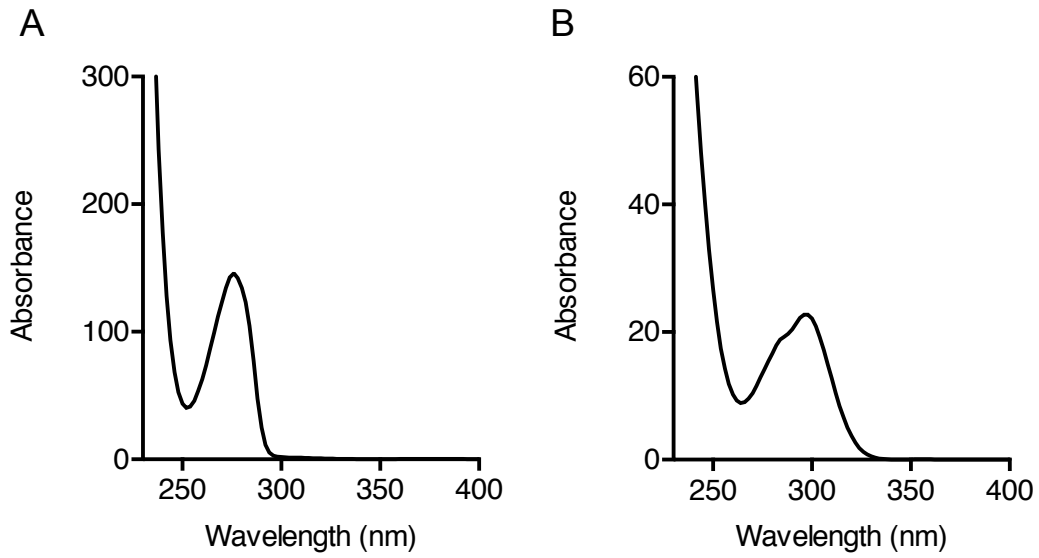

Figure S47. UV-Vis spectra of A) substrate **25**; B) product **26**.

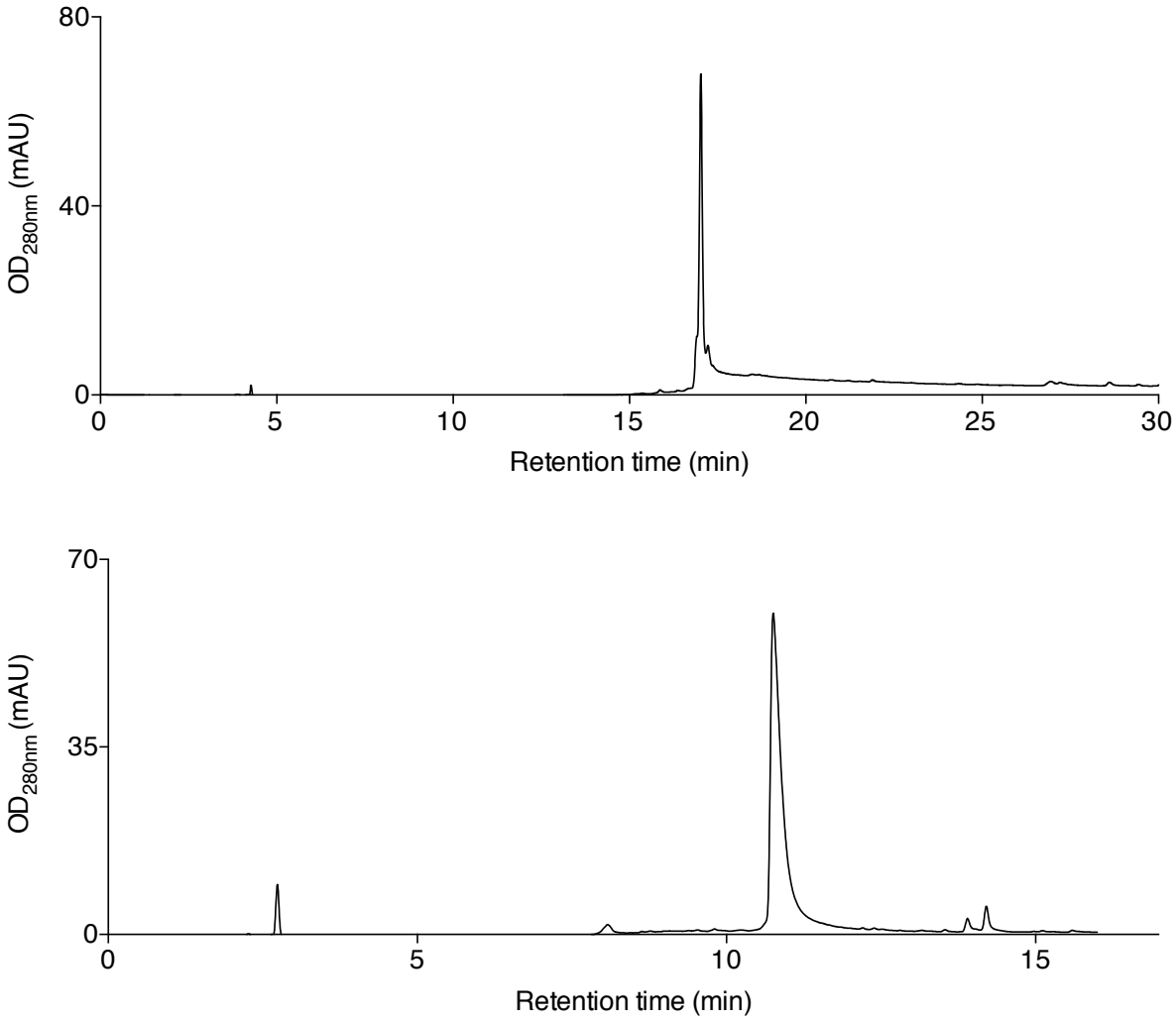

Figure S48. HPLC-MS analysis of pure peptide containing *ortho*-$^{2}H_2$-L-Tyr1, L-Phe2, D-Hpg3, D-Hpg4 as a 7mer hydrazide (top) and as a CoA thioester adduct (bottom).

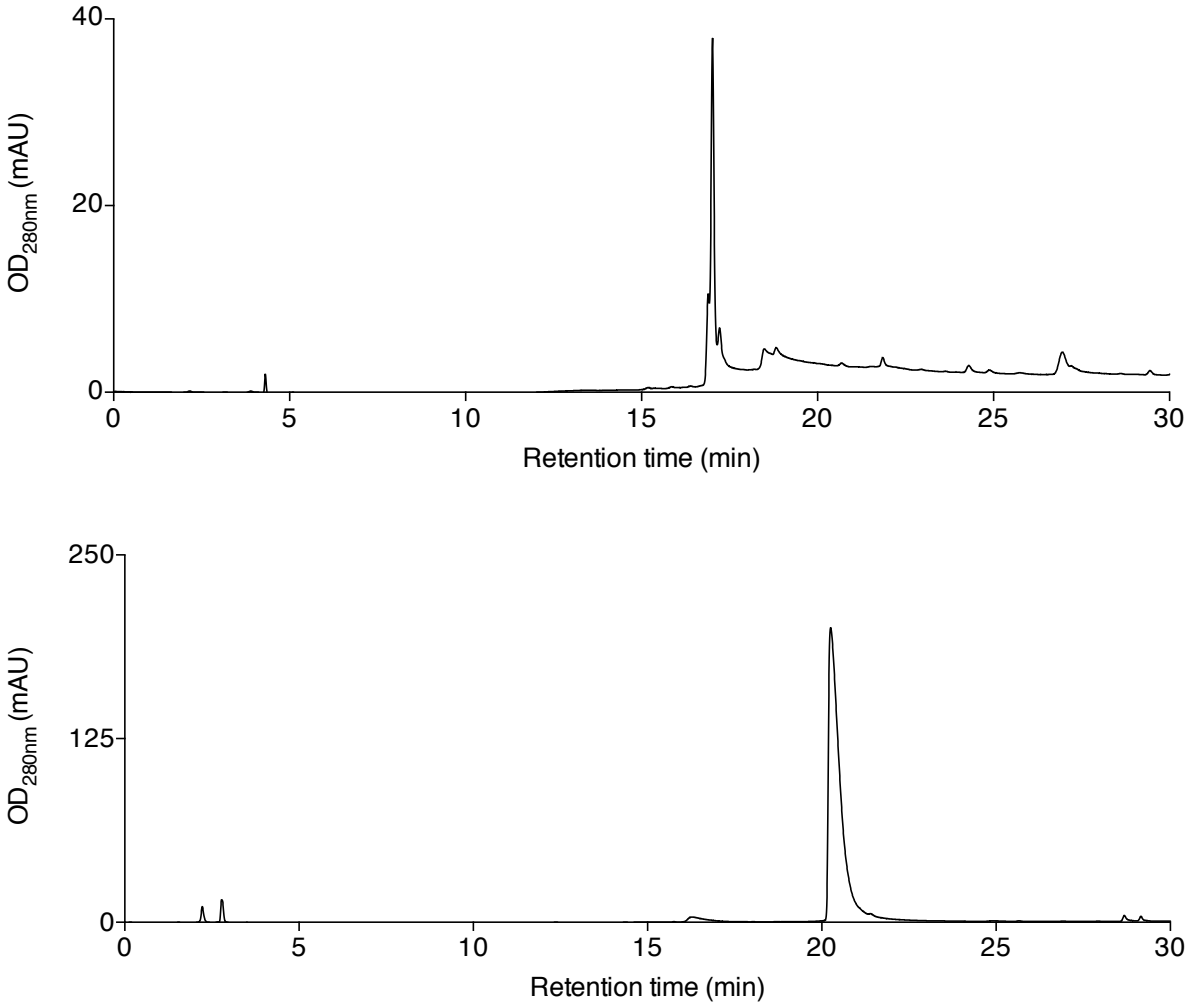

Figure S49. HPLC-MS analysis of pure peptide containing L-Tyr1, ring-$^{2}H_5$-L-Phe2, D-Hpg3, D-Hpg4 as a 7mer hydrazide (top) and as a CoA thioester adduct (bottom).

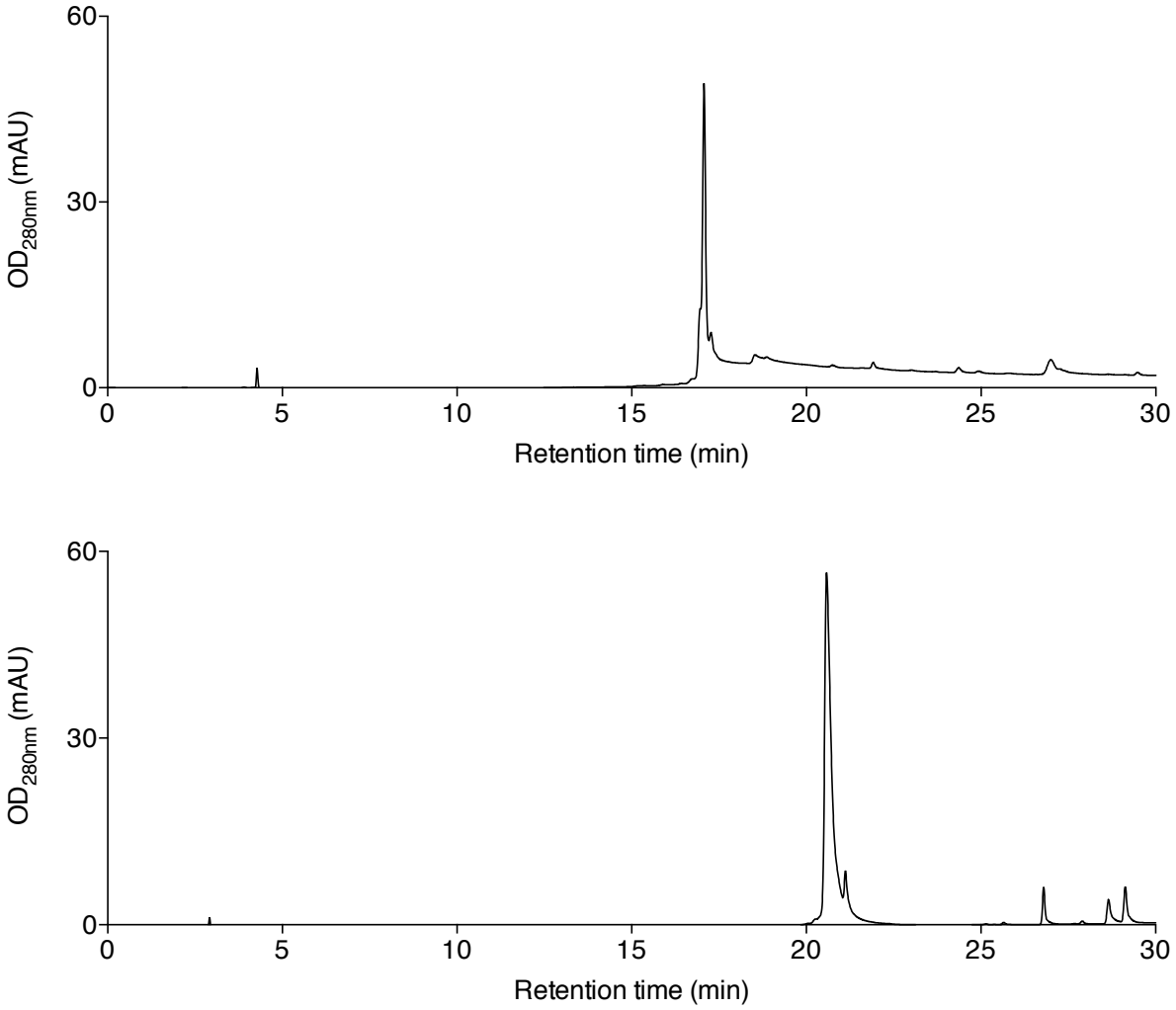

Figure S50. HPLC-MS analysis of pure peptide containing L-Tyr1, L-Phe2, *ortho*-$^{2}H_{2}$-D-Hpg3, D-Hpg4 as a 7mer hydrazide (top) and as a CoA thioester adduct (bottom).

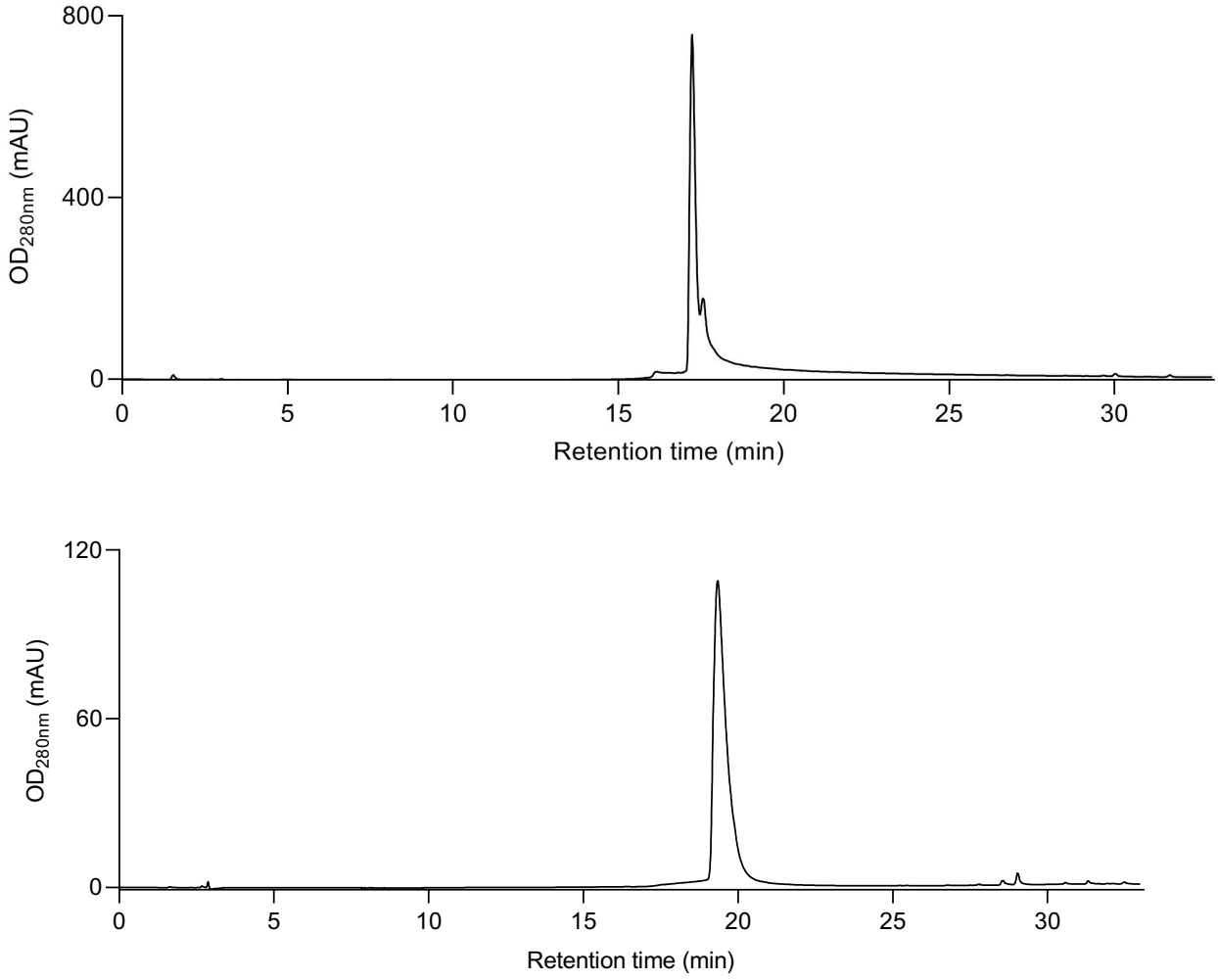

Figure S51. HPLC-MS analysis of pure peptide containing L-Tyr1, L-Phe2, D-Hpg3, *ortho*-$^{2}H_{2}$-D-Hpg4 as a 7mer hydrazide (top) and as a CoA thioester adduct (bottom).

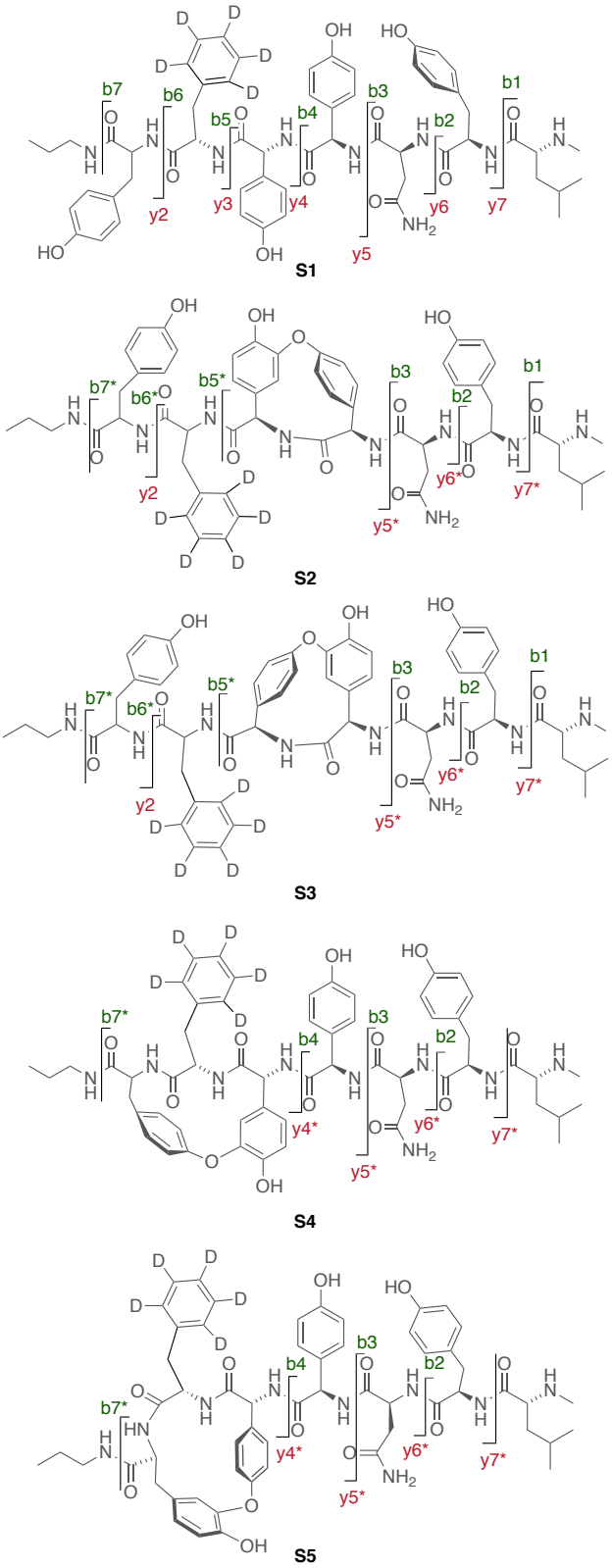

Figure S52. HR-MS/MS for substrate **S1**, with isotopically labelled AA2 ($^{2}H_5$-L-Phe), and products obtained upon reaction with OxyB (-2 Da products: **S2, S3, S4, S5**).

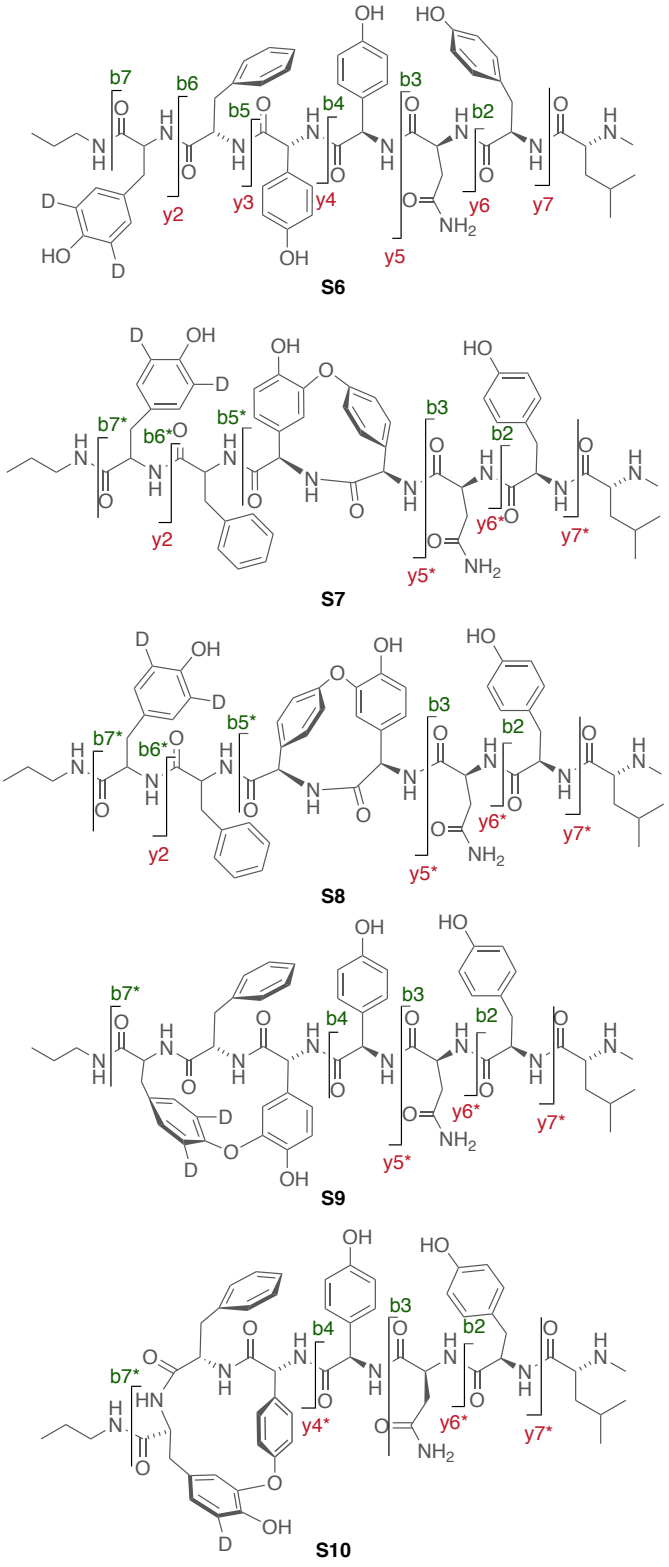

Figure S53. HR-MS/MS for substrate **S6**, with isotopically labelled AA1 (3,5-$^{2}H_2$-L-Tyr), and products obtained upon reaction with OxyB (-2 Da products, **S7**, **S8**, **S9**; -3Da product, **S10**).

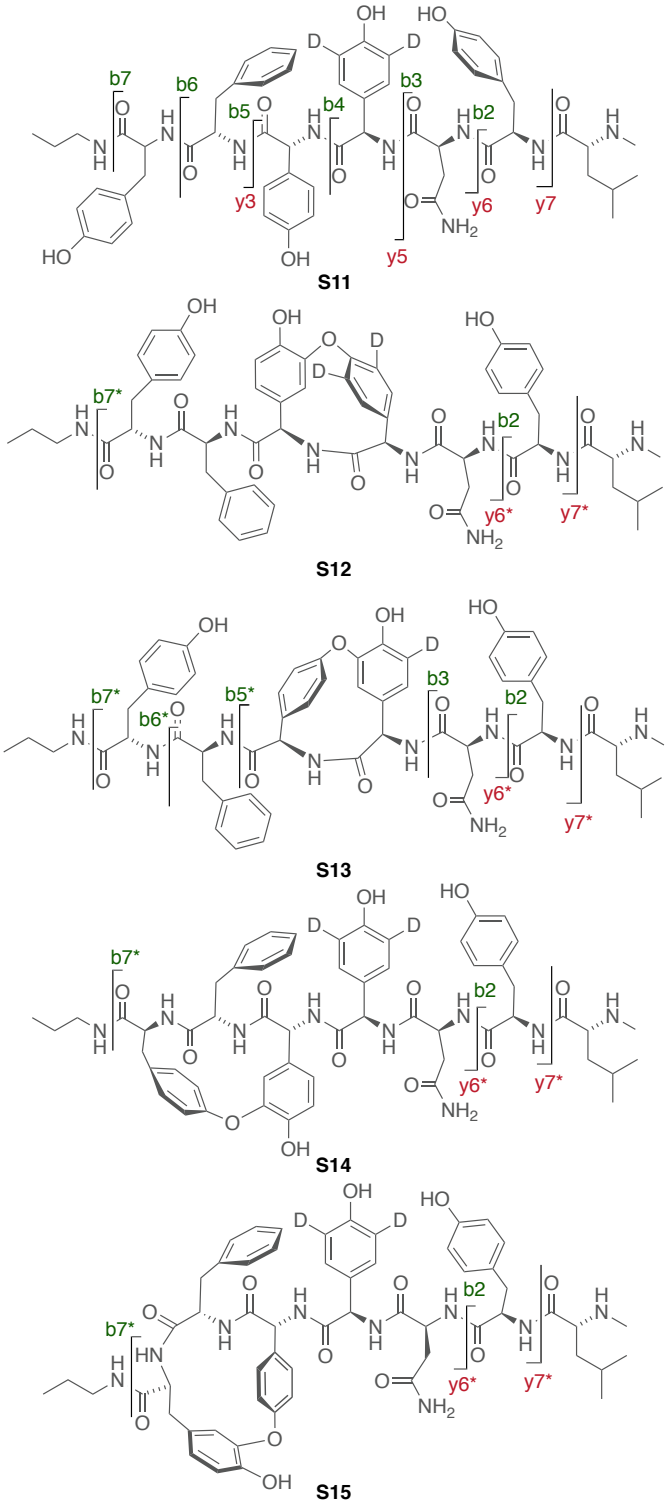

Figure S54. HR-MS/MS for substrate **S11**, with isotopically labelled AA4 (3,5-$^{2}H_2$-D-Hpg4), and products obtained upon reaction with OxyB (-2 Da products, **S12**, **S14**, **S15**; -3Da product, **S13**).

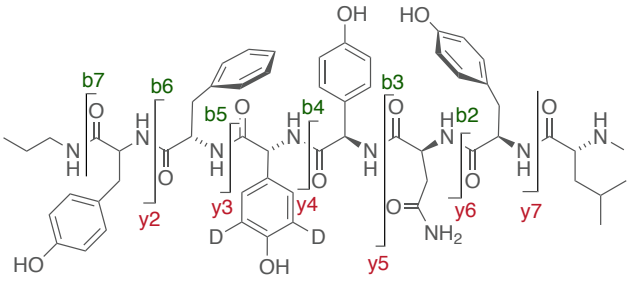

S16

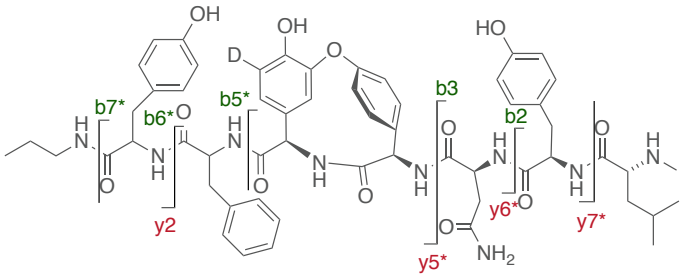

S17

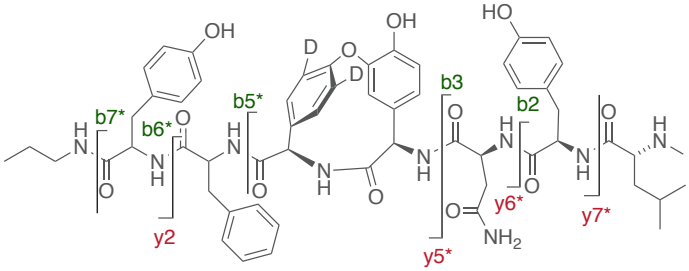

S18

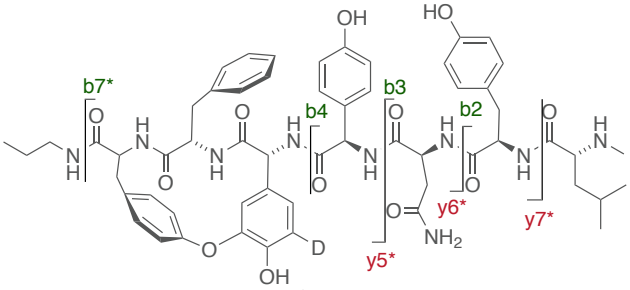

S19

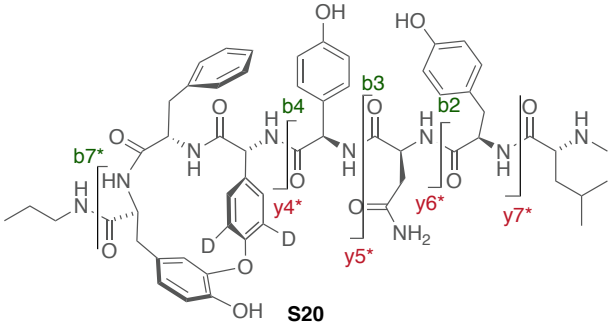

S20

Figure S55. HR-MS/MS for substrate **S16**, with isotopically labelled AA3 (3,5-$^{2}H_2$-D-Hpg), and products obtained upon reaction with OxyB (-2 Da products, **S18**, **S20**; -3Da product, **S17, S19**).

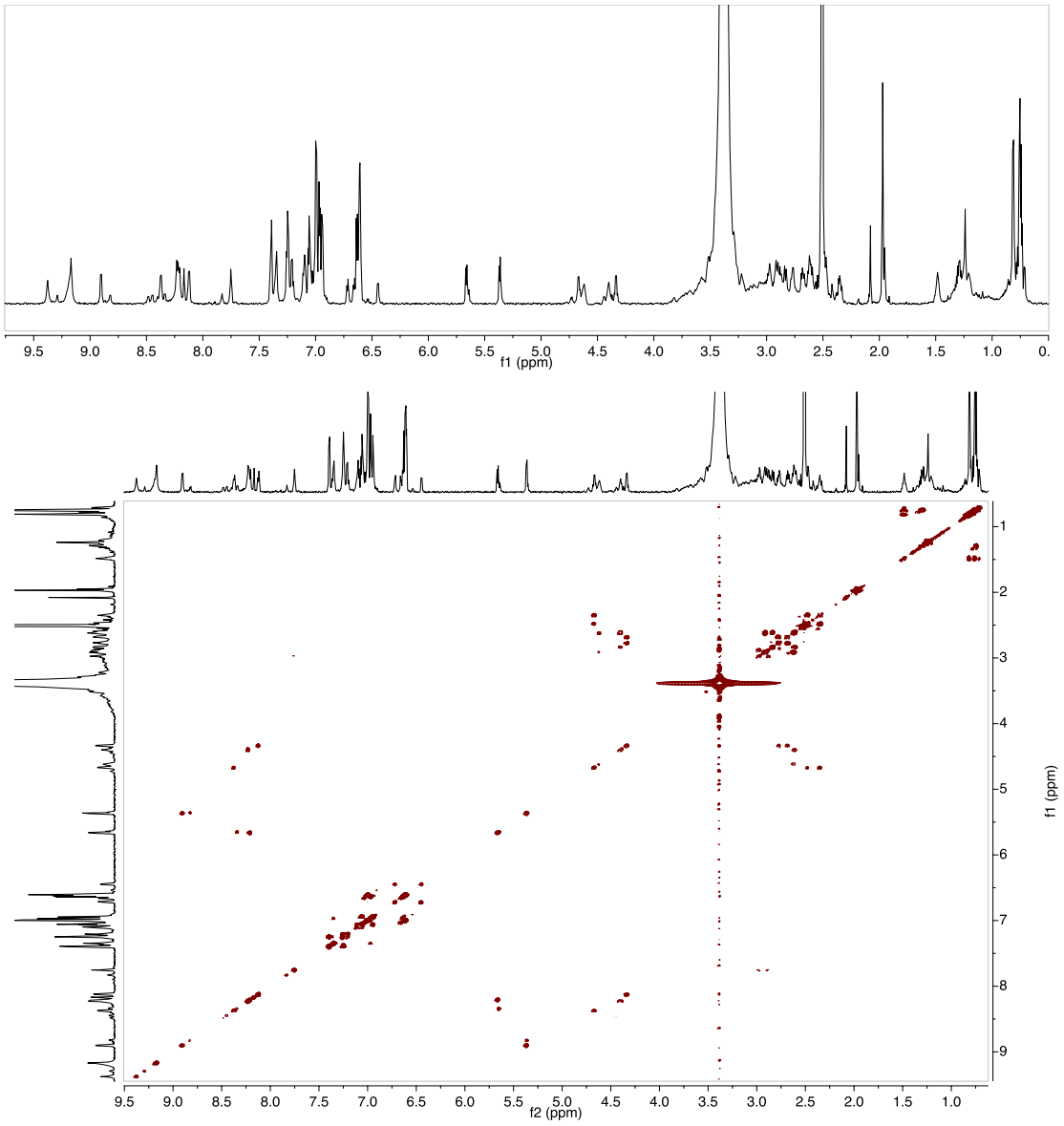

Figure S56. 800 MHz ^{1}H NMR of **32** in $(CD_3)_2SO$ (top). 800 MHz COSY spectra of **32** in $(CD_3)_2SO$ (bottom).

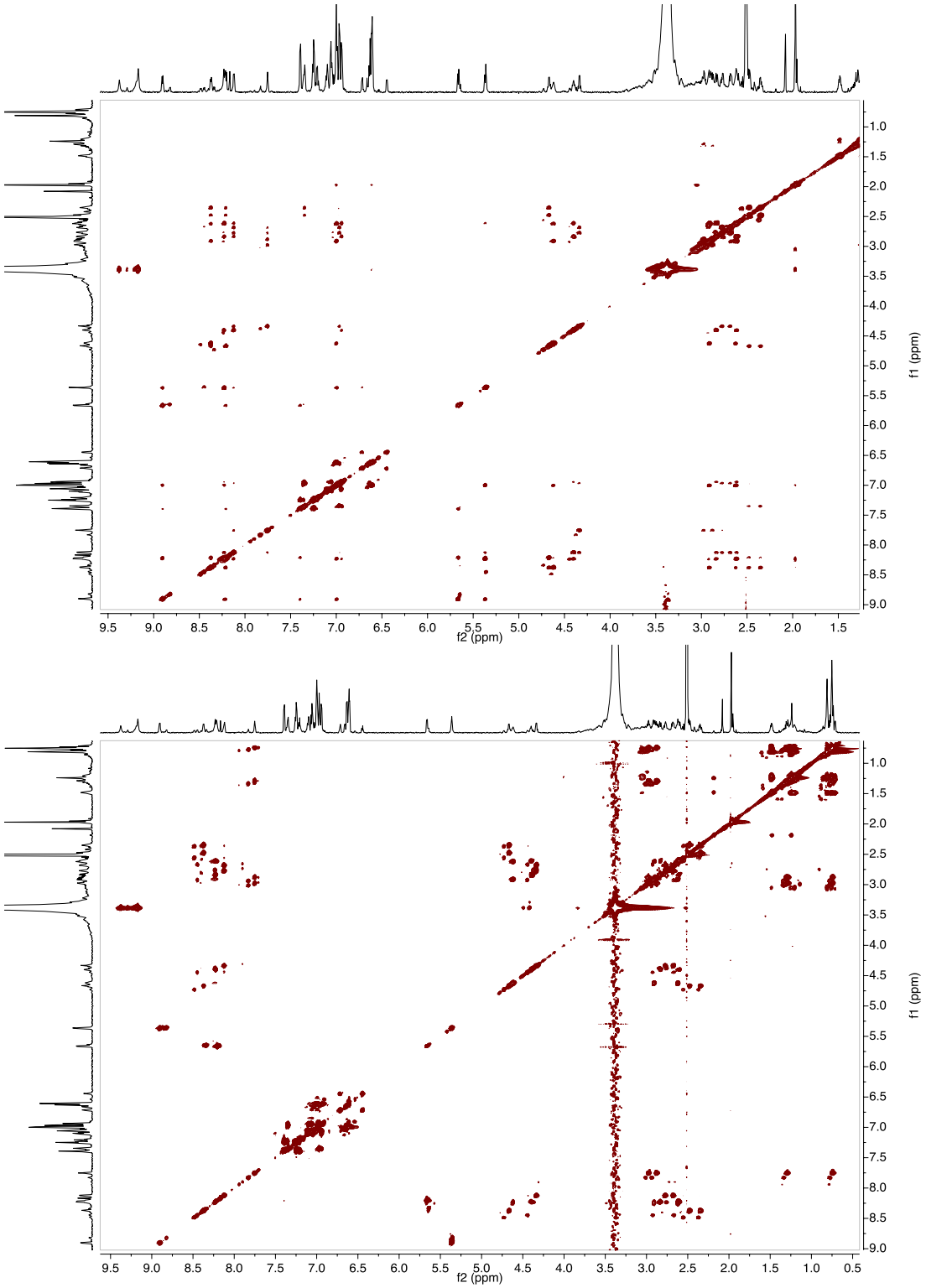

Figure S57. 800 MHz TOCSY spectra of **32** in $(CD_3)_2SO$ (top). 800 MHz NOESY spectra of **32** in $(CD_3)_2SO$ (bottom).

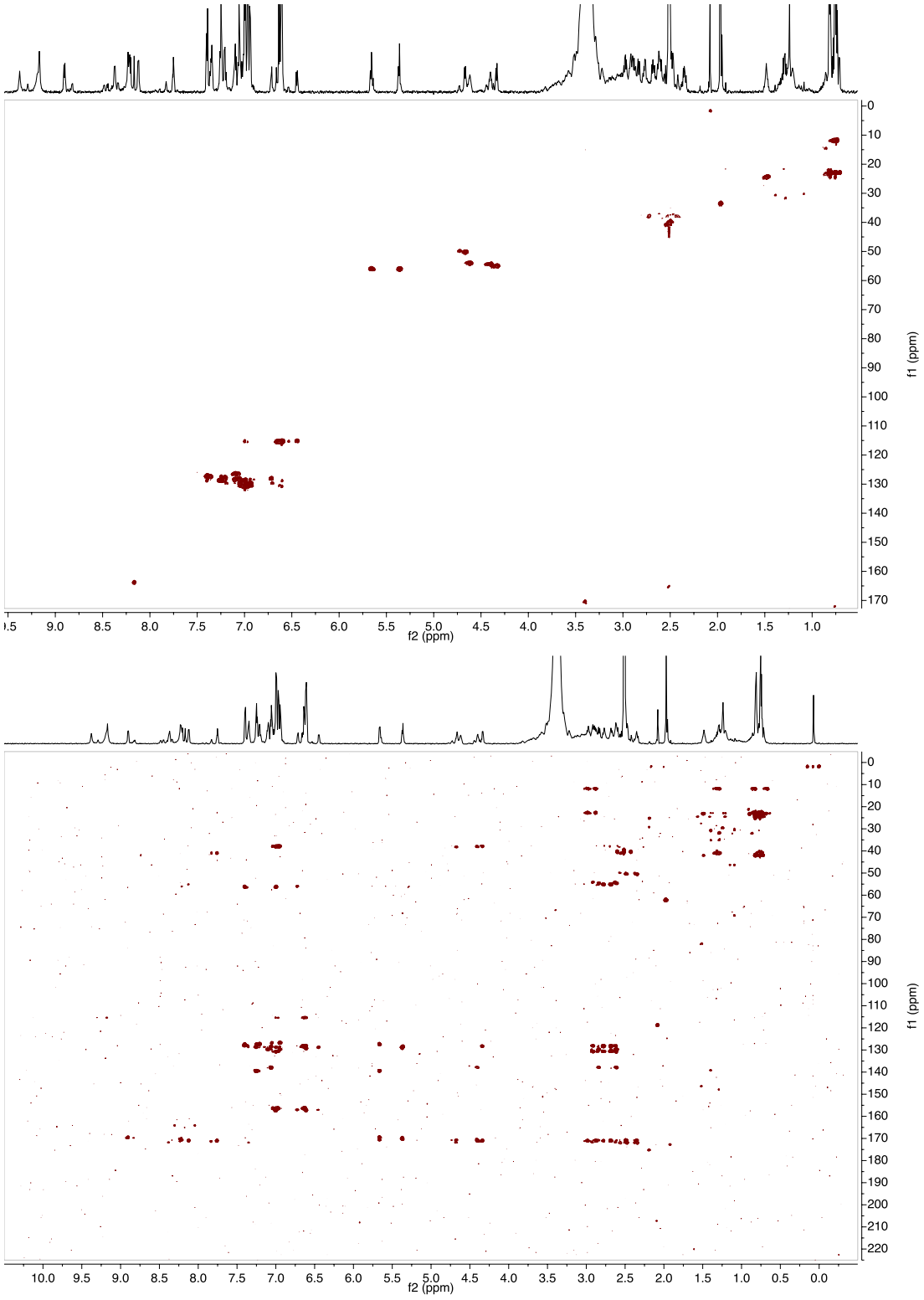

Figure S58. 800 MHz HSQC spectra of **32** in $(CD_3)_2SO$ (top). 800 MHz HMBC spectra of **32** in $(CD_3)_2SO$ (bottom).

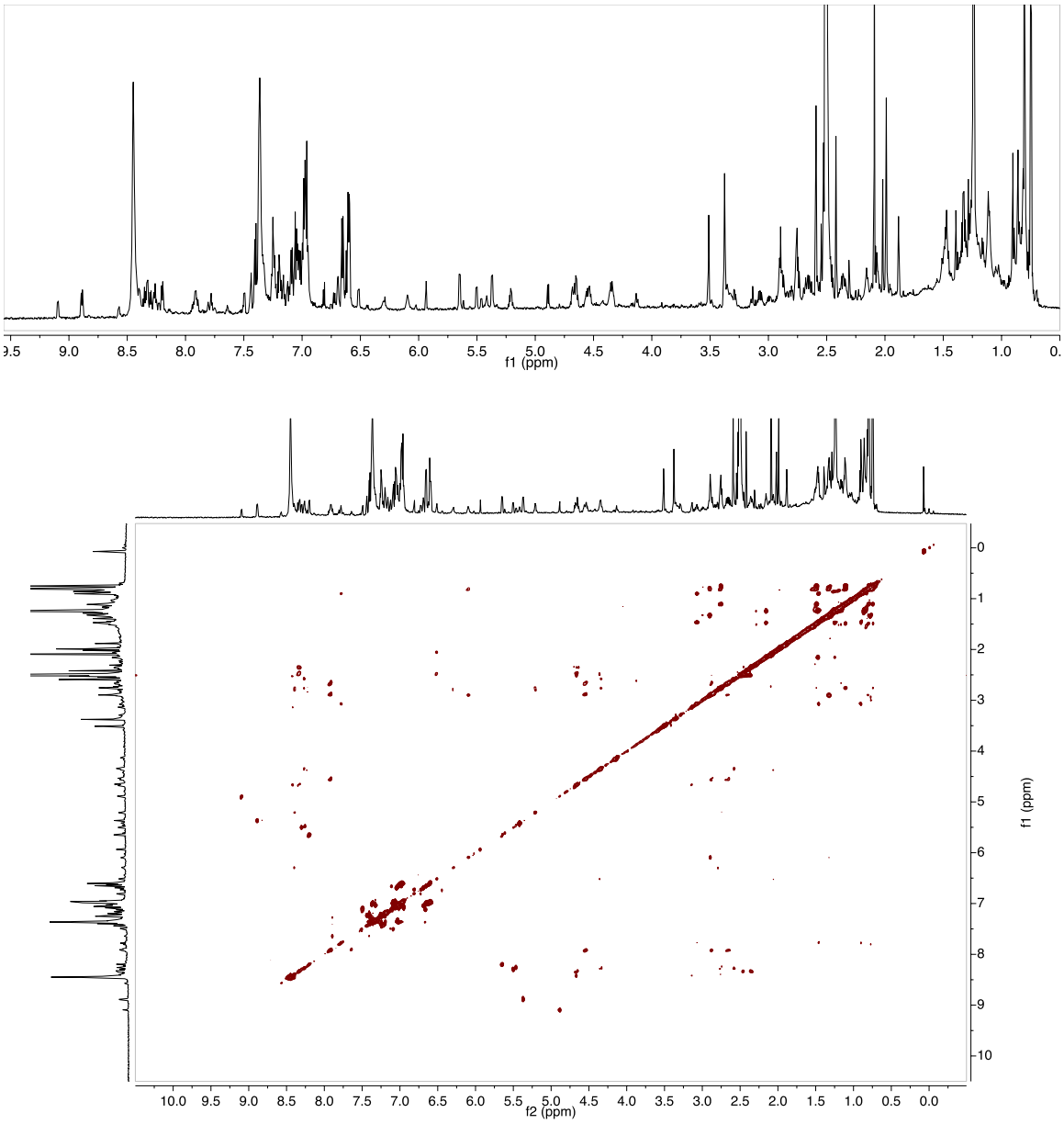

Figure S59. 800 MHz ^{1}H NMR of **33** in $(CD_3)_2SO$ (top). 800 MHz COSY spectra of **33** in $(CD_3)_2SO$ (bottom).

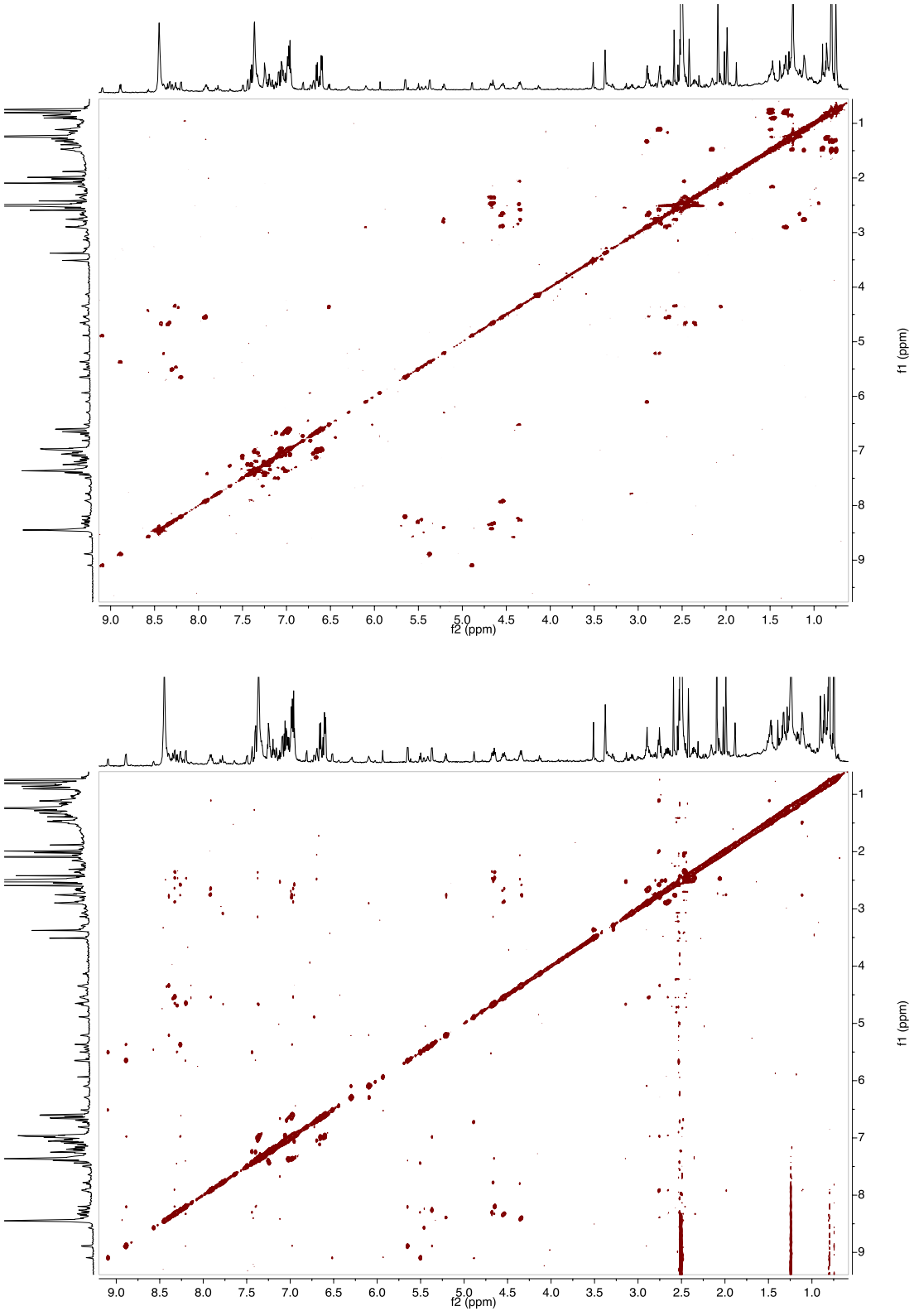

Figure S60. 800 MHz TOCSY spectra of **33** in $(CD_3)_2SO$ (top). 800 MHz NOESY spectra of **33** in $(CD_3)_2SO$ (bottom).

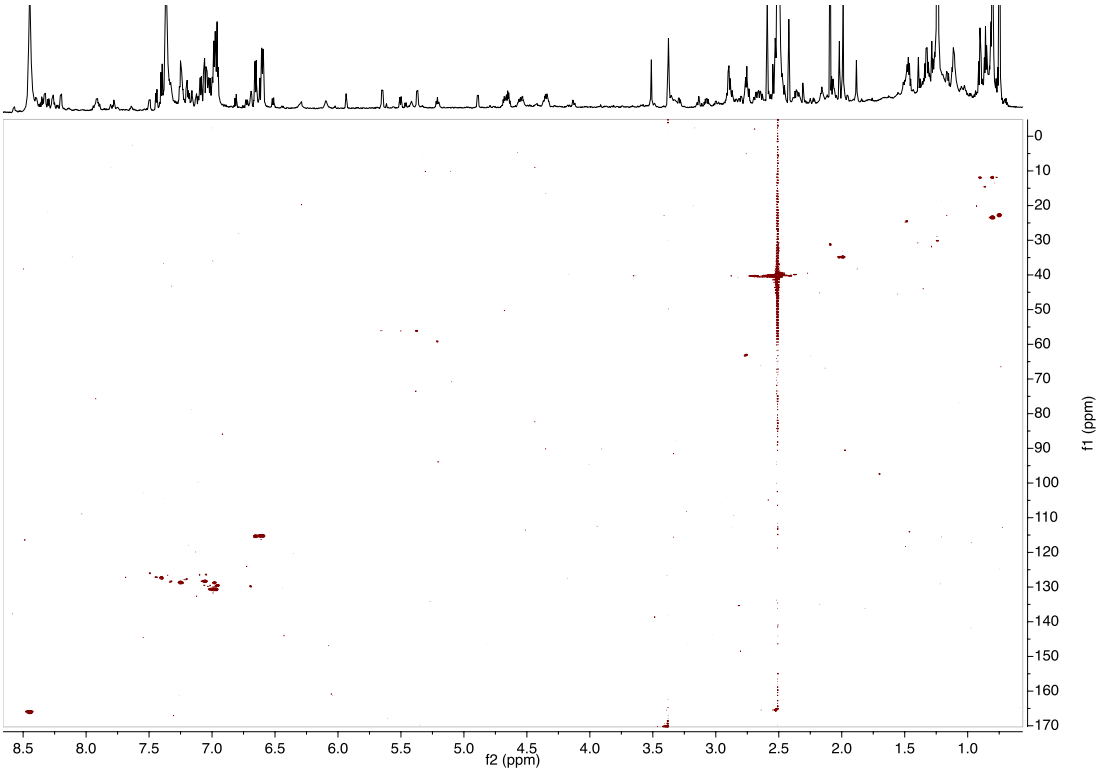

Figure S61. 800 MHz HSQC spectra of **33** in $(CD_3)_2SO$.

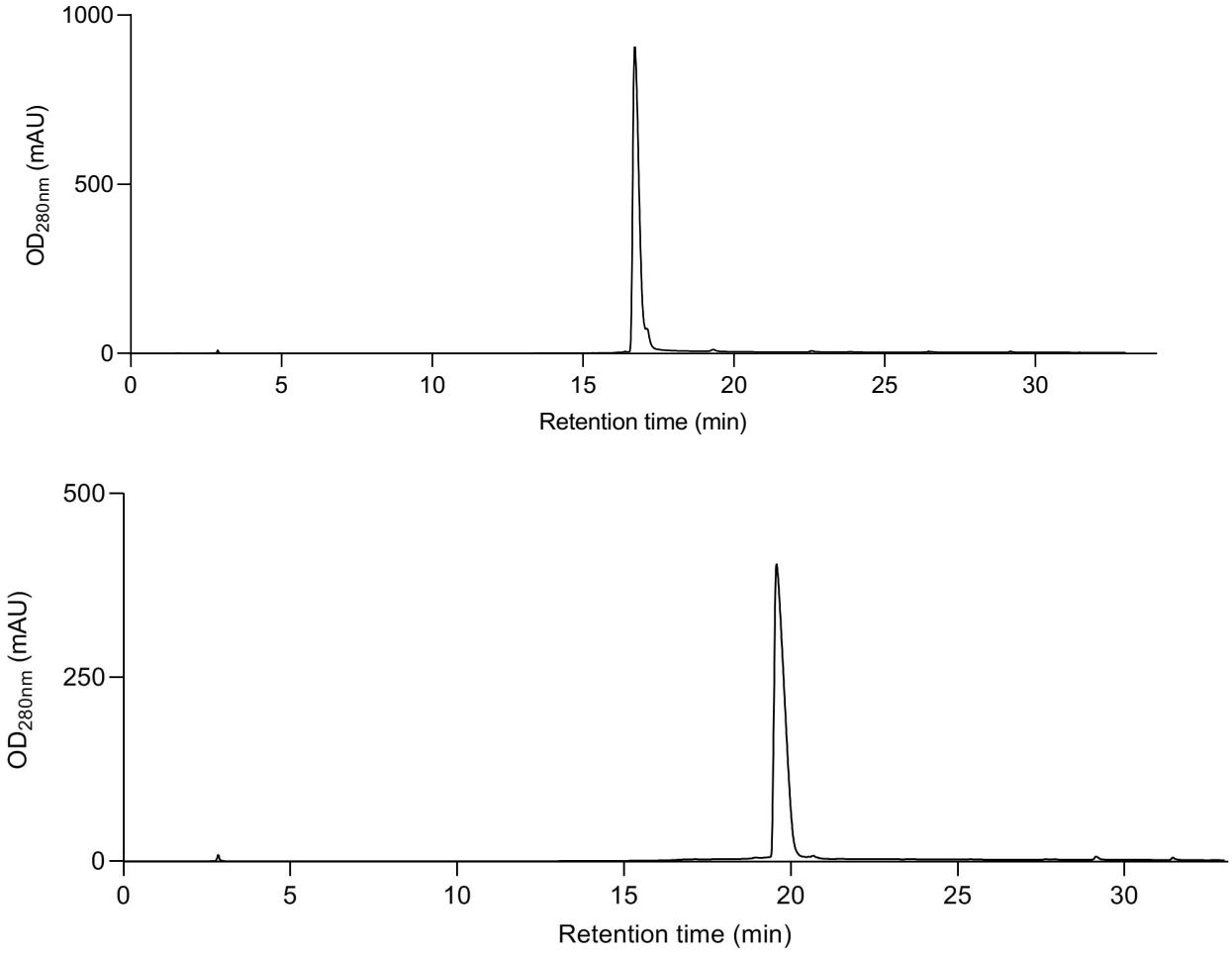

Figure S62. HPLC-MS analysis of pure **34** as a 7mer hydrazide (top) and as a CoA thioester adduct (bottom).

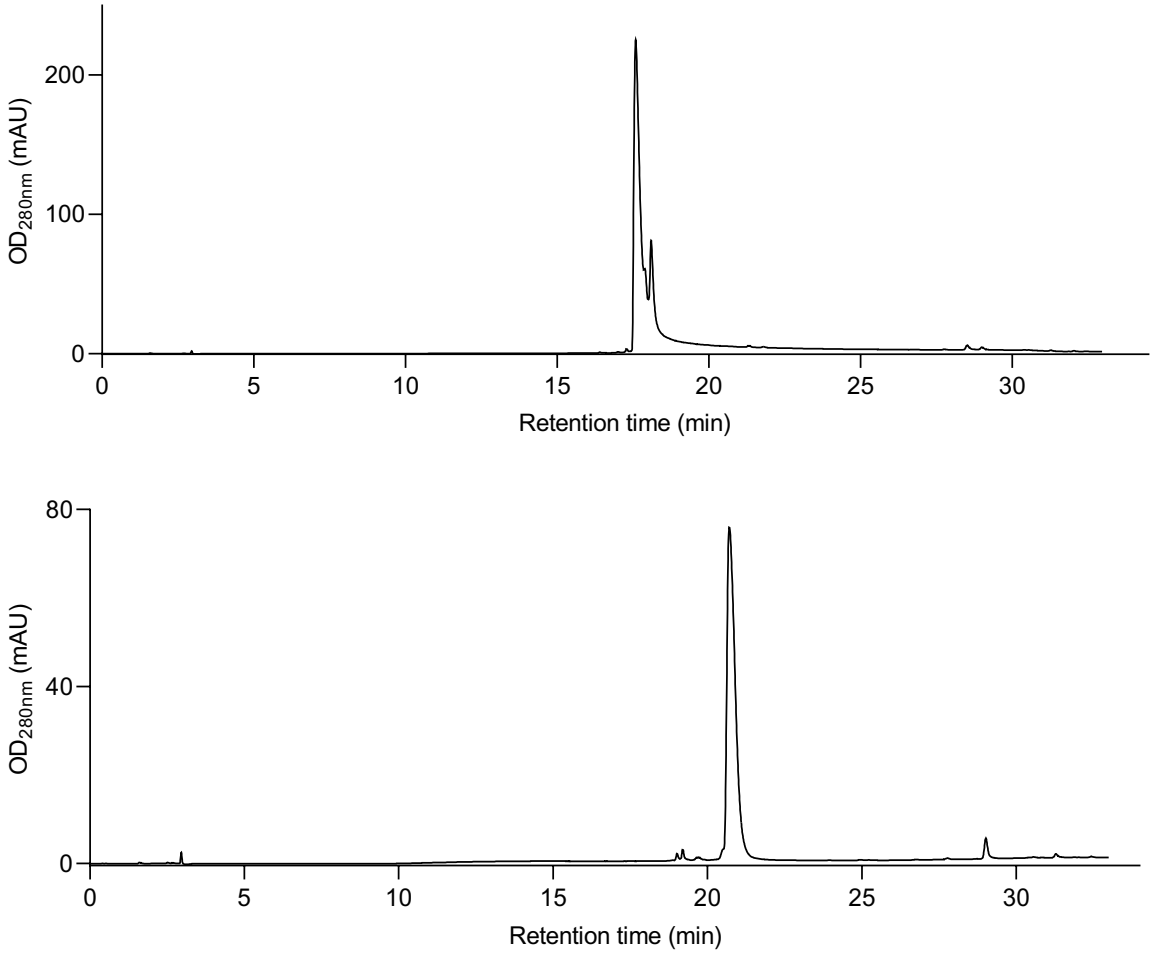

Figure S63. HPLC-MS analysis of pure **39** as a 7mer hydrazide (top) and as a CoA thioester adduct (bottom).

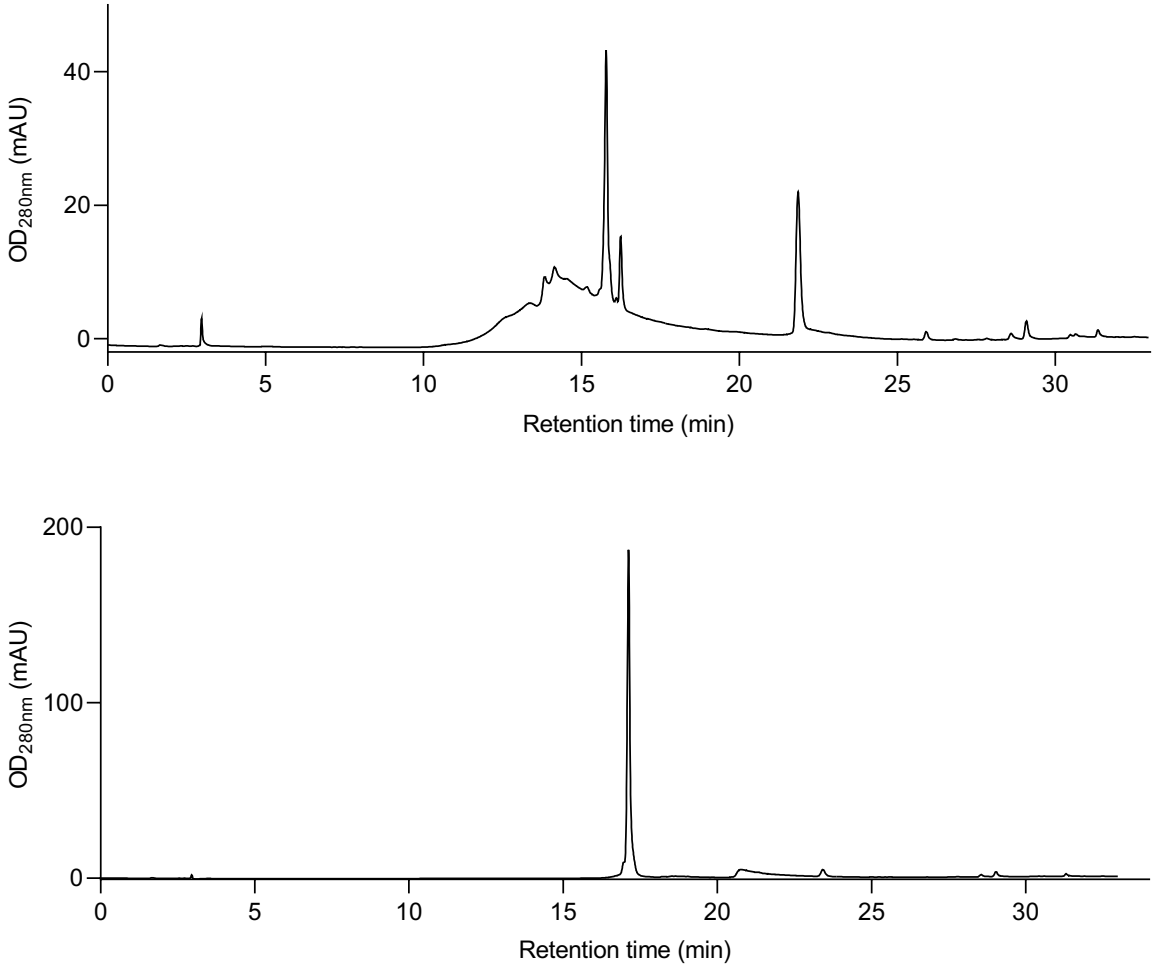

Figure S64. HPLC-MS analysis of pure **43** as a 7mer CoA thioester adduct (top). HPLC-MS analysis of pure **46** as CoA thioester adduct (bottom).

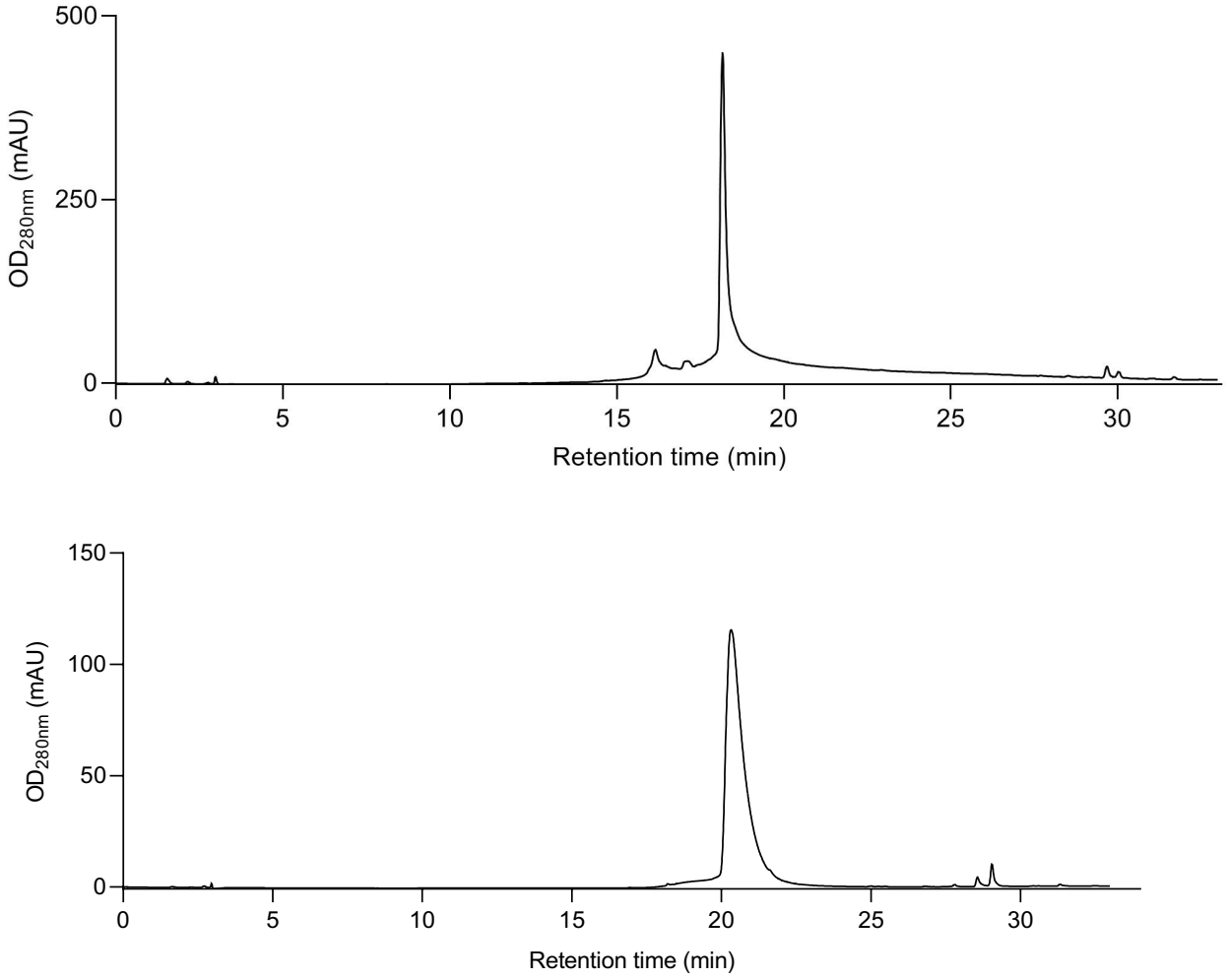

Figure S65. HPLC-MS analysis of pure peptide containing 4-Me-L-Phe2 and 3,5-$^{2}H_2$-D-Hpg4 (precursor to **36**) as a 7mer hydrazide (top) and as a CoA thioester adduct (bottom).

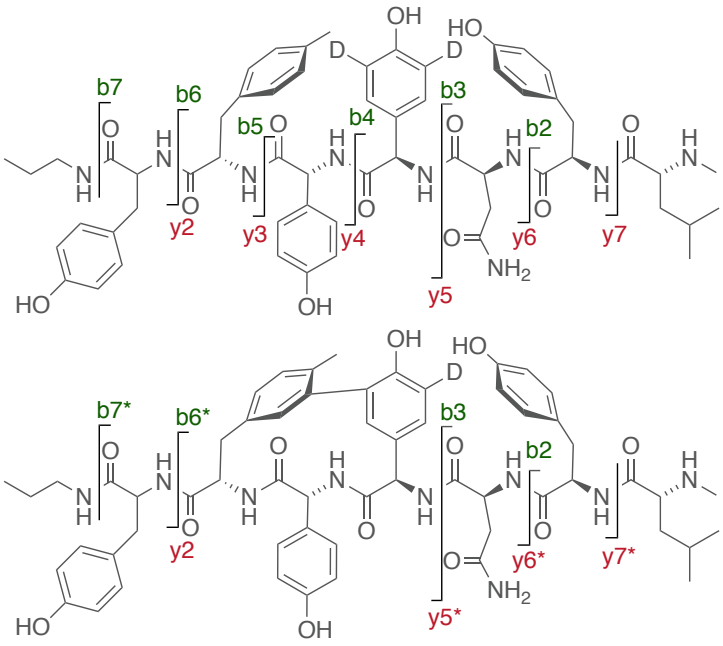

Figure S66. HR-MS/MS fragmentation for starting material with 4-Me-L-Phe as AA2 and *ortho*-$^{2}H_2$-D-Hpg as AA4 and -3 Da product upon reaction with OxyB (**36**).

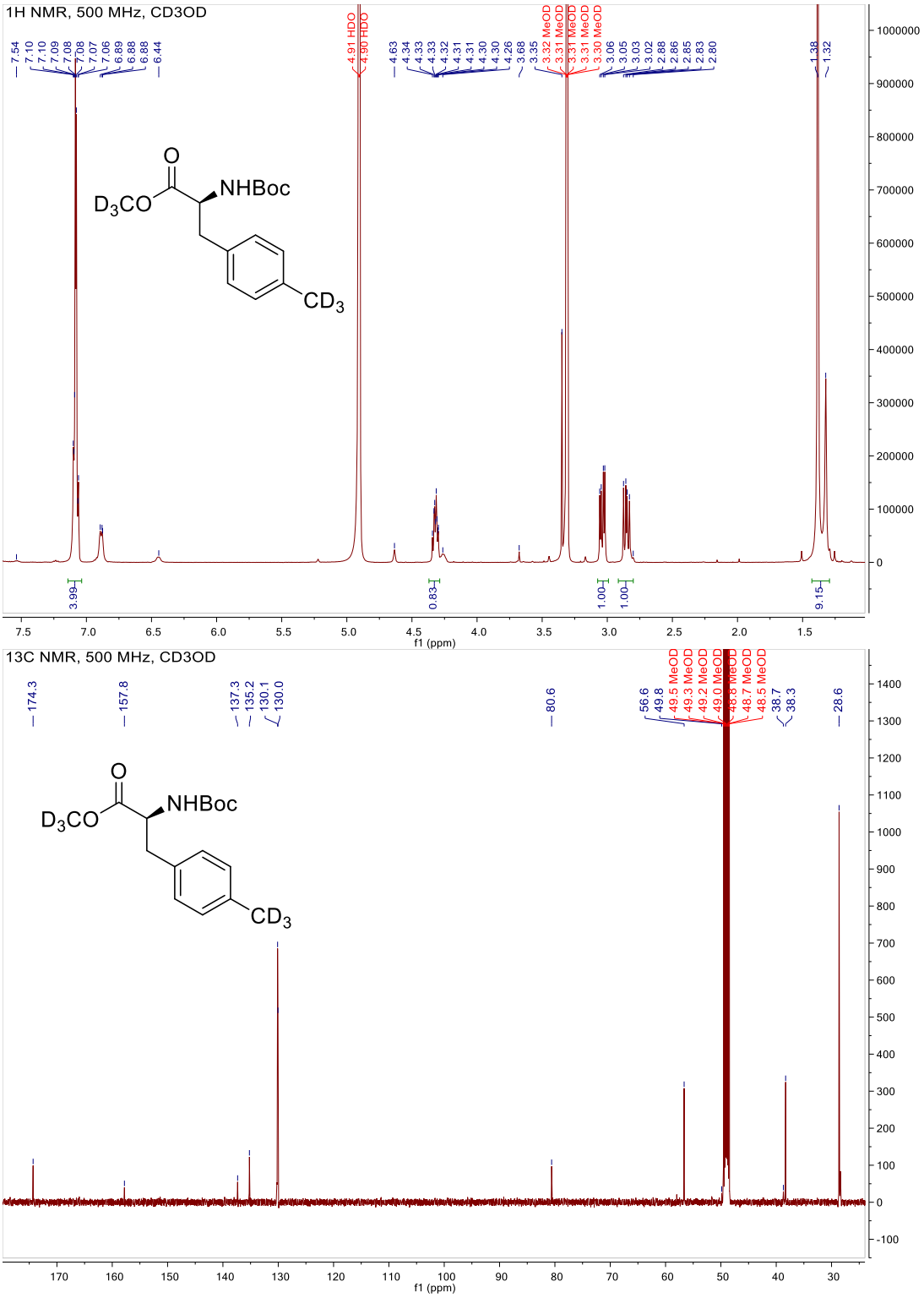

Figure S67. ^{1}H NMR spectrum (top) and ^{13}C NMR spectrum (bottom) of *N*-Boc-4-CD_3-L-phenylalanine methyl ester.

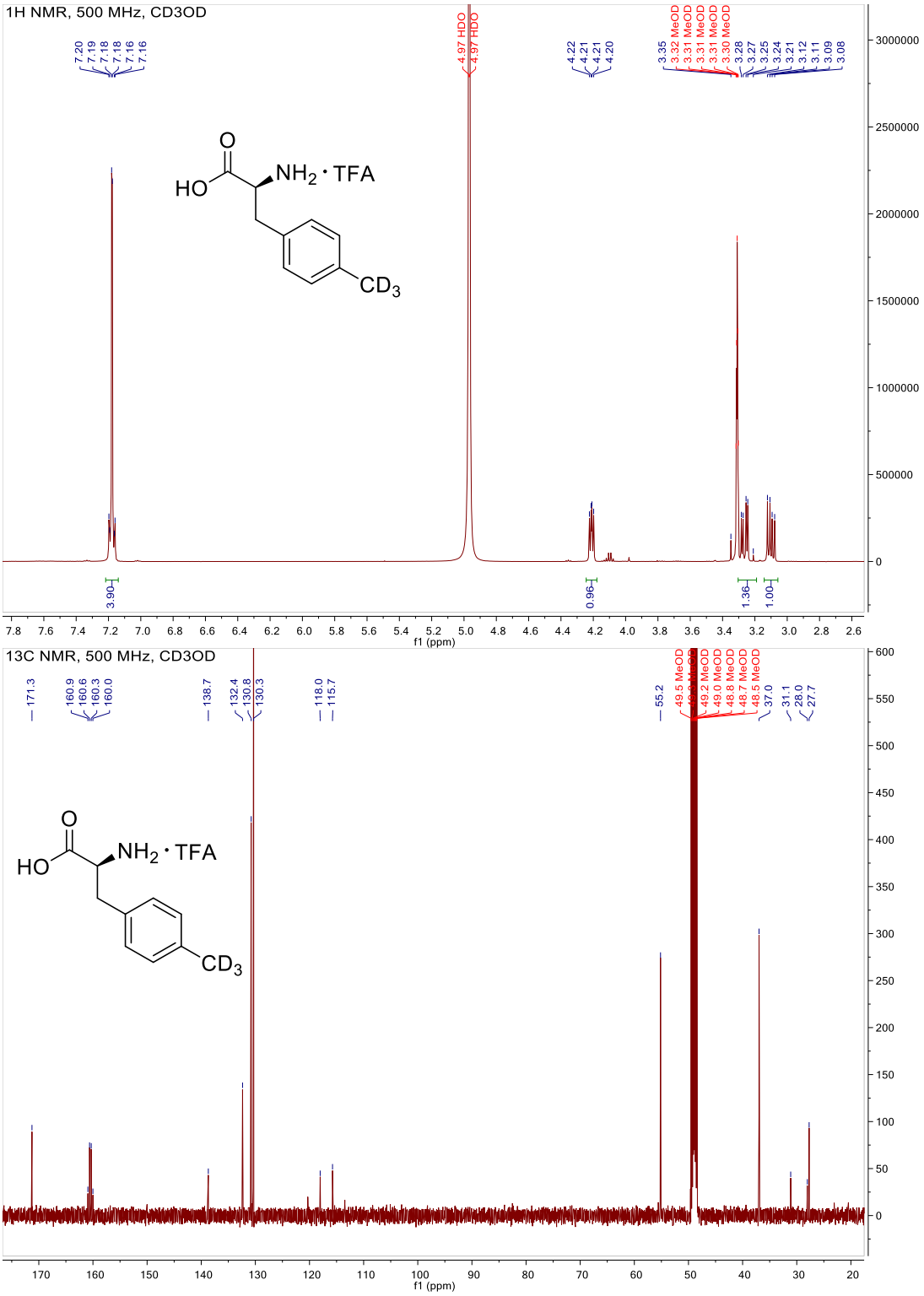

Figure S68. ^{1}H NMR spectrum (top) and ^{13}C NMR spectrum (bottom) of 4-CD_3-L-phenylalanine.

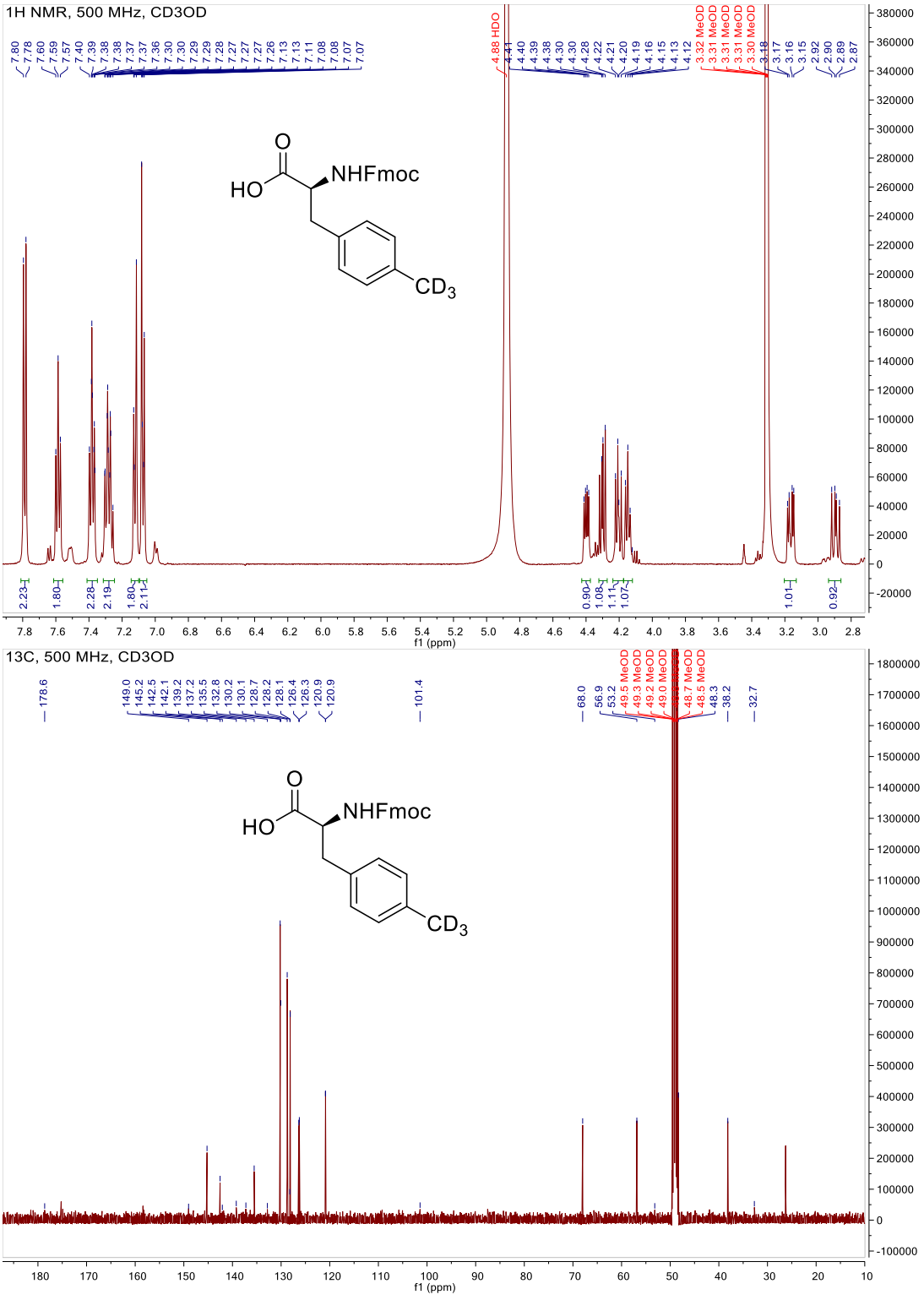

Figure S69. ^{1}H NMR spectrum (top) and ^{13}C NMR spectrum (bottom) of *N*-Fmoc-4-CD$_3$-L-phenylalanine.

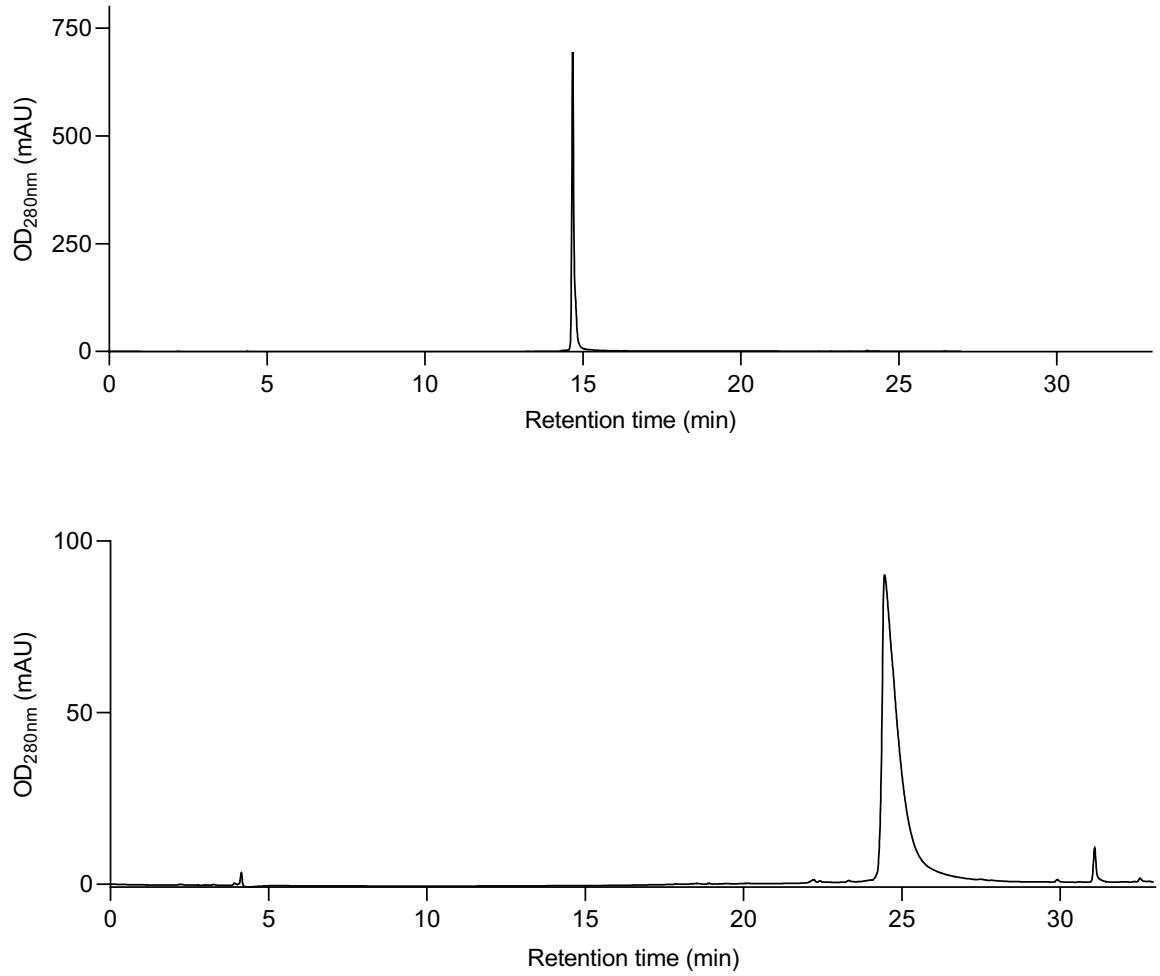

Figure S70. HPLC-MS analysis of pure peptide containing 4-C^2H_3-L-Phe2 and D-Hpg4 (precursor to **37**) as a 7mer hydrazide (top) and as a CoA thioester adduct (bottom).

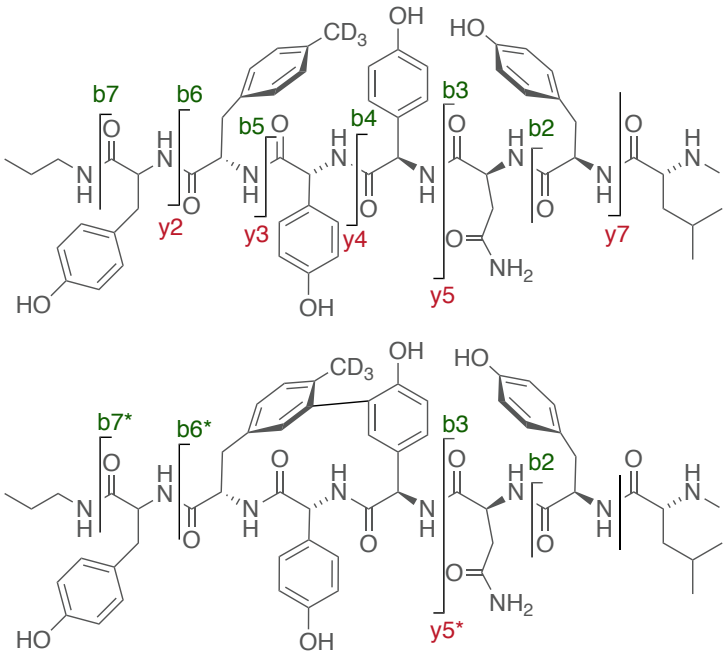

Figure S71. HR-MS/MS for starting material with 4-CD_3-L-Phe as AA2 and D-Hpg as AA4 and -2 Da product upon reaction with OxyB (**37**).

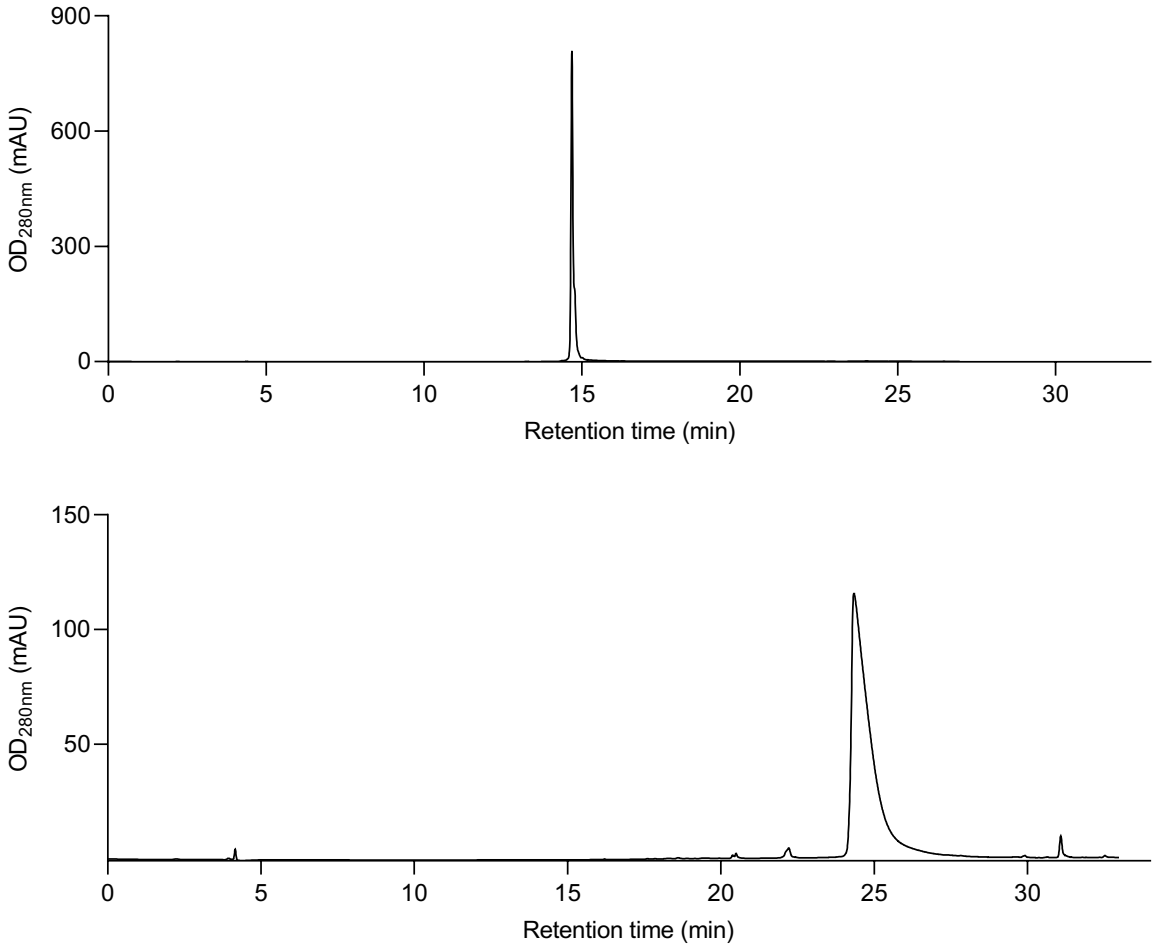

Figure S72. HPLC-MS analysis of pure peptide containing 4-C^2H_3-L-Phe2 and *ortho*-$^2H_2$-D-Hpg4 (precursor to **38**) as a 7mer hydrazide (top) and as a CoA thioester adduct (bottom).

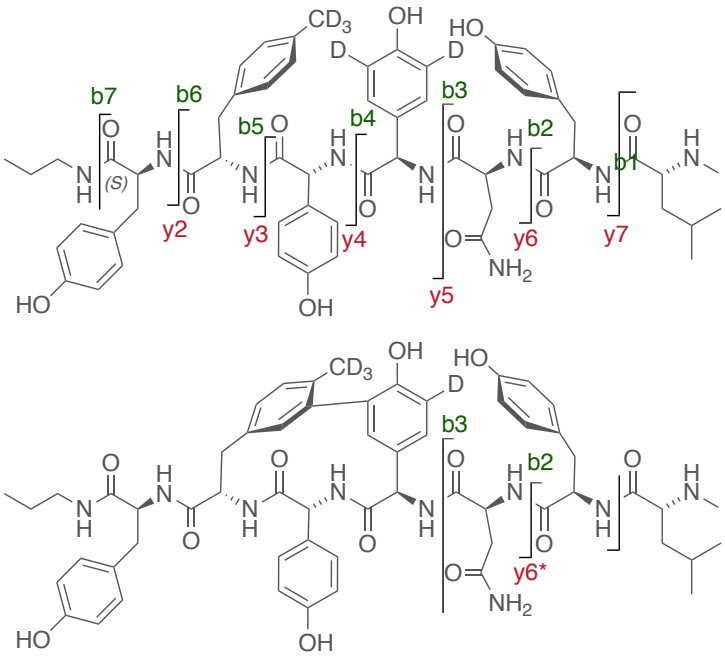

Figure S73. HR-MS/MS data for starting material AA2 = 4-CD_3-L-Phe and AA4 = *ortho*-$^2H_2$-D-Hpg and -3 Da product upon reaction with OxyB (**38**).

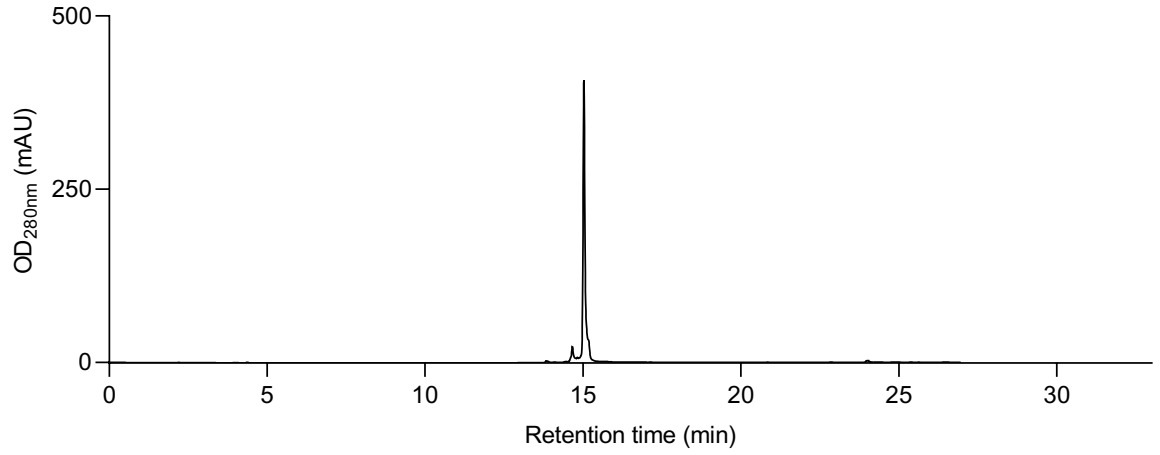

Figure S74. HPLC-MS analysis of pure peptide containing 4-C^2H_3-L-Phe2 and D-PhGly4 (precursor to **41**) as a 7mer hydrazide. Coenzyme A adduct of this peptide was purified via mass-detected HPLC and pure fractions containing desired mass were collected and submitted to assays without further characterization.

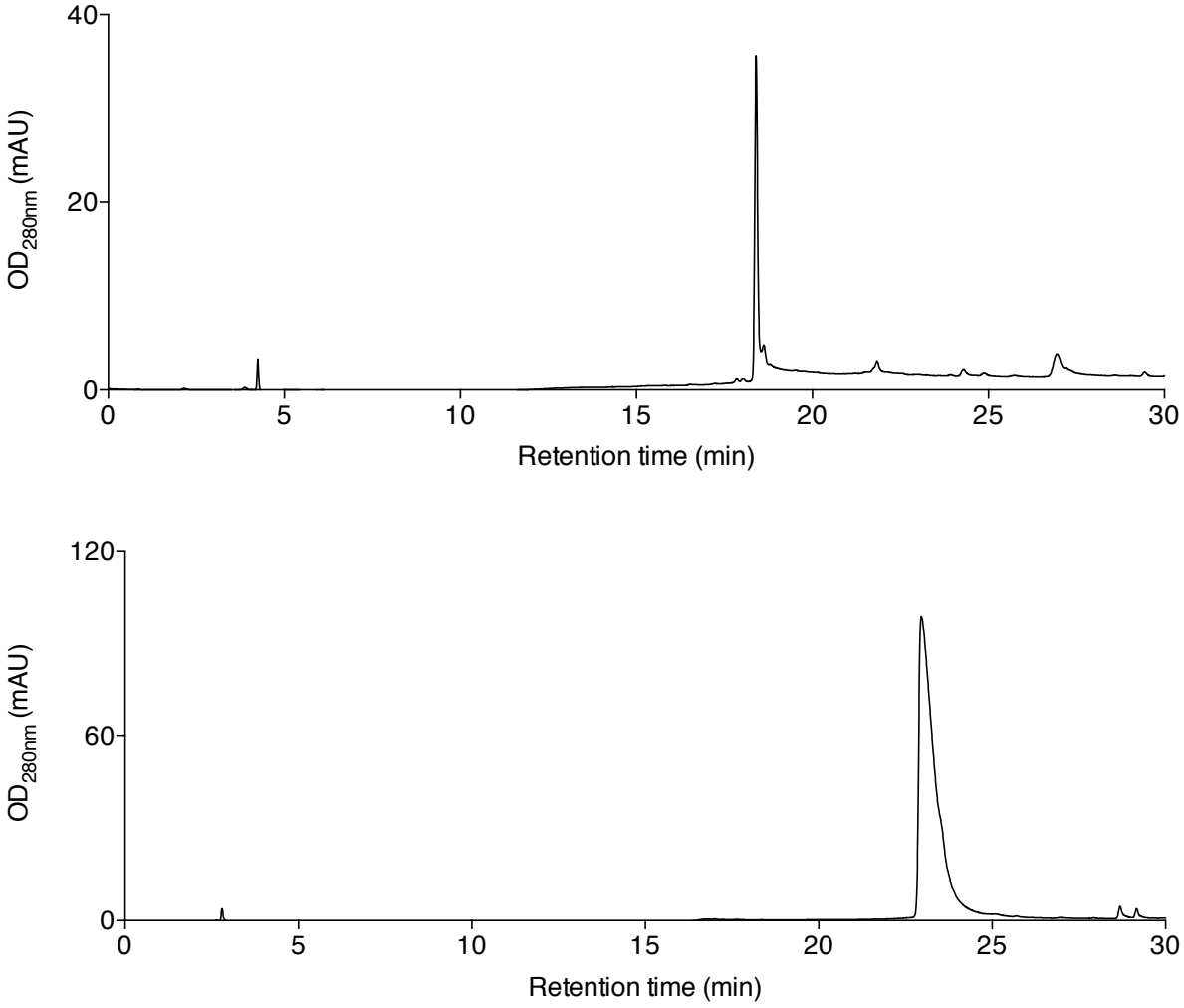

Figure S75. HPLC-MS analysis of pure peptide containing L-Phe2, *ortho*-$^{2}H_2$-D-Hpg3 and D-PhGly4 (precursor to **42**) as a 7mer hydrazide (top) and as a CoA thioester adduct (bottom).

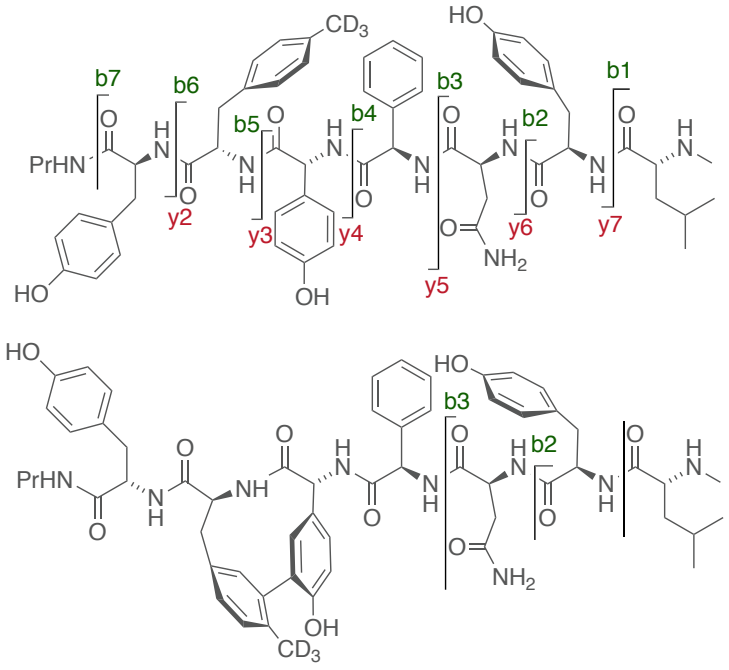

Figure S76. HR-MS/MS for starting material with AA2 = 4-CD_3-L-Phe and AA4 = D-PhGly and -2 Da product upon reaction with OxyB (**41**).

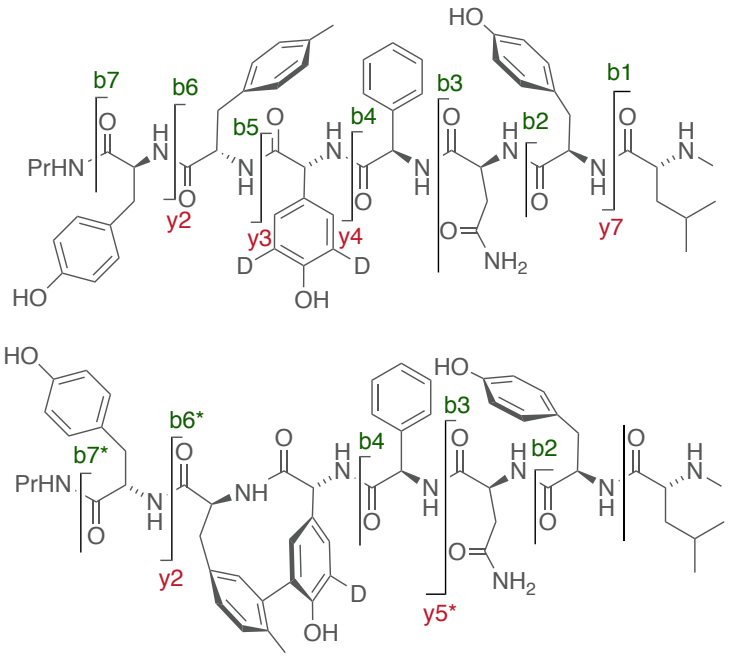

Figure S77. HR-MS/MS data for starting material AA2 = L-Phe, AA3 = *ortho*-$^{2}H_2$-D-Hpg, AA4 = D-PhGly and -3 Da product upon reaction with OxyB (**42**).

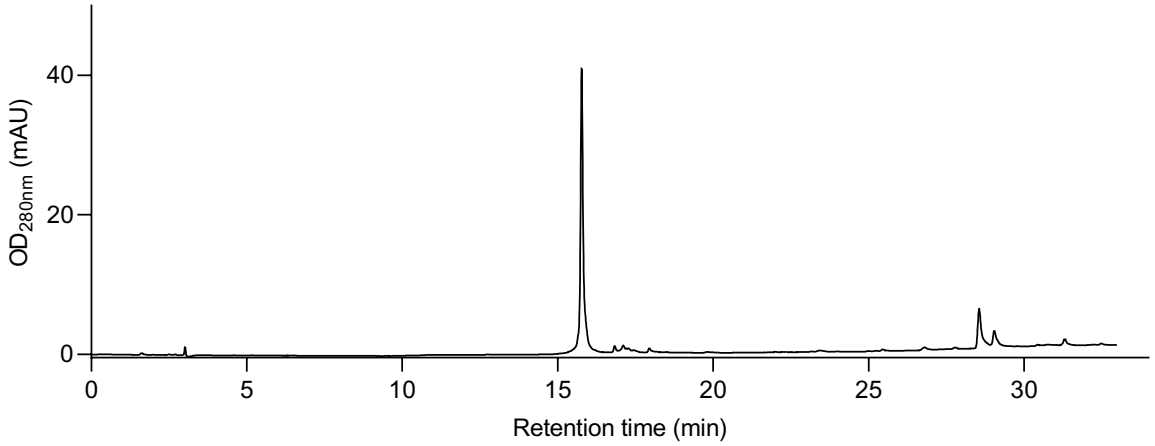

Figure S78. HPLC-MS analysis of pure peptide containing 4-NH_2-L-Phe2 and *ortho*-$^2H_2$-D-Hpg4 (precursor to **45**) as a 7mer CoA thioester adduct.

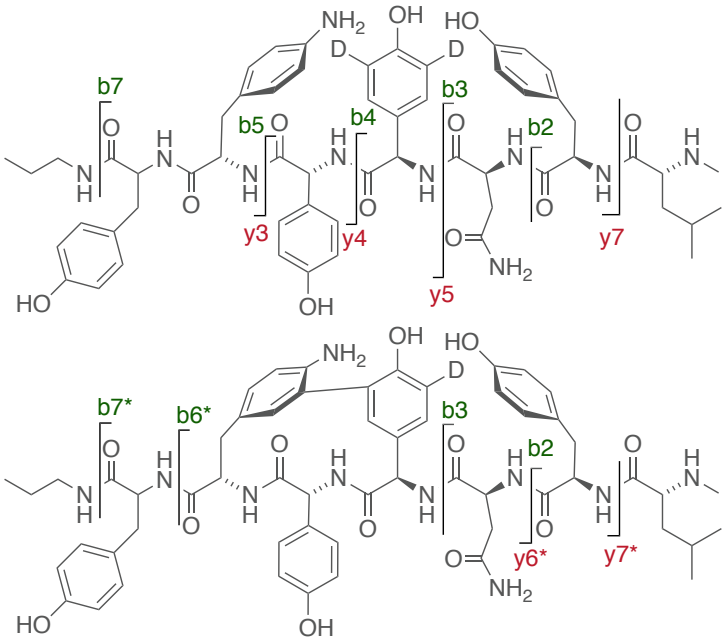

Figure S79. HR-MS/MS fragmentation for starting material with AA2 = 4-NH_2-L-Phe and AA4 = *ortho*-$^2H_2$-D-Hpg and -3 Da product upon reaction with OxyB (**45**).

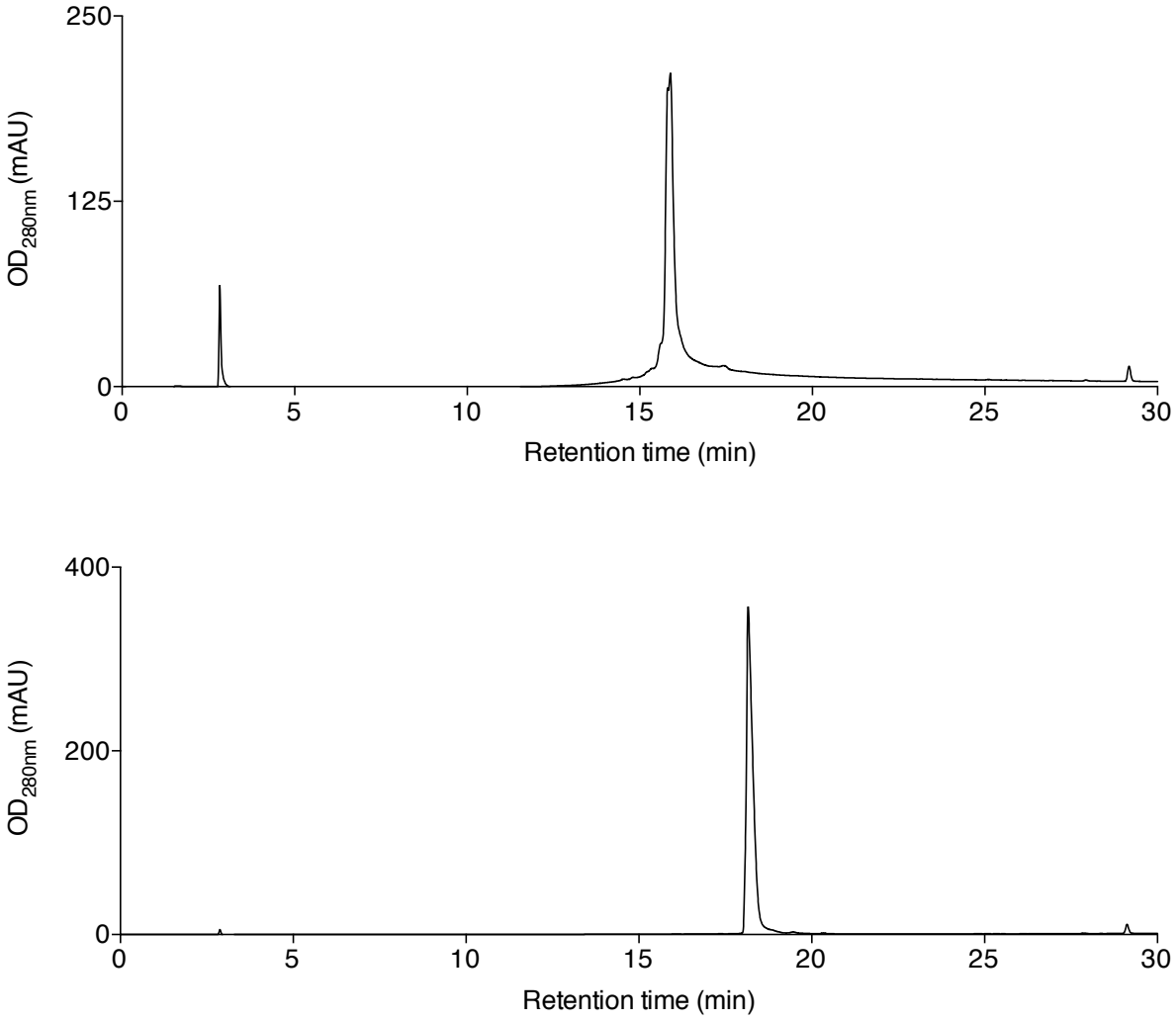

Figure S80. HPLC-MS analysis of pure **48** as a 7mer hydrazide (top) and as a CoA thioester adduct (bottom).

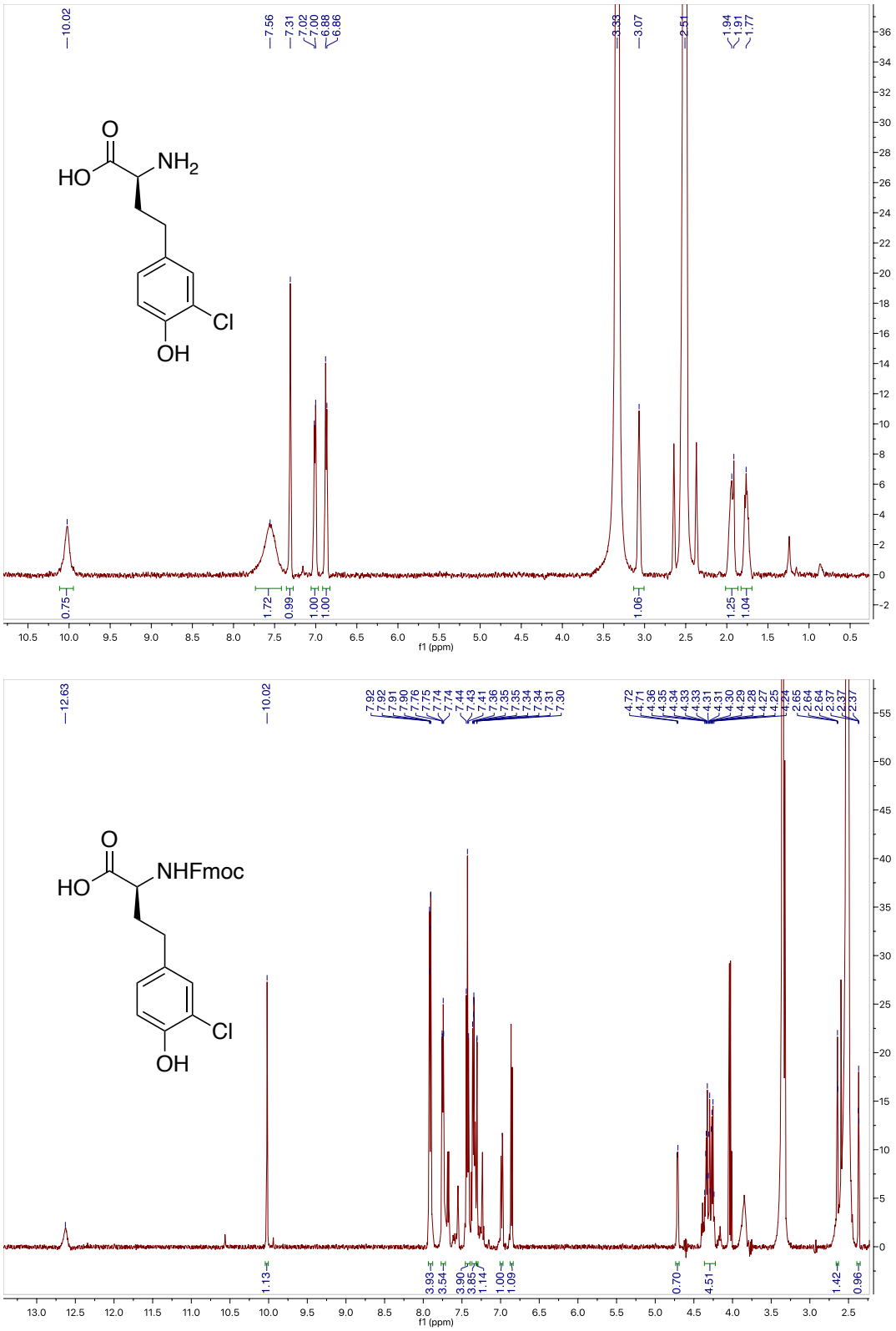

Figure S81. ^{1}H NMR spectrum for 3-Cl-L-homotyrosine (top) and ^{1}H NMR spectrum for *N*-Fmoc-3-Cl-L-homotyrosine (bottom).

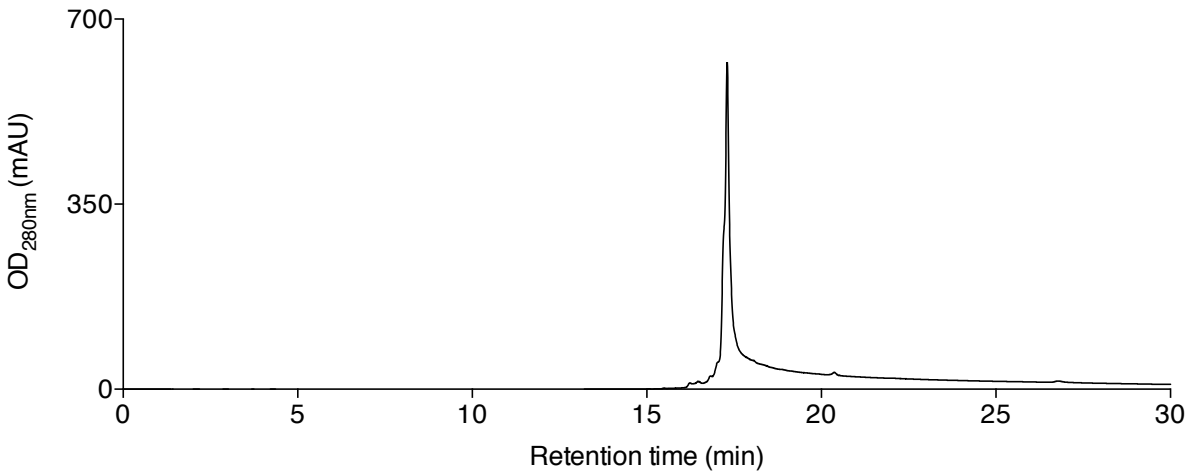

Figure S82. HPLC-MS analysis of pure **50** as a 7mer hydrazide. Coenzyme A adduct of this peptide was purified via mass-detected HPLC and pure fractions containing desired mass were collected and submitted to assays without further characterization.

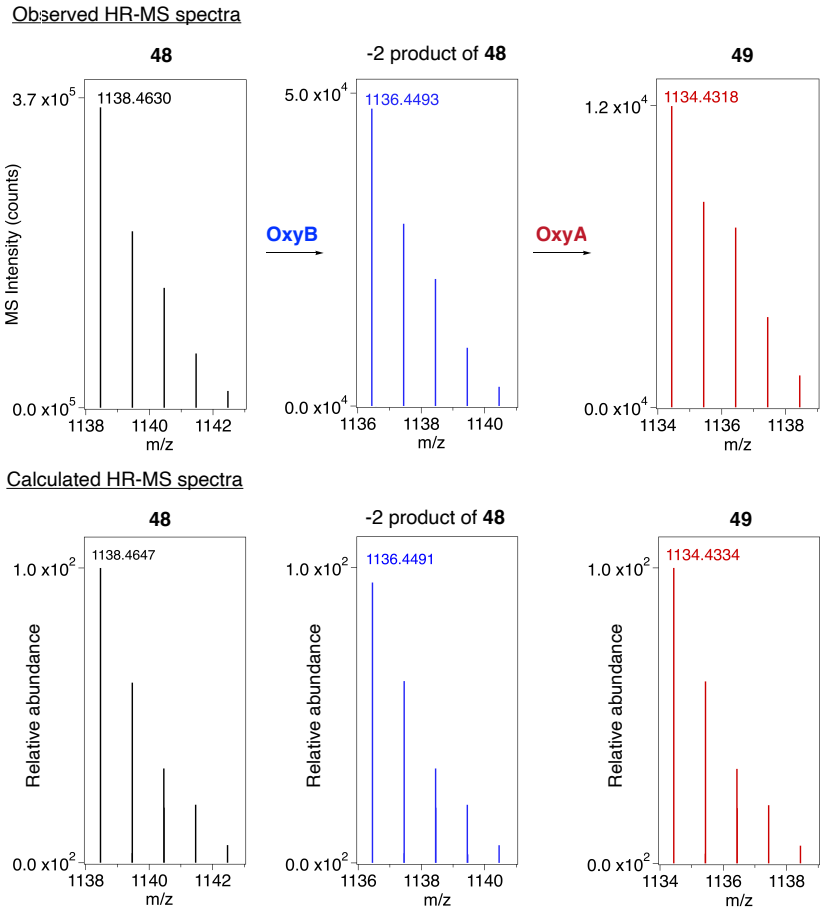

Figure S83. Observed and calculated HR-MS spectra for substrate **48** and its products upon reaction with OxyB and OxyA.

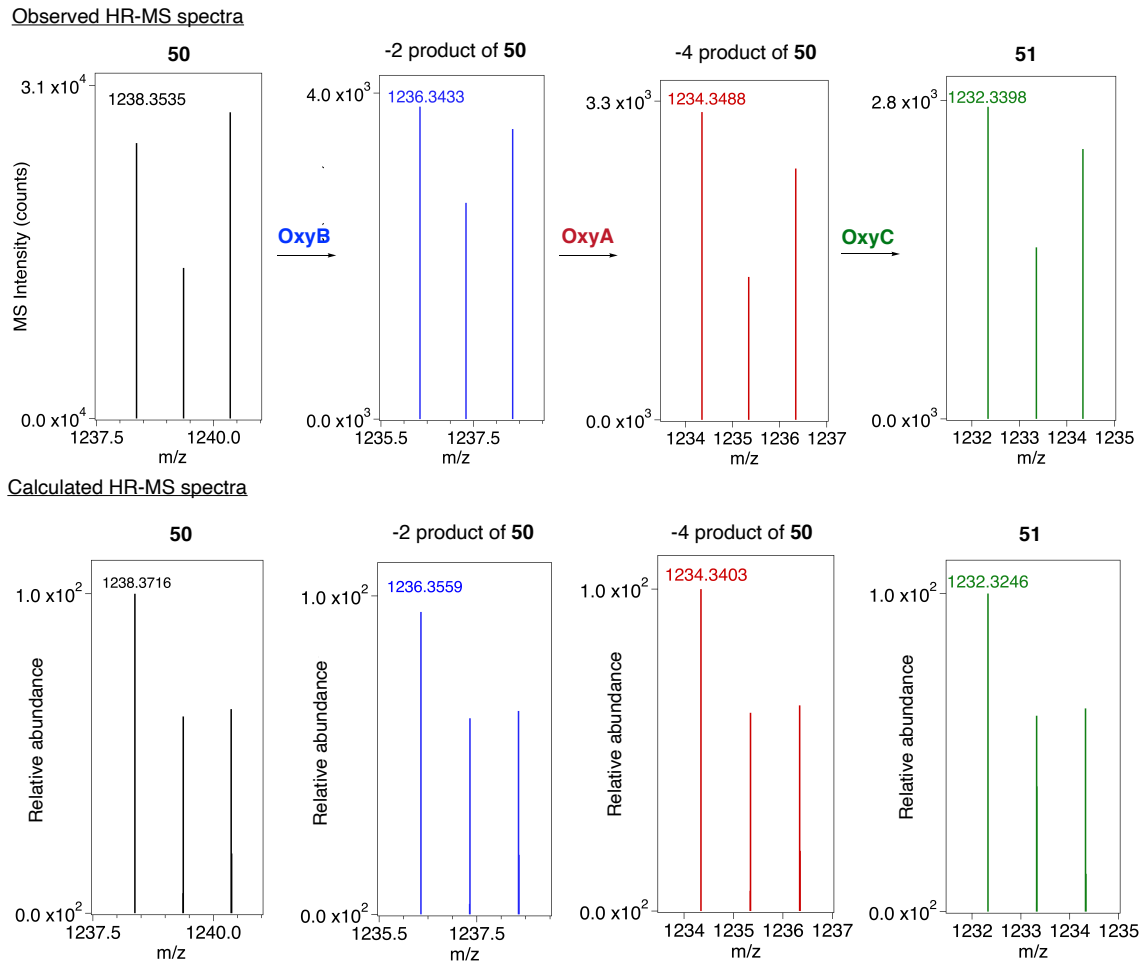

Figure S84. Observed and calculated HR-MS spectra for the trisodium salt of substrate **50** and its products upon reaction with OxyB, OxyA and OxyC.

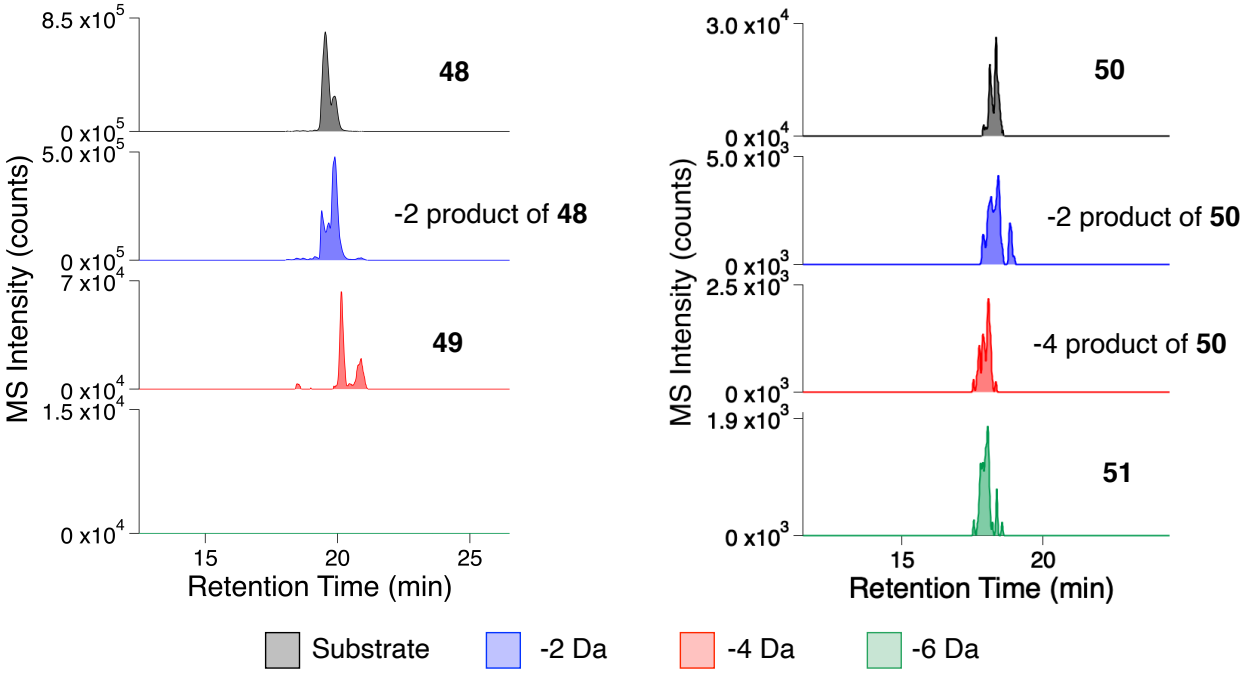

Figure S85. (Left) Extracted ion counts for derivatized substrate **48**, monocrosslinked product from reaction of **48** with OxyB and bicyclic product **49**. (Right) Extracted ion counts for derivatized substrate **50**, monocrosslinked product from reaction of **50** with OxyB, bicyclic product from reaction of **50** with OxyB and OxyA, and tricyclic product **51**.

Table S1. HR-MS data for substrates and products of OxyB enzymatic reactions to generate analogs with varying macrocycle sizes and various stereochemistries. Sequence of peptides shown is (LTyr1)-AA2-(D-Hpg3)-AA4-(L-Asn5)-(D-Tyr6)-(*N*-Me-D-Leu7).

Compound	AA2	AA4	Charge State	Calculated mass	Observed mass	Δppm
4	L-Hpg	D-Hpg	$[M+H]^+$	1074.4931	1074.49646	3.1
5	L-Hpg	D-Hpg	$[M+H]^+$	1072.4775	1072.48163	3.9
6	L-Tyr	D-Tyr	$[M+H]^+$	1102.5223	1102.52646	3.8
7	L-Tyr	D-Tyr	$[M+H]^+$	1100.51	1100.50982	0.2
8	L-homoTyr	D-Hpg	$[M+H]^+$	1102.5244	1102.52625	1.7
9/10	L-homoTyr	D-Hpg	$[M+H]^+$	1100.5088	1100.5108	1.8
-	$^2H_2$-L-homoTyr	D-Hpg	$[M+H]^+$	1104.537	1104.53553	1.3
11	$^2H_2$-L-homoTyr	D-Hpg	$[M+H]^+$	1102.5213	1102.528	6.1
12	$^2H_2$-L-homoTyr	D-Hpg	$[M+H]^+$	1101.515	1101.52318	7.4
-	L-homoTyr	$^2H_2$-D-Hpg	$[M+H]^+$	1104.5369	1104.54332	5.8
13	L-homoTyr	$^2H_2$-D-Hpg	$[M+H]^+$	1102.5213	1102.53378	11.3
14	L-homoTyr	$^2H_2$-D-Hpg	$[M+H]^+$	1101.515	1101.52832	12.1
15	L-Tyr	L-Hpg	$[M+H]^+$	1088.5088	1088.51177	2.7
16	L-Tyr	L-Hpg	$[M+H]^+$	1086.4931	1086.49495	1.7
17	D-Tyr	D-Hpg	$[M+H]^+$	1088.5088	1088.50973	0.8
18	D-Tyr	D-Hpg	$[M+H]^+$	1086.4931	1086.4941	0.9
-	D-Tyr	$^2H_2$-D-Hpg	$[M+H]^+$	1090.5213	1090.52589	4.2
19	D-Tyr	$^2H_2$-D-Hpg	$[M+H]^+$	1087.4994	1087.50414	4.3
20	D-Tyr	L-Hpg	$[M+H]^+$	1088.5088	1088.51149	2.4
21/22	D-Tyr	L-Hpg	$[M+H]^+$	1086.4931	1086.49454	1.3
-	D-Tyr	$^2H_2$-L-Hpg	$[M+H]^+$	1090.5213	1090.52889	6.9
23	D-Tyr	$^2H_2$-L-Hpg	$[M+H]^+$	1088.5057	1088.50927	3.2
24	D-Tyr	$^2H_2$-L-Hpg	$[M+H]^+$	1087.4994	1087.5074	7.3

Table S2. HR-MS/MS data for **4** and its product upon reaction with OxyB, **5**.

*HR-MS/MS for substrate **4** (AA2 = L-Hpg; AA4 = D-Hpg)*

Charge State	Calculated m/z	Observed m/z	Δppm	Sequence
b_2^{+1}	291.1709	291.1755	15.8	MeLeu-Tyr
b_3^{+1}	405.2138	405.2201	15.7	MeLeu-Tyr-Asn
b_4^{+1}	554.2615	554.2704	16.0	MeLeu-Tyr-Asn-Hpg
b_5^{+1}	703.3092	703.3182	12.9	MeLeu-Tyr-Asn-Hpg-Hpg
b_6^{+1}	852.3568	852.3691	14.5	MeLeu-Tyr-Asn-Hpg-Hpg-Hpg-Tyr
b_7^{+1}	1015.4202	1015.4264	6.1	MeLeu-Tyr-Asn-Hpg-Hpg-Hpg-Tyr
y_2^{+1}	223.1436	223.1481	20.5	Tyr-propyl
y_3^{+1}	372.1912	371.197	15.6	Hpg-Tyr-propyl
y_4^{+1}	521.2389	521.2479	17.4	Hpg-Hpg-Tyr-propyl
y_5^{+1}	670.2866	670.2956	13.4	Asn-Hpg-Hpg-Hpg-Tyr-propyl
y_7^{+1}	947.3928	947.4057	13.6	Tyr-Asn-Hpg-Hpg-Hpg-Tyr-propyl

*HR-MS/MS for product **5** (AA2 = L-Hpg; AA4 = D-Hpg)*

Charge State	Calculated m/z	Observed m/z	Δppm	Sequence
b_2^{+1}	291.1709	291.1759	17.4	MeLeu-Tyr
b_3^{+1}	405.2138	405.2203	16.1	MeLeu-Tyr-Asn
b_6^{+1}	850.3212	850.3512	11.8	MeLeu-Tyr-Asn-Hpg$_m$-Hpg-Hpg$_m$
b_7^{+1}	1013.4045	1013.4183	13.6	MeLeu-Tyr-Asn-Hpg$_m$-Hpg-Hpg$_m$
y_2^{+1}	223.1436	223.1475	17.5	Tyr-propyl
y_5^{+1}	668.2709	668.2848	20.9	Hpg$_m$-Hpg-Hpg$_m$-Tyr-propyl
y_6^{+1}	782.3139	782.323	11.6	Asn-Hpg$_m$-Hpg-Hpg$_m$-Tyr-propyl
y_7^{+1}	945.3772	945.3873	10.7	Tyr-Asn-Hpg$_m$-Hpg-Hpg$_m$-Tyr-propyl

Table S3. NMR assignments for **4** in $(CD_3)_2SO$ from C- to N-terminus. The structure and number scheme for the compound is shown below the table.

Residue	Label	δH (ppm)	δC (ppm)
Pr	1	0.69	11.7
	2	1.23	22.4
	3	2.92;2.75	40.8
	NH	7.45	-
Tyr1	1	-	170.5
	2	4.26	55.2
	3	2.88;2.73	-
	5	6.98	130.5
	6	6.64	115.3
	NH	8.20	-
Hpg2	1	-	169.9
	2	5.13	56.6
	4	6.80	128.8
	5	6.54	115.2
	NH	8.47	-
Hpg3	1	-	170.5
	2	5.40	56.4
	4	7.18	128.5
	5	6.68	115.3
	NH	8.78	-
Hpg4	1	-	170.3
	2	5.49	55.6
	4	7.18	129.3
	5	6.65	115.3
	NH	8.19	-
Asn5	1	-	170.4
	2	4.63	50.1
	3	2.34;2.45	-
	NH	8.30	-
Tyr6	1	-	171.5
	2	4.53	53.9
	3	2.63;2.87	-
	5	6.98	130.5
	6	6.59	115.2
	NH	8.31	-
NMeLeu7	1	-	171.7

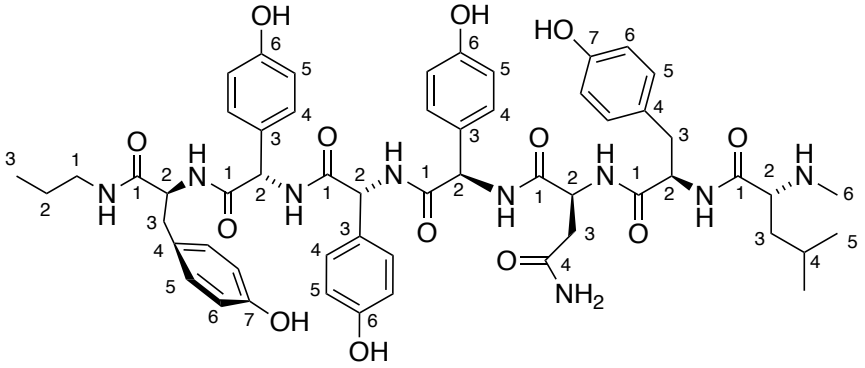

Table S4. NMR assignments for **5** in $(CD_3)_2SO$ from C- to N-terminus. The structure and number scheme for the compound is shown below the table.

Residue	Label	δH (ppm)	δC (ppm)
Propyl	2	0.76	11.8
	3	1.32	22.7
	4	2.95	-
	NH	7.98	-
Tyr1	2	4.49	55.1
	3	2.73; 2.81	63.3
	5	7.00	130.6
	6	6.65	115.3
Hpg2	2	-	-
	4	7.39	131.8
	5	6.92	123.6
Hpg3	2	5.28	-
	4	7.06	127.9
	5	6.71	115.8
	NH	9.00	-
Hpg4	2	-	-
	4	5.21	114.3
	7	6.74	115.9
	8	6.59	130.5
Asn	2	4.65	50.3
	3	2.36; 2.51	-
	NH	8.30	-
Tyr6	2	4.54	53.7
	3	2.85; 2.61	-
	5	6.95	115.2
	6	6.59	130.5
	NH	7.89	-

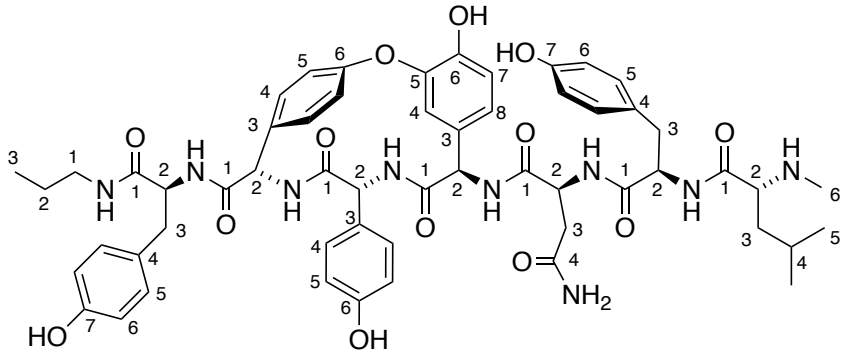

Table S5. Partial NMR assignment for vancomycin (**1**) in $(CD_3)_2SO$ and 2D correlations of relevant portions of the molecule [7].

Residue	Label	δH (ppm)	δC (ppm)
L-Dpg1	2	4.42	56.7
	6	6.42	102.3
	8	6.26	105.8
	NH	8.48	-
3-Cl-β-OH-L-Tyr2	2	4.19	61.9
	5	7.86	127.3
	8	7.34	123.3
	9	7.47	127.3
	NH	6.67	-
D-Hpg3	2	4.43	53.7
	4	7.18	135.6
	7	6.72	116.2
	8	6.77	125.4
	NH	8.64	-
D-Hpg4	2	5.75	54.9
	4	5.21	104.6
	8	5.55	107.1
	NH	8.25	-

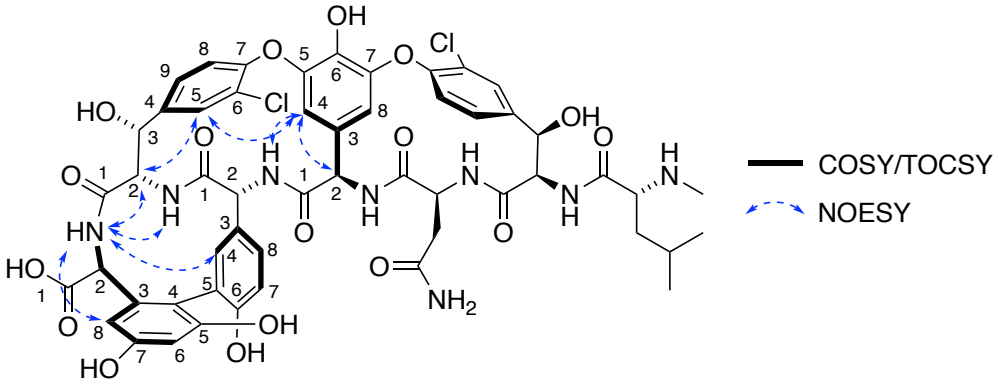

Table S6. HR-MS/MS data for **6** and its product upon reaction with OxyB, **7**.

*HR-MS/MS for substrate **6** (AA2 = L-Tyr; AA4 = D-Tyr)*

Charge State	Calculated m/z	Observed m/z	Δppm	Sequence
b_2^{+1}	291.1709	291.1672	12.4	MeLeu-Tyr
b_3^{+1}	405.2138	405.2154	3.9	MeLeu-Tyr-Asn
b_4^{+1}	568.2771	568.278	1.6	MeLeu-Tyr-Asn-Tyr
b_5^{+1}	717.3248	717.3233	2.0	MeLeu-Tyr-Asn-Tyr-Hpg
b_6^{+1}	880.3881	880.3851	3.3	MeLeu-Tyr-Asn-Tyr-Hpg-Tyr
b_7^{+1}	1043.4458	1043.4515	5.4	MeLeu-Tyr-Asn-Tyr-Hpg-Tyr-Tyr
y_2^{+1}	223.1436	223.1326	4.9	Tyr-propyl
y_3^{+1}	386.2069	386.2094	6.6	Tyr-Tyr-propyl
y_4^{+1}	535.2546	535.2555	1.7	Hpg-Tyr-Tyr-propyl
y_5^{+1}	698.3179	698.3137	5.9	Tyr-Hpg-Tyr-Tyr-propyl
y_6^{+1}	812.3539	821.3608	8.4	Asn-Tyr-Hpg-Tyr-Tyr-propyl
y_7^{+1}	975.4203	975.4241	3.8	Tyr-Asn-Tyr-Hpg-Tyr-Tyr-propyl

*HR-MS/MS for product **7** (AA2 = L-Tyr; AA4 = D-Tyr)*

Charge State	Calculated m/z	Observed m/z	Δppm	Sequence
b_2^{+1}	291.1709	291.1759	17.4	MeLeu-Tyr
b_3^{+1}	405.2138	405.2203	16.1	MeLeu-Tyr-Asn
b_6^{+1}	850.3212	850.3512	11.8	MeLeu-Tyr-Asn-Tyr_m-Hpg-Tyr_m
b_7^{+1}	1013.4045	1013.4183	13.6	MeLeu-Tyr-Asn-Tyr_m-Hpg-Tyr_m
y_2^{+1}	223.1436	223.1475	17.5	Tyr-propyl
y_5^{+1}	668.2709	668.2848	20.9	Tyr_m-Hpg-Tyr_m-Tyr-propyl
y_6^{+1}	782.3139	782.323	11.6	Asn-Tyr_m-Hpg-Tyr_m-Tyr-propyl
y_7^{+1}	945.3772	945.3873	10.7	Tyr-Asn-Tyr_m-Hpg-Tyr_m-Tyr-propyl

Table S7. NMR assignments for **6** in $(CD_3)_2SO$ from C- to N-terminus. The structure and number scheme for the compound is shown below the table.

Residue	Label	δH (ppm)	δC (ppm)
Pr	1	0.74	-
	2	1.32	-
	3	2.88;2.99	40.7
	NH	7.72	170.9
Tyr1	1	-	170.9
	2	4.36	55.0
	3	2.77;2.84	37.4
	4	-	128.1
	5	7.00	130.6
	6	6.62	115.3
	NH	8.14	-
Tyr2	1	-	171.1
	2	4.57	54.2
	3	2.60;2.90	-
	5	7.00	130.6
	6	6.61	115.3
	NH	-	-
Hpg3	1	-	170.6
	2	5.38	56.2
	3	-	128.5
	4	7.03	128.8
	5	6.60	115.3
	6	-	157.2
	NH	8.57	-
Tyr4	1	-	171.0
	2	4.32	55.1
	3	2.77;2.61	-
	5	6.82	130.6
	6	6.52	115.3
	7	-	156.2
	NH	8.35	-
Asn5	1	-	170.6
	2	4.57	-
	3	2.22;2.25	-
	NH	8.28	-
Tyr6	2	4.57	50.0
	3	2.90;2.60	-
	5	7.00	130.6
	6	6.62	115.3

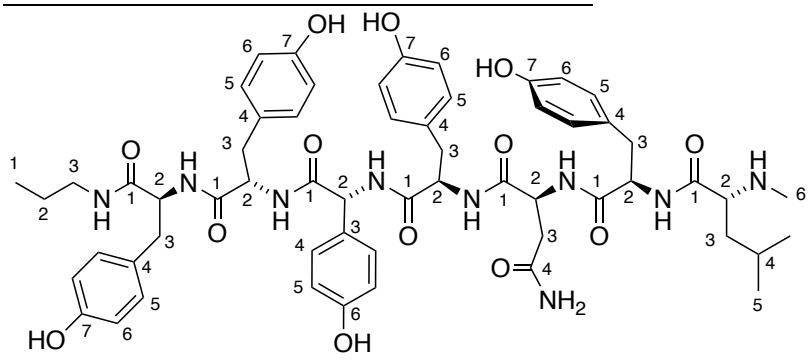

Table S8. NMR assignments for **7** in $(CD_3)_2SO$ from C- to N-terminus. The structure and number scheme for the compound is shown below the table.

Residue	Label	δH (ppm)	δC (ppm)
Pr	1	0.84	-
	2	1.26;1.46	-
	3	2.90;3.12	-
	NH	7.45	-
Tyr1	2	4.50	49.6
	3	2.58/2.80	-
	5	6.97	130.5
	6	6.62	115.3
	NH	8.06	-
Tyr2	2	4.25	57.1
	3	3.02;3.15	-
	5	7.13	140.5
	8	6.67	115.3
	9	7.03	128.5
	NH	8.21	-
Hpg3	2	5.42	56.9
	4	7.22	129.8
	5	6.77	115.6
	NH	8.63	-
Tyr4	2	4.50	54.2
	3	2.18;2.51	-
	5	6.64	139.5
	8	7.23	-
	9	6.90	129.5
	NH	8.12	-
Asn5	2	4.49	55.8
	3	2.17;2.42	-
	NH	7.99	-
Tyr6	2	4.46	53.8
	3	2.57;2.82	-
	5	6.95	130.6
	6	6.58	115.1
	NH	7.85	-
NMeLeu7	2	2.73	-
	3	1.10	-
	4	1.48	-
	5	0.78;0.73	-

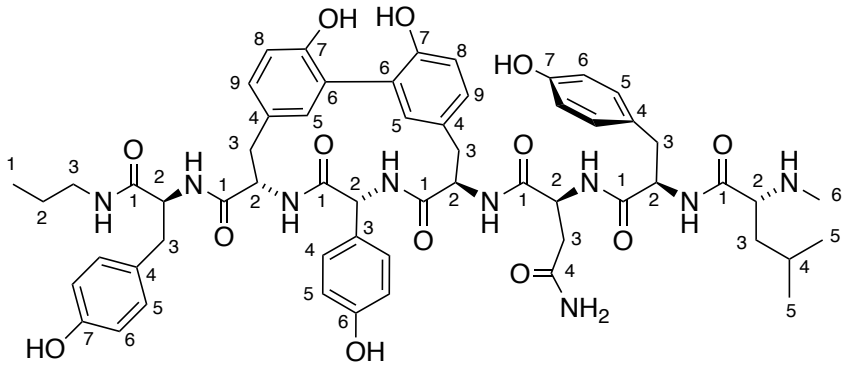

Table S9. NMR assignment for mycocyclosin in $(CD_3)_2SO$.[8]

Residue	Label	δH (ppm)	δC (ppm)
Tyr	2	4.32	55.6
	3	3.46;2.64	33.3
	5	6.57	141.4
	8	6.62	114.7
	9	6.84	129.8
	NH	7.99	-

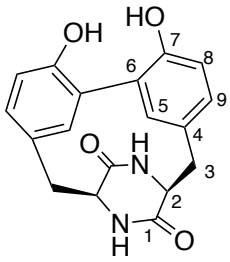

Table S10. NMR Assignment for arylomycin variant shown below in CD_3OH. Labelling of residues was assigned from C- to N-terminus.[9]

Residue	Label	δH (ppm)	δC (ppm)
L-Tyr1	2	4.57	55.6
	3	3.38;3.07	35.4
	5	6.78	134.2
	8	6.74	116.7
	9	7.03	130.5
L-Ala2	2	4.81	50.3
	3	1.32	19.0
L-Hpg3	2	6.33	61.5
	4	6.99	136.3
	7	7.31	116.6
	8	7.21	130.4

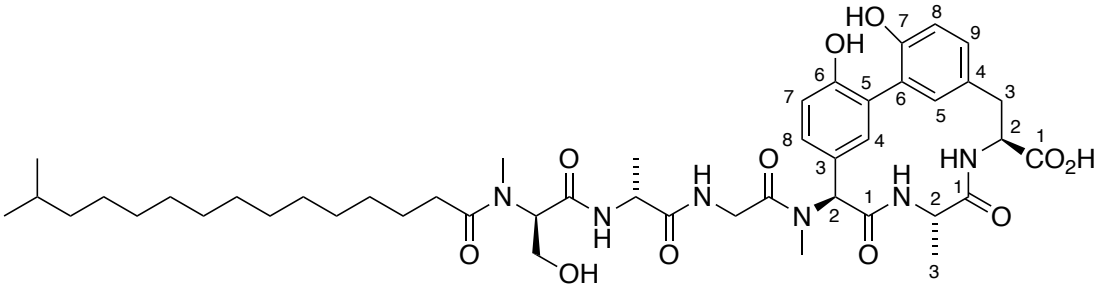

Table S11. HR-MS/MS data for **8** and its products upon reaction with OxyB, **9** and **10**.

*HR-MS/MS for substrate **8** (AA2 = L-homoTyr; AA4 = D-Hpg)*

Charge State	Calculated m/z	Observed m/z	Δppm	Sequence
b_1^{+1}	128.1075	128.1061	10.7	MeLeu
b_2^{+1}	291.1709	291.172	3.9	MeLeu-Tyr
b_3^{+1}	405.2138	405.2155	4.4	MeLeu-Tyr-Asn
b_4^{+1}	554.2615	554.2636	3.8	MeLeu-Tyr-Asn-Hpg
b_5^{+1}	703.3092	703.3105	1.8	MeLeu-Tyr-Asn-Hpg-Hpg
b_6^{+1}	880.3881	880.3884	0.4	MeLeu-Tyr-Asn-Hpg-Hpg-HomoTyr
b_7^{+1}	1043.4515	1043.4508	0.6	MeLeu-Tyr-Asn-Hpg-Hpg-HomoTyr-Tyr
y_2^{+1}	223.1436	223.1449	5.8	Tyr-propyl
y_3^{+1}	400.2225	400.2222	0.5	HomoTyr-Tyr-propyl
y_4^{+1}	549.2702	549.2678	4.2	Hpg-HomoTyr-Tyr-propyl
y_5^{+1}	698.3179	698.3157	3.1	Hpg-Hpg-HomoTyr-Tyr-propyl
y_6^{+1}	812.3608	812.3611	0.4	Asn-Hpg-Hpg-HomoTyr-Tyr-propyl
y_7^{+1}	975.4241	975.4265	2.4	Tyr-Asn-Hpg-Hpg-HomoTyr-Tyr-propyl

*HR-MS/MS for products **9** and **10** (AA2 = L-homoTyr; AA4 = D-Hpg)*

Charge State	Calculated m/z	Observed m/z	Δppm	Sequence
b_2^{+1}	291.1709	291.1719	3.4	MeLeu-Tyr
b_3^{+1}	405.2138	405.2152	6	MeLeu-Tyr-Asn
b_6^{+1}	878.3725	878.3745	2.2	MeLeu-Tyr-Asn-Hpg$_m$-Hpg-HomoTyr$_m$
b_7^{+1}	1041.4358	1041.4376	1.7	MeLeu-Tyr-Asn-Hpg$_m$-Hpg-HomoTyr$_m$
y_2^{+1}	223.1436	223.1446	4.8	Tyr-propyl
y_5^{+1}	696.3022	696.3031	1.3	Hpg$_m$-Hpg-HomoTyr$_m$-Tyr-propyl
y_6^{+1}	810.3452	810.3502	6.1	Asn-Hpg$_m$-Hpg-HomoTyr$_m$-Tyr-propyl
y_7^{+1}	973.4085	973.4118	3.4	Tyr-Asn-Hpg$_m$-Hpg-HomoTyr$_m$-Tyr-propyl

Table S12. HR-MS/MS data for starting material AA2 = *ortho*-$^2H_2$-L-homoTyr and AA4 = D-Hpg and products upon reaction with OxyB (-2 Da product, **11**; and -3 Da product, **12**).

HR-MS/MS for starting material AA2 = ortho-$^2H_2$- homo-L-Tyr and AA4 = D-Hpg

Charge State	Calculated m/z	Observed m/z	Δppm	Sequence
b_2^{+1}	291.1709	291.168	9.8	MeLeu-Tyr
b_3^{+1}	405.2138	405.2181	10.7	MeLeu-Tyr-Asn
b_4^{+1}	554.2615	554.2656	7.4	MeLeu-Tyr-Asn-Hpg
b_5^{+1}	703.3092	703.3133	5.9	MeLeu-Tyr-Asn-Hpg-Hpg
b_6^{+1}	882.4007	882.4	0.2	MeLeu-Tyr-Asn-Hpg-Hpg-$^2H_2$HomoTyr
b_7^{+1}	1045.4640	1045.4629	1.0	MeLeu-Tyr-Asn-Hpg-Hpg-$^2H_2$HomoTyr-Tyr
y_3^{+1}	402.2351	402.2404	13.2	$^2H_2$HomoTyr-Tyr-propyl
y_4^{+1}	551.2828	551.2761	12.1	Hpg-$^2H_2$HomoTyr-Tyr-propyl
y_5^{+1}	700.3304	700.3374	10.1	Hpg-Hpg-$^2H_2$HomoTyr-Tyr-propyl
y_6^{+1}	814.3734	814.3833	12.1	Asn-Hpg-Hpg-$^2H_2$HomoTyr-Tyr-propyl
y_7^{+1}	977.4367	977.4377	1.1	Tyr-Asn-Hpg-Hpg-$^2H_2$HomoTyr-Tyr-propyl

*HR-MS/MS for product **11** (-2Da product)*

Charge State	Calculated m/z	Observed m/z	Δppm	Sequence
b_2^{+1}	291.1709	291.1681	9.3	MeLeu-Tyr
b_3^{+1}	405.2138	405.218	10.5	MeLeu-Tyr-Asn
b_6^{+1}	880.3850	880.3845	0.4	MeLeu-Tyr-Asn-Hpg$_m$-Hpg-$^2H_2$HomoTyr$_m$
b_7^{+1}	1043.4484	1043.4446	3.6	MeLeu-Tyr-Asn-Hpg$_m$-Hpg-$^2H_2$HomoTyr$_m$
y_6^{+1}	812.3577	812.3594	2.1	Asn-Hpg$_m$-Hpg-$^2H_2$HomoTyr$_m$-Tyr-propyl
y_7^{+1}	975.4211	975.4296	0.4	Tyr-Asn-Hpg$_m$-Hpg-$^2H_2$HomoTyr$_m$-Tyr-propyl

*HR-MS/MS for product **12** (-3Da product)*

Charge State	Calculated m/z	Observed m/z	Δppm	Sequence
b_2^{+1}	291.1709	291.1705	1.0	MeLeu-Tyr
b_3^{+1}	405.2138	405.216	5.5	MeLeu-Tyr-Asn
b_6^{+1}	879.3788	879.3772	1.7	MeLeu-Tyr-Asn-Hpg$_m$-Hpg-$^2H_2$HomoTyr$_m$
y_7^{+1}	974.4148	974.4166	1.9	Tyr-Asn-Hpg$_m$-Hpg-$^2H_2$HomoTyr$_m$-Tyr-propyl

Table S13. HR-MS/MS data for starting material AA2 = L-homoTyr and AA4 = *ortho*-$^{2}H_2$-D-Hpg and products upon reaction with OxyB (-2 Da product, **13**; and -3 Da product, **14**).

HR-MS/MS for starting material AA2 = homo-L-Tyr and AA4 = ortho-$^{2}H_2$-D-Hpg

Charge State	Calculated m/z	Observed m/z	Δppm	Sequence
b_2^{+1}	291.1709	291.1669	13.5	MeLeu-Tyr
b_3^{+1}	405.2138	405.2154	3.9	MeLeu-Tyr-Asn
b_4^{+1}	556.274	556.2784	7.9	MeLeu-Tyr-Asn-Hpg
b_5^{+1}	705.3216	705.3216	0.1	MeLeu-Tyr-Asn-Hpg-$^{2}H_2$Hpg
b_6^{+1}	882.4007	882.3984	2.5	MeLeu-Tyr-Asn-Hpg-$^{2}H_2$Hpg-HomoTyr
b_7^{+1}	1045.464	1045.4598	4.0	MeLeu-Tyr-Asn-Hpg-$^{2}H_2$Hpg-HomoTyr-Tyr
y_3^{+1}	400.2225	400.2131	23.3	HomoTyr-Tyr-propyl
y_4^{+1}	549.2702	549.268	3.9	Hpg-HomoTyr-Tyr-propyl
y_5^{+1}	700.3304	700.3256	6.7	$^{2}H_2$Hpg-Hpg-HomoTyr-Tyr-propyl
y_6^{+1}	814.3732	814.3657	9.4	Asn-$^{2}H_2$Hpg-Hpg-HomoTyr-Tyr-propyl
y_7^{+1}	977.4367	977.4254	11.4	Tyr-Asn-$^{2}H_2$Hpg-Hpg-HomoTyr-Tyr-propyl

*HR-MS/MS for product **13** (-2Da product)*

Charge State	Calculated m/z	Observed m/z	Δppm	Sequence
b_3^{+1}	405.2138	405.2126	2.8	MeLeu-Tyr-Asn
b_6^{+1}	880.385	880.3772	8.8	MeLeu-Tyr-Asn-$^{2}H_2$Hpg$_m$-Hpg-HomoTyr$_m$
b_7^{+1}	1043.4484	1043.439	9.0	MeLeu-Tyr-Asn-$^{2}H_2$Hpg$_m$-Hpg-HomoTyr$_m$
y_6^{+1}	812.3577	812.3626	6.1	Asn-$^{2}H_2$Hpg$_m$-Hpg-HomoTyr$_m$-Tyr-propyl
y_7^{+1}	975.4211	975.411	10.2	Tyr-Asn-$^{2}H_2$Hpg$_m$-Hpg-HomoTyr$_m$-Tyr-propyl

*HR-MS/MS for product **14** (-3 Da product)*

Charge State	Calculated m/z	Observed m/z	Δppm	Sequence
b_2^{+1}	291.1709	291.1652	19.3	MeLeu-Tyr
b_3^{+1}	405.2138	405.2137	0.2	MeLeu-Tyr-Asn
b_6^{+1}	879.3788	879.3812	2.7	MeLeu-Tyr-Asn-$^{2}H_2$Hpg$_m$-Hpg-HomoTyr$_m$
b_7^{+1}	1042.4421	1042.4326	9.0	MeLeu-Tyr-Asn-$^{2}H_2$Hpg$_m$-Hpg-HomoTyr$_m$
y_6^{+1}	811.3514	811.3393	14.8	Asn-$^{2}H_2$Hpg$_m$-Hpg-HomoTyr$_m$-Tyr-propyl
y_7^{+1}	974.4148	974.4125	2.3	Tyr-Asn-$^{2}H_2$Hpg$_m$-Hpg-HomoTyr$_m$-Tyr-propyl

Table S14. HR-MS/MS data for starting material **15** (AA2 = L-Tyr, AA4 = L-Hpg) and its product upon reaction with OxyB, **16**.

*HR-MS/MS for starting material **15** (AA2 = L-Tyr; AA4 = L-Hpg)*

Charge State	Calculated m/z	Observed m/z	Δppm	Sequence
b_2^{+1}	291.1709	291.1756	16.3	MeLeu-Tyr
b_3^{+1}	405.2138	405.2199	15.2	MeLeu-Tyr-Asn
b_4^{+1}	554.2615	554.2701	15.5	MeLeu-Tyr-Asn-(L)Hpg
b_5^{+1}	703.3092	703.3198	15.1	MeLeu-Tyr-Asn-(L)Hpg-Hpg
b_6^{+1}	866.3725	866.3827	11.8	MeLeu-Tyr-Asn-(L)Hpg-Hpg-(L)Tyr
b_7^{+1}	1029.4358	1029.4463	10.2	MeLeu-Tyr-Asn-(L)Hpg-Hpg-(L)Tyr-Tyr
y_3^{+1}	386.2069	386.2137	17.6	(L)Tyr-Tyr-propyl
y_4^{+1}	535.2546	535.2647	18.9	Hpg-(L)Tyr-Tyr-propyl
y_5^{+1}	684.3022	684.3126	15.3	(L)Hpg-Hpg-(L)Tyr-Tyr-propyl
y_6^{+1}	798.3452	798.35	6.0	Asn-(L)Hpg-Hpg-(L)Tyr-Tyr-propyl
y_7^{+1}	961.4085	961.4222	14.2	Tyr-Asn-(L)Hpg-Hpg-(L)Tyr-Tyr-propyl

*HR-MS/MS for starting material **16** (AA2 = L-Tyr; AA4 = L-Hpg)*

Charge State	Calculated m/z	Observed m/z	Δppm	Sequence
b_2^{+1}	291.1709	291.1751	14.5	MeLeu-Tyr
b_3^{+1}	405.2138	405.2205	16.6	MeLeu-Tyr-Asn
b_4^{+1}	554.2615	554.2632	1.3	MeLeu-Tyr-Asn-(L)Hpg
b_6^{+1}	864.3491	864.362	6.1	MeLeu-Tyr-Asn-(L)Hpg-Hpg$_m$-(L)Tyr$_m$
b_7^{+1}	1027.4202	1027.4229	2.7	MeLeu-Tyr-Asn-(L)Hpg-Hpg$_m$-(L)Tyr$_m$-Tyr
y_2^{+1}	223.1472	223.1468	16.2	Tyr-propyl
y_4^{+1}	533.2389	533.2445	10.5	Hpg$_m$-(L)Tyr$_m$-Tyr-propyl
y_5^{+1}	682.2866	682.2964	14.4	(L)Hpg-Hpg$_m$-(L)Tyr$_m$-Tyr-propyl
y_6^{+1}	796.3295	796.3391	12.1	Asn-(L)Hpg-Hpg$_m$-(L)Tyr$_m$-Tyr-propyl
y_7^{+1}	959.3928	959.4035	11.1	Tyr-Asn-(L)Hpg-Hpg$_m$-(L)Tyr$_m$-Tyr-propyl

Table S15. NMR assignments for **15** in $(CD_3)_2SO$ from C- to N-terminus. The structure and number scheme for the compound is shown below the table.

Residue	Label	δH (ppm)	δC (ppm)
Pr	1	0.76	11.7
	2	1.32	22.7
	3	2.93;3.00	40.7
	NH	7.76	-
Tyr1	1	-	171.1
	2	4.34	55.0
	3	2.75;2.84	37.5
	5	7.02	130.6
	6	6.64	115.0
	NH	8.19	-
Tyr2	1	-	171.1
	2	4.34	55.0
	3	2.55;2.80	37.4
	5	6.84	130.6
	6	6.51	115.1
	NH	8.38	-
Hpg3	1	-	170.1
	2	5.35	55.8
	4	6.73	128.1
	5	6.48	115.0
	NH	8.64	-
Hpg4	1	-	170.0
	2	5.50	55.7
	4	7.15	128.7
	5	6.63	115.3
	NH	8.25	-
Asn5	1	-	170.3
	2	4.70	-
	3	2.37;2.55	37.4
	4	-	172.0
Tyr6	1	-	171.7
	2	4.61	53.7
	3	2.62;2.91	38.0
	5	6.99	130.6
	6	6.60	115.1

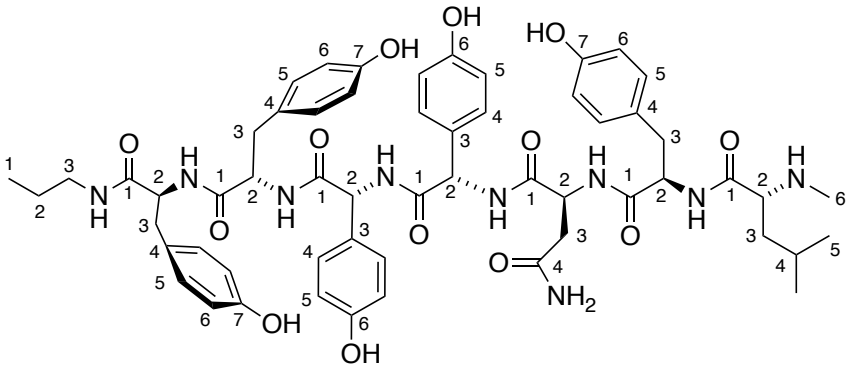

Table S16. NMR assignments for **16** in $(CD_3)_2SO$ from C- to N-terminus. The structure and number scheme for the compound is shown below the table.

Residue	Label	δH (ppm)	δC (ppm)
Tyr1	2	4.54	55.6
	3	3.37;2.31	-
	5	7.06	129.2
	6	6.71	115.6
	NH	7.76	-
Tyr2	2	4.31	57.1
	3	3.14;2.89	-
	5	7.14	140.8
	8	6.67	114.9
	9	7.00	128.4
	NH	8.21	-
Hpg3	2	5.38	56.5
	4	6.63	139.7
	7	6.62	115.2
	8	6.55	133.6
	NH	8.86	-
Hpg4	2	5.55	55.2
	4	7.11	128.4
	5	6.61	115.2
	NH	8.21	-
Asn5	2	4.68	49.9
	3	2.38;2.52	-
	NH	8.38	-
Tyr6	2	4.54	53.5
	3	2.62;2.87	-
	5	6.96	130.6
	6	6.60	115.2
NMeLeu7	2	4.65	-
	3	2.38;2.48	-
	4	1.48	-
	5	0.79;0.74	-
	NH	8.43	-

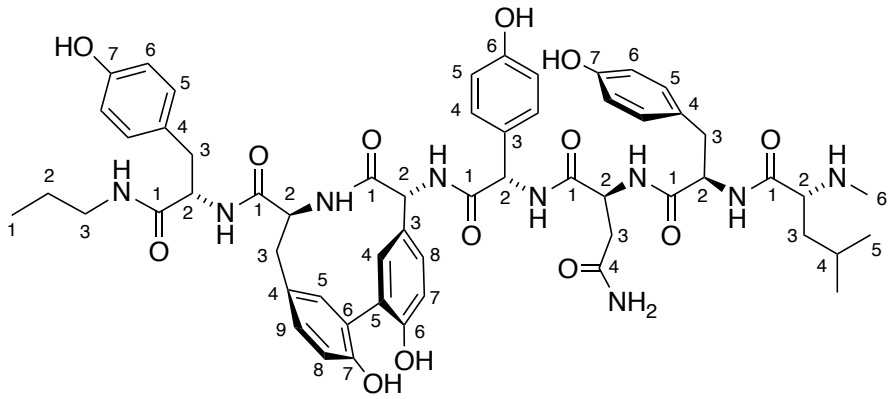

Table S17. HR-MS/MS data for starting material **17** (AA2 = D-Tyr, AA4 = D-Hpg) and its product upon reaction with OxyB, **18**.

*HR-MS/MS for starting material **17** (AA2 = D-Tyr, AA4 = D-Hpg)*

Charge State	Calculated m/z	Observed m/z	Δppm	Sequence
b_1^{+1}	128.1075	128.1097	17.0	MeLeu
b_2^{+1}	291.1709	291.1737	9.7	MeLeu-Tyr
b_3^{+1}	405.2138	405.2178	9.8	MeLeu-Tyr-Asn
b_4^{+1}	554.2615	554.2664	8.9	MeLeu-Tyr-Asn-(D)Hpg
b_5^{+1}	703.3092	703.3138	6.5	MeLeu-Tyr-Asn-(D)Hpg-Hpg
b_6^{+1}	866.3725	866.3781	6.5	MeLeu-Tyr-Asn-(D)Hpg-Hpg-(D)Tyr
b_7^{+1}	1029.4358	1029.4406	4.6	MeLeu-Tyr-Asn-(D)Hpg-Hpg-(D)Tyr-Tyr
y_2^{+1}	223.1426	223.1458	14.6	Tyr-propyl
y_3^{+1}	386.2069	386.21306	15.9	(D)Tyr-Tyr-propyl
y_4^{+1}	535.2546	535.2634	16.4	Hpg-(D)Tyr-Tyr-propyl
y_5^{+1}	684.3022	684.3067	6.6	(D)Hpg-Hpg-(D)Tyr-Tyr-propyl
y_7^{+1}	961.4085	961.4152	7.0	Tyr-Asn-(D)Hpg-Hpg-(D)Tyr-Tyr-propyl

*HR-MS/MS for product **18** (AA2 = D-Tyr, AA4 = D-Hpg)*

Charge State	Calculated m/z	Observed m/z	Δppm	Sequence
b_2^{+1}	291.1709	291.174	10.7	MeLeu-Tyr
b_3^{+1}	405.2138	405.2182	10.8	MeLeu-Tyr-Asn
b_6^{+1}	864.3491	864.3568	8.8	MeLeu-Tyr-Asn-(D)Hpg$_m$-Hpg-(D)Tyr$_m$
b_7^{+1}	1027.4202	1027.4109	9	MeLeu-Tyr-Asn-(D)Hpg$_m$-Hpg-(D)Tyr$_m$-Tyr
y_2^{+1}	223.1436	223.1455	8.8	Tyr-propyl
y_5^{+1}	682.2866	682.2931	9.6	(D)Hpg$_m$-Hpg-(D)Tyr$_m$-Tyr-propyl
y_6^{+1}	796.3295	796.338	10.7	Asn-(D)Hpg$_m$-Hpg-(D)Tyr$_m$-Tyr-propyl
y_7^{+1}	959.3928	959.4027	10.3	Tyr-Asn-(D)Hpg$_m$-Hpg-(D)Tyr$_m$-Tyr-propyl

Table S18. HR-MS/MS data for starting material AA2 = D-Tyr and AA4 = *ortho*-$^{2}H_2$-D-Hpg and -3 Da product upon reaction with OxyB (**19**).

HR-MS/MS for starting material AA2 = D-Tyr and AA4 =ortho-$^{2}H_2$-D-Hpg

Charge State	Calculated m/z	Observed m/z	Δppm	Sequence
b_2^{+1}	291.1709	291.1711	0.9	MeLeu-Tyr
b_3^{+1}	405.2138	405.2162	6.0	MeLeu-Tyr-Asn
b_4^{+1}	556.274	556.2765	4.6	MeLeu-Tyr-Asn-(D)$^{2}H_2$Hpg
b_5^{+1}	705.3217	705.3238	2.9	MeLeu-Tyr-Asn-(D)$^{2}H_2$Hpg-Hpg
b_6^{+1}	868.3879	868.385	3.3	MeLeu-Tyr-Asn-(D)$^{2}H_2$Hpg-Hpg-(D)Tyr
b_7^{+1}	1031.4484	1031.4515	3.0	MeLeu-Tyr-Asn-(D)$^{2}H_2$Hpg-Hpg-(D)Tyr-Tyr
y_2^{+1}	223.1426	223.1418	7.7	Tyr-propyl
y_3^{+1}	386.2069	386.2103	8.8	(D)Tyr-Tyr-propyl
y_4^{+1}	535.2546	535.2569	4.3	Hpg-(D)Tyr-Tyr-propyl
y_5^{+1}	686.3148	686.3152	0.6	(D)$^{2}H_2$Hpg-Hpg-(D)Tyr-Tyr-propyl
y_6^{+1}	800.3577	800.3598	2.6	Asn-(D)$^{2}H_2$Hpg-Hpg-(D)Tyr-Tyr-propyl
y_7^{+1}	963.4211	963.4242	3.2	Tyr-Asn-(D)$^{2}H_2$Hpg-Hpg-(D)Tyr-Tyr-propyl

*HR-MS/MS for product **19***

Charge State	Calculated m/z	Observed m/z	Δppm	Sequence
b_2^{+1}	291.1709	291.1702	2.2	MeLeu-Tyr
b_3^{+1}	405.2138	405.2151	3.4	MeLeu-Tyr-Asn
b_6^{+1}	865.3631	865.368	5.6	MeLeu-Tyr-Asn-(D)$^{2}H_2$Hpg$_m$-Hpg-(D)Tyr$_m$
b_7^{+1}	1028.4264	1028.429	2.5	MeLeu-Tyr-Asn-(D)$^{2}H_2$Hpg$_m$-Hpg-(D)Tyr$_m$-Tyr
y_2^{+1}	223.1436	223.1411	11.1	Tyr-propyl
y_5^{+1}	683.2929	683.2944	2.2	(D)$^{2}H_2$Hpg$_m$-Hpg-(D)Tyr$_m$-Tyr-propyl
y_6^{+1}	797.3358	797.3409	6.4	Asn-(D)$^{2}H_2$Hpg$_m$-Hpg-(D)Tyr$_m$-Tyr-propyl
y_7^{+1}	960.3991	960.4027	3.8	Tyr-Asn-(D)$^{2}H_2$Hpg$_m$-Hpg-(D)Tyr$_m$-Tyr-propyl

Table S19. HR-MS/MS data for starting material **20** (AA2 = D-Tyr, AA4 = L-Hpg) and products **21**, **22**.

*HR-MS/MS for starting material **20** (AA2 = D-Tyr, AA4 = L-Hpg)*

Charge State	Calculated m/z	Observed m/z	Δppm	Sequence
b_1^{+1}	128.1075	128.1079	3.6	MeLeu
b_2^{+1}	291.1709	291.1752	14.9	MeLeu-Tyr
b_3^{+1}	405.2138	405.2205	16.5	MeLeu-Tyr-Asn
b_4^{+1}	554.2615	554.2699	15.5	MeLeu-Tyr-Asn-(L)Hpg
b_5^{+1}	703.3092	703.3199	15.2	MeLeu-Tyr-Asn-(L)Hpg-Hpg
b_6^{+1}	866.3725	866.3818	10.8	MeLeu-Tyr-Asn-(L)Hpg-Hpg-(D)Tyr
b_7^{+1}	1029.4358	1029.4459	9.8	MeLeu-Tyr-Asn-(L)Hpg-Hpg-(D)Tyr-Tyr
y_3^{+1}	386.2069	386.2122	13.8	(D)Tyr-Tyr-propyl
y_4^{+1}	535.2546	535.2633	16.4	Hpg-(D)Tyr-Tyr-propyl
y_5^{+1}	684.3022	684.3104	12.0	(L)Hpg-Hpg-(D)Tyr-Tyr-propyl
y_6^{+1}	798.3452	798.3561	13.7	Asn-(L)Hpg-Hpg-(D)Tyr-Tyr-propyl
y_7^{+1}	961.4085	961.4276	19.9	Tyr-Asn-(L)Hpg-Hpg-(D)Tyr-Tyr-propyl

*HR-MS/MS for products **21**,**22** (AA2 = D-Tyr, AA4 = L-Hpg)*

Charge State	Calculated m/z	Observed m/z	Δppm	Sequence
b_2^{+1}	291.1709	291.174	19.1	MeLeu-Tyr
b_3^{+1}	405.2138	405.2204	16.3	MeLeu-Tyr-Asn
b_6^{+1}	864.3491	864.368	13.1	MeLeu-Tyr-Asn-(L)Hpg$_m$-Hpg-(D)Tyr$_m$
b_7^{+1}	1027.4202	1027.4375	16.9	MeLeu-Tyr-Asn-(L)Hpg$_m$-Hpg-(D)Tyr$_m$-Tyr
y_2^{+1}	223.1436	223.1468	19	Tyr-propyl
y_6^{+1}	796.3295	796.3424	16.3	Asn-(L)Hpg$_m$-Hpg-(D)Tyr$_m$-Tyr-propyl
y_7^{+1}	959.3928	959.3989	6.3	Tyr-Asn-(L)Hpg$_m$-Hpg-(D)Tyr$_m$-Tyr-propyl

Table S20. HR-MS/MS data for starting material AA2 = D-Tyr and AA4 = *ortho*-$^2H_2$-L-Hpg and products upon reaction with OxyB (-2 Da product, **23**; and -3 Da product, **24**).

HR-MS/MS for starting material AA2 =D-Tyr and AA4 = ortho-$^2H_2$-L-Hpg

Charge State	Calculated m/z	Observed m/z	Δppm	Sequence
b_2^{+1}	291.1709	291.1708	0.1	MeLeu-Tyr
b_3^{+1}	405.2138	405.2161	5.7	MeLeu-Tyr-Asn
b_4^{+1}	556.274	556.2767	4.9	MeLeu-Tyr-Asn-(L)$^2H_2$Hpg
b_5^{+1}	705.3217	705.3244	3.9	MeLeu-Tyr-Asn-(L)$^2H_2$Hpg-Hpg
b_6^{+1}	868.385	868.3877	3.1	MeLeu-Tyr-Asn-(L)$^2H_2$Hpg-Hpg-(D)Tyr
b_7^{+1}	1031.4484	1031.452	3.5	MeLeu-Tyr-Asn-(L)$^2H_2$Hpg-Hpg-(D)Tyr-Tyr
y_2^{+1}	223.1436	223.1413	9.9	Tyr-propyl
y_3^{+1}	386.2069	386.2087	4.6	(D)Tyr-Tyr-propyl
y_4^{+1}	535.2566	535.2566	0.1	Hpg-(D)Tyr-Tyr-propyl
y_5^{+1}	686.3148	686.3179	4.5	(L)$^2H_2$Hpg-Hpg-(D)Tyr-Tyr-propyl
y_6^{+1}	800.3577	800.3615	4.8	Asn-(L)$^2H_2$Hpg-Hpg-(D)Tyr-Tyr-propyl
y_7^{+1}	963.4211	963.4254	4.5	Tyr-Asn-(L)$^2H_2$Hpg-Hpg-(D)Tyr-Tyr-propyl

*HR-MS/MS for product **23** (-2Da product)*

Charge State	Calculated m/z	Observed m/z	Δppm	Sequence
b_2^{+1}	291.1709	291.1683	8.8	MeLeu-Tyr
b_3^{+1}	405.2138	405.2131	1.7	MeLeu-Tyr-Asn
b_6^{+1}	866.3694	866.3734	4.6	MeLeu-Tyr-Asn-(L)$^2H_2$Hpg$_m$-Hpg-(D)Tyr$_m$
b_7^{+1}	1029.4327	1029.4341	1.3	MeLeu-Tyr-Asn-(L)$^2H_2$Hpg$_m$-Hpg-(D)Tyr$_m$-Tyr
y_2^{+1}	223.1436	223.1436	15.7	Tyr-propyl
y_5^{+1}	684.2991	684.2931	8.6	(L)$^2H_2$Hpg$_m$-Hpg-(D)Tyr$_m$-Tyr-propyl
y_7^{+1}	961.4054	961.4013	4.2	Tyr-Asn-(L)$^2H_2$Hpg$_m$-Hpg-(D)Tyr$_m$-Tyr-propyl

*HR-MS/MS for product **24** (-3Da product)*

Charge State	Calculated m/z	Observed m/z	Δppm	Sequence
b_2^{+1}	291.1709	291.1679	9.9	MeLeu-Tyr
b_3^{+1}	405.2138	405.2146	2.0	MeLeu-Tyr-Asn
b_6^{+1}	865.3631	865.3581	5.6	MeLeu-Tyr-Asn-(L)$^2H_2$Hpg$_m$-Hpg-(D)Tyr$_m$
b_7^{+1}	1028.4264	1028.4303	3.7	MeLeu-Tyr-Asn-(L)$^2H_2$Hpg$_m$-Hpg-(D)Tyr$_m$-Tyr
y_2^{+1}	223.1436	223.1436	6.9	Tyr-propyl
y_5^{+1}	683.2929	683.2947	2.6	Asn-(L)$^2H_2$Hpg$_m$-Hpg-(D)Tyr$_m$-Tyr-propyl
y_7^{+1}	960.3991	960.3942	5.0	Tyr-Asn-(L)$^2H_2$Hpg$_m$-Hpg-(D)Tyr$_m$-Tyr-propyl

Table S21. HR-MS data for substrates and products of OxyB enzymatic reactions to generate analogs with varying hydroxyl group substituents. Sequence of peptides shown is (AA1)-AA2-(AA3)-AA4-(L-Asn5)-(D-Tyr6)-(*N*-Me-D-Leu7).

Compound	AA1	AA2	AA3	AA4	Charge State	Calculated mass	Observed mass	Δppm
25	L-Tyr	L-Tyr	D-Hpg	D-PhGly	$[M+H]^+$	1072.5138	1072.51447	0.6
26	L-Tyr	L-Tyr	D-Hpg	D-PhGly	$[M+H]^+$	1070.4982	1070.49859	0.3
27	L-Tyr	L-Phe	D-Hpg	D-Hpg	$[M+H]^+$	1072.5138	1072.51447	0.7
28-31	L-Tyr	L-Phe	D-Hpg	D-Hpg	$[M+H]^+$	1070.4982	1070.49859	0.1
S1	L-Tyr	$^2H_5$-L-Phe	D-Hpg	D-Hpg	$[M+H]^+$	1077.5452	1077.55852	12.3
S1-S5	L-Tyr	$^2H_5$-L-Phe	D-Hpg	D-Hpg	$[M+H]^+$	1075.5296	1075.54143	10.9
S6	$^2H_2$-L-Tyr	L-Phe	D-Hpg	D-Hpg	$[M+H]^+$	1074.5264	1074.53947	12.1
S7-S9	$^2H_2$-L-Tyr	L-Phe	D-Hpg	D-Hpg	$[M+H]^+$	1072.5107	1072.516	4.9
S10	$^2H_2$-L-Tyr	L-Phe	D-Hpg	D-Hpg	$[M+H]^+$	1071.5045	1071.50939	4.5
S11	L-Tyr	L-Phe	D-Hpg	$^2H_2$-D-Hpg	$[M+H]^+$	1074.5264	1074.53615	9.0
S12, 14, 15	L-Tyr	L-Phe	D-Hpg	$^2H_2$-D-Hpg	$[M+H]^+$	1072.5107	1072.51929	8.0
S13	L-Tyr	L-Phe	D-Hpg	$^2H_2$-D-Hpg	$[M+H]^+$	1071.5045	1071.5139	8.7
S16	L-Tyr	L-Phe	$^2H_2$-D-Hpg	D-Hpg	$[M+H]^+$	1074.5264	1074.54043	13.0
S18, S20	L-Tyr	L-Phe	$^2H_2$-D-Hpg	D-Hpg	$[M+H]^+$	1072.5107	1072.51987	8.5
S17, S19	L-Tyr	L-Phe	$^2H_2$-D-Hpg	D-Hpg	$[M+H]^+$	1071.5045	1071.51482	9.6
32	L-Tyr	L-Phe	D-Hpg	D-PhGly	$[M+H]^+$	1056.5189	1056.52202	2.9
33	L-Tyr	L-Phe	D-Hpg	D-PhGly	$[M+H]^+$	1054.5033	1054.50517	1.7

Table S22. HR-MS/MS data for starting material **25** (AA2 = L-Tyr, AA4 = D-PhGly) and product **26**.

*HR-MS/MS for starting material **25** (AA2 = L-Tyr, AA4 = D-PhGly)*

Charge State	Calculated m/z	Observed m/z	Δppm	Sequence
b_2^{+1}	291.1709	291.1713	1.6	MeLeu-Tyr
b_3^{+1}	405.2138	405.2147	2.4	MeLeu-Tyr-Asn
b_4^{+1}	538.2666	538.2690	4.6	MeLeu-Tyr-Asn-PhGly
b_5^{+1}	687.3142	687.3164	3.3	MeLeu-Tyr-Asn-PhGly-Hpg
b_6^{+1}	850.3776	850.3811	4.1	MeLeu-Tyr-Asn-PhGly-Hpg-Tyr
b_7^{+1}	1013.4409	1013.4449	3.9	MeLeu-Tyr-Asn-PhGly-Hpg-Tyr-Tyr
y_2^{+1}	223.1436	223.1450	6.6	Tyr-propyl
y_3^{+1}	386.2069	386.2075	1.7	Tyr-Tyr-propyl
y_4^{+1}	535.2536	535.2627	17.1	Hpg-Tyr-Tyr-propyl
y_5^{+1}	668.3073	668.3117	6.6	PhGly-Hpg-Tyr-Tyr-propyl
y_6^{+1}	782.3503	782.3610	13.6	Asn-PhGly-Hpg-Tyr-Tyr-propyl
y_7^{+1}	945.4136	945.4128	0.7	Tyr-Asn-PhGly-Hpg-Tyr-Tyr-propyl

*HR-MS/MS for product **26** (AA2 = L-Tyr, AA4 = D-PhGly)*

Charge State	Calculated m/z	Observed m/z	Δppm	Sequence
b_2^{+1}	291.1709	291.1715	2.2	MeLeu-Tyr
b_3^{+1}	405.2138	405.2149	2.9	MeLeu-Tyr-Asn
b_4^{+1}	538.2666	538.2679	2.4	MeLeu-Tyr-Asn-PhGly
b_5^{+1}	687.3142	687.3072	10	MeLeu-Tyr-Asn-PhGly-Hpg-Tyr_m-Tyr_m
b_7^{+1}	1011.4252	1011.4225	2.6	MeLeu-Tyr-Asn-PhGly-Hpg-Tyr_m-Tyr_m
y_3^{+1}	384.1912	384.1930	4.7	Tyr_m-Tyr_m-propyl
y_4^{+1}	533.2389	533.2468	14.9	Hpg-Tyr_m-Tyr_m-propyl
y_5^{+1}	666.2917	666.2963	6.9	PhGly-Hpg-Tyr_m-Tyr_m-propyl
y_6^{+1}	780.3346	780.3365	2.5	Asn-PhGly-Hpg-Tyr_m-Tyr_m-propyl
y_7^{+1}	943.3979	943.4005	2.7	Tyr-Asn-PhGly-Hpg-Tyr_m-Tyr_m-propyl

Table S23. NMR assignments for **25** in $(CD_3)_2SO$ from C- to N-terminus. The structure and number scheme for the compound is shown below the table.

Residue	Label	δH (ppm)	δC (ppm)
Tyr1	2	4.33	54.8
	3	2.75	-
	5	6.95	115.3
	6	6.62	130.4
	NH	8.04	-
Tyr2	2	4.30	54.9
	3	2.68;2.53	-
	5	6.73	130.6
	6	6.47	115.2
	NH	8.14	-
Hpg3	1	-	170.1
	2	5.38	56.2
	4	7.02	128.8
	5	6.63	115.3
	NH	8.86	-
PhGly4	1	-	169.4
	2	5.65	56.1
	4	7.39	127.3
	5	7.23	128.6
	NH	8.19	-
Asn5	1	-	170.7
	2	4.64	50.2
	3	2.47;2.34	-
	NH	8.29	-
Tyr6	2	4.53	53.9
	3	2.64;2.88	-
	5	6.96	130.6
	6	6.59	115.1
	NH	7.94	-

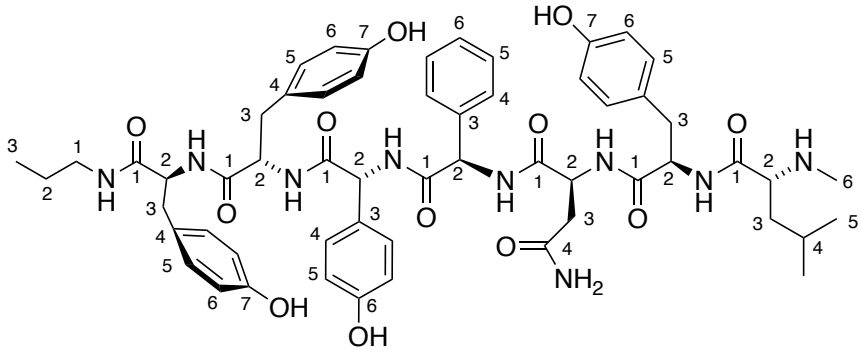

Table S24. NMR assignments for **26** in $(CD_3)_2SO$ from C- to N-terminus. The structure and number scheme for the compound is shown below the table.

Residue	Label	δH (ppm)	δC (ppm)
Pr	NH	7.50	-
Tyr1	2	4.23	56.9
	3	2.94;2.81	-
	5	7.02	140.8
	8	6.64	115.7
	9	6.97	130.6
	NH	8.09	-
Tyr2	2	4.50	55.6
	3	2.28;3.32	-
	5	6.55	139.6
	8	6.55	115.3
	9	6.39	129.6
	NH	7.46	-
Hpg3	2	5.45	56.6
	4	7.17	129.4
	5	6.78	115.7
	NH	8.94	-
PhGly4	2	5.62	56.1
	4	7.39	127.4
	5	7.28	128.6
	6	7.26	-
	NH	8.37	-
Asn5	2	4.63	50.0
	3	2.34;2.45	-
	NH	8.32	-
Tyr6	2	4.51	53.9
	3	2.86;2.64	-
	5	6.97	128.5
	6	6.61	115.2
	NH	7.93	-

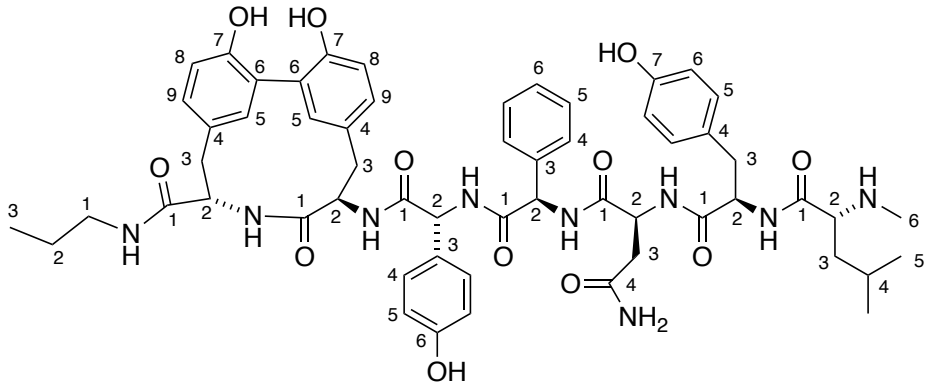

Table S25. HR-MS/MS for substrate **S1**, with isotopically labelled AA2 ($^2H_5$-L-Phe), and -2 Da products obtained upon reaction with OxyB (**S2**, **S3**, **S4**).

*HR-MS/MS for substrate **S1**, containing labelled AA2 ($^2H_5$-L-Phe)*

Charge State	Calculated m/z	Observed m/z	Δppm	Sequence
b_1^{+1}	128.1075	128.1094	14.8	MeLeu
b_2^{+1}	291.1709	291.1755	15.7	MeLeu-Tyr
b_3^{+1}	405.2138	405.2206	16.7	MeLeu-Tyr-Asn
b_4^{+1}	554.2615	554.2708	16.7	MeLeu-Tyr-Asn-Hpg
b_5^{+1}	703.3092	703.3205	16.0	MeLeu-Tyr-Asn-Hpg-Hpg
b_6^{+1}	855.4089	855.4222	15.5	MeLeu-Tyr-Asn-Hpg-Hpg-$^2H_5$Phe
b_7^{+1}	1018.472	1018.488	15.6	MeLeu-Tyr-Asn-Hpg-Hpg-$^2H_5$Phe-Tyr
y_2^{+1}	223.1426	223.1482	20.6	Tyr-propyl
y_3^{+1}	375.2434	375.2499	17.3	$^2H_5$Phe-Tyr-propyl
y_4^{+1}	524.291	524.299	15.2	Hpg-$^2H_5$Phe-Tyr-propyl
y_5^{+1}	673.2287	673.349	15.2	Hpg-Hpg-$^2H_5$Phe-Tyr-propyl
y_6^{+1}	787.3816	787.3934	14.9	Asn-Hpg-Hpg-$^2H_5$Phe-Tyr-propyl
y_7^{+1}	950.445	950.4607	16.5	Tyr-Asn-Hpg-Hpg-$^2H_5$Phe-Tyr-propyl

*HR-MS/MS for -2 Da products **S2**, **S3**, **S4**, containing labelled AA2 ($^2H_5$-L-Phe)*

Charge State	Calculated m/z	Observed m/z	Δppm	Sequence
b_2^{+1}	291.1709	291.1756	16.1	MeLeu-Tyr
b_3^{+1}	405.2138	405.22	15.3	MeLeu-Tyr-Asn
b_4^{+1}	554.2615	554.2615	15.5	MeLeu-Tyr-Asn-Hpg
b_5^{+1}	701.2935	701.3025	12.8	MeLeu-Tyr-Asn-Hpg-Hpg
b_5^{+1}	703.3092	703.3192	14.2	MeLeu-Tyr-Asn-Hpg-Hpg
b_6^{+1}	853.3933	853.4071	16.1	MeLeu-Tyr-Asn-Hpg-Hpg-$^2H_5$Phe
b_7^{+1}	1016.4566	1016.4707	13.8	MeLeu-Tyr-Asn-Hpg-Hpg-$^2H_5$Phe-Tyr
y_2^{+1}	223.1436	223.1478	18.8	Tyr-propyl
y_4^{+1}	522.2754	522.2848	17.9	Hpg-$^2H_5$Phe-Tyr-propyl
y_5^{+1}	671.3231	671.3294	9.3	Hpg-Hpg-$^2H_5$Phe-Tyr-propyl
y_6^{+1}	785.366	785.3785	15.9	Asn-Hpgm-Hpg-$^2H_5$Phe-Tyr-propyl
y_7^{+1}	948.4423	948.4293	13.7	Tyr-Asn-Hpg-Hpg-$^2H_5$Phe-Tyr-propyl

Table S26. HR-MS/MS for substrate **S6**, with isotopically labelled AA1 (*ortho*-$^2H_2$-L-Tyr), and products obtained upon reaction with OxyB (-2 Da products, **S7**, **S8**, **S9**; -3Da product, **S10**).

*HR-MS/MS for substrate **S6**, containing labelled AA1 (ortho-$^2H_2$-L-Tyr)*

Charge State	Calculated m/z	Observed m/z	Δppm	Sequence
b_2^{+1}	291.1709	291.1771	21.2	MeLeu-Tyr
b_3^{+1}	405.2138	405.2229	22.4	MeLeu-Tyr-Asn
b_4^{+1}	554.2615	554.2741	22.7	MeLeu-Tyr-Asn-Hpg
b_5^{+1}	703.3092	703.3237	20.6	MeLeu-Tyr-Asn-Hpg-Hpg
b_6^{+1}	850.3776	850.3958	21.4	MeLeu-Tyr-Asn-Hpg-Hpg-Phe
b_7^{+1}	1015.453	1015.475	21.2	MeLeu-Tyr-Asn-Hpg-Hpg-Phe-$^2H_2$Tyr
y_2^{+1}	225.1561	225.1619	25.7	$^2H_2$Tyr-propyl
y_3^{+1}	372.2245	372.2331	23.1	Phe-$^2H_2$Tyr-propyl
y_4^{+1}	521.2722	521.2831	20.9	Hpg-Phe-$^2H_2$Tyr-propyl
y_5^{+1}	670.3199	670.3263	9.5	Hpg-Hpg-Phe-$^2H_2$Tyr-propyl
y_6^{+1}	784.3628	784.3791	20.7	Asn-Hpg-Hpg-Phe-$^2H_2$Tyr-propyl
y_7^{+1}	947.4261	947.4468	21.8	Tyr-Asn-Hpg-Hpg-Phe-$^2H_2$Tyr-propyl

*HR-MS/MS for -2 Da products **S7**, **S8**, **S9**, containing labelled AA1 (ortho-$^2H_2$-L-Tyr)*

Charge State	Calculated m/z	Observed m/z	Δppm	Sequence
b_2^{+1}	291.1709	291.1771	21.2	MeLeu-Tyr
b_3^{+1}	405.2138	405.222	20.2	MeLeu-Tyr-Asn
b_4^{+1}	554.2615	554.2746	23.6	MeLeu-Tyr-Asn-Hpg
b_5^{+1}	701.2935	701.3042	15.2	MeLeu-Tyr-Asn-Hpg-Hpg
b_5^{+1}	703.3092	703.319	13.9	MeLeu-Tyr-Asn-Hpg-Hpg
b_6^{+1}	848.3619	848.3733	13.4	MeLeu-Tyr-Asn-Hpg-Hpg-Phe
b_6^{+1}	850.3776	850.3933	18.4	MeLeu-Tyr-Asn-Hpg-Hpg-Phe
b_7^{+1}	1013.438	1013.456	18.4	MeLeu-Tyr-Asn-Hpg-Hpg-Phe-$^2H_2$Tyr
y_2^{+1}	225.1561	225.1613	23.1	$^2H_2$Tyr-propyl
y_5^{+1}	668.3042	668.3211	25.2	Hpg-Hpg-Phe-$^2H_2$Tyr-propyl
y_6^{+1}	782.3472	782.3674	25.8	Asn-Hpg-Hpg-Phe-$^2H_2$Tyr-propyl
y_7^{+1}	945.4105	945.429	19.5	Tyr-Asn-Hpg-Hpg-Phe-$^2H_2$Tyr-propyl

*HR-MS/MS for -3 Da products **S10**, containing labelled AA1 (ortho-$^2H_2$-L-Tyr)*

Charge State	Calculated m/z	Observed m/z	Δppm	Sequence
b_2^{+1}	291.1709	291.1757	16.4	MeLeu-Tyr
b_3^{+1}	405.2138	405.2218	19.7	MeLeu-Tyr-Asn
b_4^{+1}	554.2615	554.2692	13.8	MeLeu-Tyr-Asn-Hpg
b_7^{+1}	1012.432	1012.446	13.9	MeLeu-Tyr-Asn-Hpg-Hpg$_m$-Phe-$^2H_2$Tyr$_m$
y_4^{+1}	518.2503	518.2556	10.2	$^2H_2$Tyr$_m$-propyl
y_6^{+1}	781.3409	781.3564	19.8	Asn-Hpg-Hpg$_m$-Phe-$^2H_2$Tyr$_m$-propyl
y_7^{+1}	944.4042	944.4178	14.4	Tyr-Asn-Hpg-Hpg$_m$-Phe-$^2H_2$Tyr$_m$-propyl

Table S27. HR-MS/MS for substrate **S11**, with isotopically labelled AA4 (*ortho*-$^2H_2$-D-Hpg4), and products obtained upon reaction with OxyB (-2 Da products, **S12**, **S14**, **S15**; -3Da product, **S13**).

*HR-MS/MS for substrate **38**, containing labelled AA4 (ortho-$^2H_2$-D-Hpg4)*

Charge State	Calculated m/z	Observed m/z	Δppm	Sequence
b_2^{+1}	291.1709	291.1699	3.5	MeLeu-Tyr
b_3^{+1}	405.2138	405.2182	10.9	MeLeu-Tyr-Asn
b_4^{+1}	556.274	556.2789	8.8	MeLeu-Tyr-Asn-Hpg
b_5^{+1}	705.3217	705.3257	5.6	MeLeu-Tyr-Asn-$^2H_2$Hpg-Hpg
b_6^{+1}	852.3901	852.3931	3.6	MeLeu-Tyr-Asn-$^2H_2$Hpg-Hpg-Phe
b_7^{+1}	1015.4534	1015.4576	4.1	MeLeu-Tyr-Asn-$^2H_2$Hpg-Hpg-Phe-Tyr
y_3^{+1}	370.212	370.2164	11.8	Phe-Tyr-propyl
y_5^{+1}	670.3199	670.3218	2.9	$^2H_2$Hpg-Hpg-Phe-Tyr-propyl
y_6^{+1}	784.3628	784.3628	1.5	Asn-$^2H_2$Hpg-Hpg-Phe-Tyr-propyl
y_7^{+1}	947.4261	947.4315	5.7	Tyr-Asn-$^2H_2$Hpg-Hpg-Phe-Tyr-propyl

*HR-MS/MS for -2 Da products **S12, S14, S15**, containing labelled AA4 (ortho-$^2H_2$-D-Hpg4)*

Charge State	Calculated m/z	Observed m/z	Δppm	Sequence
b_2^{+1}	291.1709	291.1701	2.5	MeLeu-Tyr
b_3^{+1}	405.2138	405.2181	10.6	MeLeu-Tyr-Asn
b_6^{+1}	850.3843	850.3722	2.7	MeLeu-Tyr-Asn-$^2H_2$Hpg-Hpg-Phe
b_7^{+1}	1013.4549	1013.4349	2.8	MeLeu-Tyr-Asn-$^2H_2$Hpg-Hpg-Phe-Tyr
y_6^{+1}	782.3472	782.3493	2.7	Asn-$^2H_2$Hpg-Hpg-Phe-Tyr-propyl
y_7^{+1}	945.4105	945.403	7.9	Tyr-Asn-$^2H_2$Hpg-Hpg-Phe-Tyr-propyl

*HR-MS/MS for -3 Da product **S13** containing labelled AA4 (ortho-$^2H_2$-D-Hpg4)*

Charge State	Calculated m/z	Observed m/z	Δppm	Sequence
b_2^{+1}	291.1709	291.1726	5.9	MeLeu-Tyr
b_3^{+1}	405.2138	405.2127	8.7	MeLeu-Tyr-Asn
b_5^{+1}	702.2998	702.3038	5.6	MeLeu-Tyr-Asn-$^2H_2$Hpg$_m$-Hpg$_m$
b_6^{+1}	849.3642	849.3741	6.9	MeLeu-Tyr-Asn-$^2H_2$Hpg$_m$-Hpg$_m$-Phe
b_7^{+1}	1012.432	1012.447	15.2	MeLeu-Tyr-Asn-$^2H_2$Hpg$_m$-Hpg$_m$-Phe-Tyr
y_6^{+1}	781.3409	781.3618	26.7	Asn-$^2H_2$Hpg$_m$-Hpg$_m$-Phe-Tyr-propyl
y_7^{+1}	944.4042	944.421	17.7	Tyr-Asn-$^2H_2$Hpg$_m$-Hpg$_m$-Phe-Tyr-propyl

Table S28. HR-MS/MS for substrate **S16**, with isotopically labelled AA3 (*ortho*-$^2H_2$-D-Hpg), and products obtained upon reaction with OxyB (-2 Da products, **S18**, **S20**; -3Da product, **S17, S19**).

*HR-MS/MS for substrate **S16**, containing labelled AA3 (ortho-$^2H_2$-D-Hpg4)*

Charge State	Calculated m/z	Observed m/z	Δppm	Sequence
b_1^{+1}	128.1075	128.1096	16.3	MeLeu
b_2^{+1}	291.1709	291.1769	20.6	MeLeu-Tyr
b_3^{+1}	405.2138	405.2224	21.2	MeLeu-Tyr-Asn
b_4^{+1}	554.2615	554.2733	21.2	MeLeu-Tyr-Asn-Hpg
b_5^{+1}	705.3217	705.3352	19.1	MeLeu-Tyr-Asn-Hpg-$^2H_2$Hpg
b_6^{+1}	852.3901	852.4076	20.5	MeLeu-Tyr-Asn-Hpg-$^2H_2$Hpg-Phe
b_7^{+1}	1015.453	1015.474	19.9	MeLeu-Tyr-Asn-Hpg-$^2H_2$Hpg-Phe-Tyr
y_2^{+1}	223.1426	223.149	24.1	Tyr-propyl
y_3^{+1}	370.212	370.2213	25.1	Phe-Tyr-propyl
y_4^{+1}	521.2722	521.2822	19.1	$^2H_2$Hpg-Phe-Tyr-propyl
y_5^{+1}	670.3199	670.3337	20.5	Hpg-$^2H_2$Hpg-Phe-Tyr-propyl
y_6^{+1}	784.3628	784.3782	19.6	Asn-Hpg-$^2H_2$Hpg-Phe-Tyr-propyl
y_7^{+1}	947.4261	947.4455	20.4	Tyr-Asn-Hpg-$^2H_2$Hpg-Phe-Tyr-propyl

*HR-MS/MS for -2 Da products **S18**, **S20** containing labelled AA3 (ortho-$^2H_2$-D-Hpg4)*

Charge State	Calculated m/z	Observed m/z	Δppm	Sequence
b_2^{+1}	291.1709	291.1766	19.5	MeLeu-Tyr
b_3^{+1}	405.2138	405.2214	18.7	MeLeu-Tyr-Asn
b_4^{+1}	554.2615	554.2719	18.7	MeLeu-Tyr-Asn-Hpg
b_6^{+1}	850.3843	850.3745	11.5	MeLeu-Tyr-Asn-Hpg-$^2H_2$Hpg-Phe
b_7^{+1}	1013.4549	1013.4378	16.8	MeLeu-Tyr-Asn-Hpg-$^2H_2$Hpg-Phe-Tyr
y_3^{+1}	370.212	370.2211	24.5	Tyr-propyl
y_4^{+1}	519.2566	519.2431	25.9	$^2H_2$Hpg-Phe-Tyr-propyl
y_5^{+1}	668.3042	668.3176	20.1	Hpg-$^2H_2$Hpg-Phe-Tyr-propyl
y_6^{+1}	782.3472	782.3624	19.4	Asn-Hpg-$^2H_2$Hpg-Phe-Tyr-propyl
y_7^{+1}	945.4105	945.428	18.5	Tyr-Asn-Hpg-$^2H_2$Hpg-Phe-Tyr-propyl

*HR-MS/MS for -3 Da products **S17**, **S19** containing labelled AA3 (ortho-$^2H_2$-D-Hpg4)*

Charge State	Calculated m/z	Observed m/z	Δppm	Sequence
b_2^{+1}	291.1709	291.1756	16.1	MeLeu-Tyr
b_3^{+1}	405.2138	405.219	12.8	MeLeu-Tyr-Asn
b_4^{+1}	554.2615	554.269	13.5	MeLeu-Tyr-Asn-Hpg
b_5^{+1}	702.2998	702.3038	5.6	MeLeu-Tyr-Asn-Hpg-$^2H_2$Hpg
b_6^{+1}	849.3642	849.3741	6.9	MeLeu-Tyr-Asn-Hpg-$^2H_2$Hpg-Phe
b_7^{+1}	1012.432	1012.447	15.2	MeLeu-Tyr-Asn-Hpg-$^2H_2$Hpg-Phe-Tyr
y_2^{+1}	223.1436	223.1436	24.6	Tyr-propyl
y_5^{+1}	667.298	667.307	13.4	Hpg-$^2H_2$Hpg-Phe-Tyr-propyl
y_6^{+1}	781.3409	781.3618	26.7	Asn-Hpg-$^2H_2$Hpg-Phe-Tyr-propyl
y_7^{+1}	944.4042	944.421	17.7	Tyr-Asn-Hpg-$^2H_2$Hpg-Phe-Tyr-propyl

Table S29. NMR assignments for **32** in $(CD_3)_2SO$ from C- to N-terminus. The structure and number scheme for the compound is shown below the table.

Residue	Label	δH (ppm)	δC (ppm)
Tyr1	2	4.33	55.0
	3	2.68; 2.77	-
	5	6.96	130.5
	6	6.63	115.4
	NH	8.12	-
Phe2	1	-	170.8
	2	4.40	54.3
	3	2.61; 2.83	-
	5	6.94	129.8
	6	7.06	128.9
	7	7.35	127.4
	NH	8.22	-
Hpg3	2	5.37	56.0
	4	6.99	130.7
	5	6.61	115.2
	NH	8.90	-
PhGly4	2	5.66	55.9
	4	7.39	127.2
	5	7.25	128.6
	6	7.21	-
	NH	8.21	-
Asn5	1	-	170.4
	2	4.67	50.1
	3	2.36; 2.47	-
	4	-	171.8
	NH	8.38	-
Tyr6	1	-	171.5
	2	4.62	54.0
	3	2.91; 2.62	-
	5	6.99	128.7
	6	6.61	115.2
	NH	8.38	-

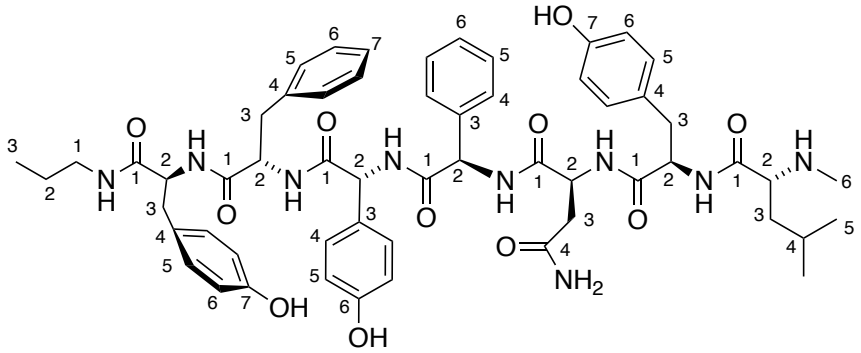

Table S30. NMR assignments for **33** in $(CD_3)_2SO$ from C- to N-terminus. The structure and number scheme for the compound is shown below the table.

Residue	Label	δH (ppm)	δC (ppm)
Pr	1	0.90	11.9
	2	1.46; 1.98	-
	3	3.07	-
	NH	7.77	-
Tyr1	2	4.65	50.0
	3	2.53; 3.14	-
	5	6.67	115.3
	6	7.11	
	NH	8.41	-
Phe2	2	4.36	
	3	2.47; 2.05	
	5	6.69	129.7
	6	7.04	128.7
	7	-	-
	NH	6.52	-
Hpg3	2	4.89	
	4	5.93	114.7
	7	6.81	116.8
	8	6.72	124.0
	NH	9.10	-
PhGly4	1	5.50	56.3
	2	7.44	127.0
	3	7.24	128.6
	4	-	-
	NH	8.29	-
Asn5	2	4.69	50.2
	3	2.35;2.47	-
	NH	8.35	-
Tyr6	2	4.56	-
	3	2.88;2.64	-
	5	6.96	
	6	6.60	115.2
	NH	7.94	-

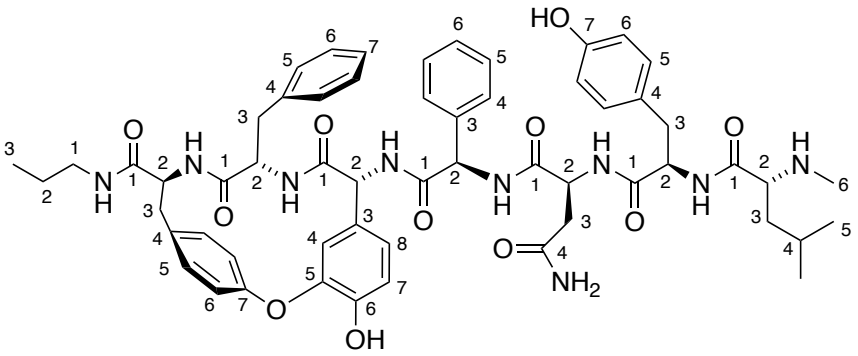

Table S31. HR-MS data for substrates and products of OxyB enzymatic reactions to generate analogs with different substituents. Sequence of peptides shown is (L-Tyr1)-AA2-AA3-AA4-(L-Asn5)-(D-Tyr6)-(*N*-Me-D-Leu7).

Compound	AA2	AA3	AA4	Charge State	Calculated mass	Observed mass	Δppm
34	4-Me-L-Phe	D-Hpg	D-Hpg	$[M+H]^+$	1086.5295	1086.52915	0.3
35	4-Me-L-Phe	D-Hpg	D-Hpg	$[M+H]^+$	1084.5138	1084.51221	1.4
-	4-Me-L-Phe	D-Hpg	$^2H_2$-D-Hpg	$[M+H]^+$	1088.542	1088.54744	4.9
36	4-Me-L-Phe	D-Hpg	$^2H_2$-D-Hpg	$[M+H]^+$	1085.5201	1085.52446	4.0
-	4-CD_3-L-Phe	D-Hpg	D-Hpg	$[M+H]^+$	1089.5483	1089.5578	8.7
37	4-CD_3-L-Phe	D-Hpg	D-Hpg	$[M+H]^+$	1087.5327	1087.54094	7.5
-	4-CD_3-L-Phe	D-Hpg	$^2H_2$-D-Hpg	$[M+H]^+$	1091.5609	1091.57447	12.4
38	4-CD_3-L-Phe	D-Hpg	$^2H_2$-D-Hpg	$[M+H]^+$	1088.539	1088.5504	10.4
39	4-Me-L-Phe	D-Hpg	D-PhGly	$[M+H]^+$	1070.5346	1070.53765	2.8
40	4-Me-L-Phe	D-Hpg	D-PhGly	$[M+H]^+$	1068.5189	1068.52095	1.9
-	4-Me-L-Phe	$^2H_2$-D-Hpg	D-PhGly	$[M+H]^+$	1072.5471	1072.56038	12.3
41	4-Me-L-Phe	$^2H_2$-D-Hpg	D-PhGly	$[M+H]^+$	1069.5252	1069.54123	14.9
-	4-CD_3-L-Phe	D-Hpg	D-PhGly	$[M+H]^+$	1073.5534	1073.56881	14.3
42	4-CD_3-L-Phe	D-Hpg	D-PhGly	$[M+H]^+$	1071.5378	1071.55087	12.1
43	4-NH_2-L-Phe	D-Hpg	D-Hpg	$[M+H]^+$	1087.52466	1087.5192	5.0
44	4-NH_2-L-Phe	D-Hpg	D-Hpg	$[M+H]^+$	1085.5091	1085.50697	1.9
-	4-NH_2-L-Phe	D-Hpg	$^2H_2$-D-Hpg	$[M+H]^+$	1089.5375	1089.54058	2.8
45	4-NH_2-L-Phe	D-Hpg	$^2H_2$-D-Hpg	$[M+H]^+$	1086.5154	1086.52363	7.5
46	4-NH_2-L-Phe	D-Hpg	D-PhGly	$[M+H]^+$	1071.5298	1071.53728	6.9
47	4-NH_2-L-Phe	D-Hpg	D-PhGly	$[M+H]^+$	1069.5142	1069.52277	8.0

Table S32. HR-MS/MS data for starting material **34** (AA2 = 4-Me-L-Phe, AA4 = L-Hpg) and product **35**.

*HR-MS/MS for starting material **34** (AA2 = 4-Me-L-Phe, AA4 = L-Hpg)*

Charge State	Calculated m/z	Observed m/z	Δppm	Sequence
b_2^{+1}	291.1709	291.1702	2.4	MeLeu-Tyr
b_3^{+1}	405.2138	405.2131	1.7	MeLeu-Tyr-Asn
b_4^{+1}	554.2615	554.2608	1.2	MeLeu-Tyr-Asn-Hpg
b_5^{+1}	703.3092	703.3081	1.5	MeLeu-Tyr-Asn-Hpg-Hpg
b_6^{+1}	864.3932	864.3918	1.6	MeLeu-Tyr-Asn-Hpg-Hpg-4MePhe
b_7^{+1}	1027.4565	1027.4565	1.6	MeLeu-Tyr-Asn-Hpg-Hpg-4MePhe-Tyr
y_2^{+1}	223.1436	223.1438	0.8	Tyr-propyl
y_3^{+1}	384.2276	384.2278	0.5	4MePhe -Tyr-propyl
y_4^{+1}	533.2853	533.2747	1.1	Hpg-4MePhe -Tyr-propyl
y_5^{+1}	682.323	682.3229	0.1	Hpg-Hpg-4MePhe -Tyr-propyl
y_6^{+1}	796.3659	796.3654	0.6	Asn-Hpg-Hpg-4MePhe -Tyr-propyl
y_7^{+1}	959.4292	959.4286	0.6	Tyr-Asn-Hpg-Hpg-4MePhe -Tyr-propyl

*HR-MS/MS for product **35** (AA2 = 4-Me-L-Phe, AA4 = L-Hpg)*

Charge State	Calculated m/z	Observed m/z	Δppm	Sequence
b_2^{+1}	291.1709	291.1701	2.7	MeLeu-Tyr
b_3^{+1}	405.2138	405.2128	2.4	MeLeu-Tyr-Asn
b_7^{+1}	1025.4409	1025.4397	1.1	MeLeu-Tyr-Asn-Hpg$_m$-Hpg-4MePhe$_m$-Tyr
y_2^{+1}	223.1436	223.1426	4.5	Tyr-propyl
y_5^{+1}	680.3073	680.3061	1.7	Hpg$_m$-Hpg-4MePhe$_m$-Tyr-propyl
y_6^{+1}	794.3503	794.3415	1.3	Asn-Hpg$_m$-Hpg-4MePhe$_m$-Tyr-propyl
y_7^{+1}	957.4136	957.4141	0.5	Tyr-Asn-Hpg$_m$-Hpg-4MePhe$_m$-Tyr-propyl

Table S33. HR-MS/MS data for starting material AA2 = 4-Me-L-Phe and AA4 = *ortho*-$^{2}H_2$-D-Hpg and -3 Da product upon reaction with OxyB (**36**).

HR-MS/MS for starting material AA2 =4-Me-L-Phe and AA4 = ortho-$^{2}H_2$-D-Hpg

Charge State	Calculated m/z	Observed m/z	Δppm	Sequence
b_2^{+1}	291.1709	291.1715	2.0	MeLeu-Tyr
b_3^{+1}	405.2138	405.2164	6.4	MeLeu-Tyr-Asn
b_4^{+1}	556.274	556.2773	5.9	MeLeu-Tyr-Asn-$^{2}H_2$Hpg
b_5^{+1}	705.3217	705.3217	0.8	MeLeu-Tyr-Asn-$^{2}H_2$Hpg-Hpg
b_6^{+1}	866.4058	866.4105	5.4	MeLeu-Tyr-Asn-$^{2}H_2$Hpg-Hpg-4MePhe
b_7^{+1}	1029.4691	1029.473	3.7	MeLeu-Tyr-Asn-$^{2}H_2$Hpg-Hpg-4MePhe-Tyr
y_2^{+1}	223.1436	223.1418	7.8	Tyr-propyl
y_3^{+1}	384.2276	384.2282	1.5	4MePhe-Tyr-propyl
y_4^{+1}	533.2753	533.2786	6.2	Hpg-4MePhe-Tyr-propyl
y_5^{+1}	684.3355	684.3366	1.6	$^{2}H_2$Hpg-Hpg-4MePhe-Tyr-propyl
y_6^{+1}	798.3785	798.3823	4.8	Asn-$^{2}H_2$Hpg-Hpg-4MePhe-Tyr-propyl
y_7^{+1}	961.4418	961.4447	3.0	4MePhe-Asn-$^{2}H_2$Hpg-Hpg-4MePhe-Tyr-propyl

*HR-MS/MS for product **36***

Charge State	Calculated m/z	Observed m/z	Δppm	Sequence
b_3^{+1}	405.2138	405.2161	5.7	MeLeu-Tyr-Asn
b_6^{+1}	864.3901	864.3952	5.9	MeLeu-Tyr-Asn-$^{2}H_2$Hpg$_m$-Hpg-4MePhe$_m$-Tyr
b_7^{+1}	1026.4472	1026.4472	4.2	MeLeu-Tyr-Asn-$^{2}H_2$Hpg$_m$-Hpg-4MePhe$_m$-Tyr
y_6^{+1}	795.3565	795.3448	14.6	Asn-$^{2}H_2$Hpg$_m$-Hpg-4MeTyr$_m$-Tyr-propyl
y_7^{+1}	958.4199	958.4166	3.4	Tyr-Asn-$^{2}H_2$Hpg$_m$-Hpg-4MeTyr$_m$-Tyr-propyl

Table S34. HR-MS/MS data for starting material AA2 = 4-CD_3-L-Phe and AA4 = D-Hpg and -2 Da product upon reaction with OxyB (**37**).

HR-MS/MS for starting material AA2 =4-CD_3-L-Phe and AA4 = D-Hpg

Charge State	Calculated m/z	Observed m/z	Δppm	Sequence
b_2^{+1}	291.1709	291.1684	8.5	MeLeu-Tyr
b_3^{+1}	405.2138	405.2099	9.5	MeLeu-Tyr-Asn
b_4^{+1}	554.2615	554.2563	9.2	MeLeu-Tyr-Asn-Hpg
b_5^{+1}	703.3092	703.3029	8.8	MeLeu-Tyr-Asn-Hpg-Hpg
b_6^{+1}	867.412	867.4037	9.4	MeLeu-Tyr-Asn-Hpg-Hpg-4CD_3Phe
b_7^{+1}	1030.4754	1030.4601	14.8	MeLeu-Tyr-Asn-Hpg-Hpg-4CD_3Phe-Tyr
y_2^{+1}	223.1436	223.143	2.6	Tyr-propyl
y_3^{+1}	387.2464	387.2433	7.9	4CD_3Phe-Tyr-propyl
y_4^{+1}	536.2941	536.2843	18.2	Hpg-4CD_3Phe-Tyr-propyl
y_5^{+1}	685.3418	685.3333	12.3	Hpg-Hpg-4CD_3Phe-Tyr-propyl
y_7^{+1}	962.4481	962.4399	8.4	Asn-Hpg-Hpg-4CD_3Phe-Tyr-propyl

*HR-MS/MS for product **37***

Charge State	Calculated m/z	Observed m/z	Δppm	Sequence
b_2^{+1}	291.1709	291.1657	8.3	MeLeu-Tyr
b_3^{+1}	405.2138	405.2091	11.4	MeLeu-Tyr-Asn
b_6^{+1}	865.3964	865.3881	9.5	MeLeu-Tyr-Asn-Hpg$_m$-Hpg-4CD_3Phe
y_5^{+1}	683.3262	683.3228	4.9	Asn-Hpg$_m$-Hpg-4CD_3Phe-Tyr-propyl

Table S35. HR-MS/MS data for starting material AA2 = 4-CD_3-L-Phe and AA4 = *ortho*-$^2H_2$-D-Hpg and -3 Da product upon reaction with OxyB (**38**).

HR-MS/MS for starting material AA2 =4-CD_3-L-Phe and AA4 = ortho-$^2H_2$-D-Hpg

Charge State	Calculated m/z	Observed m/z	Δppm	Sequence
b_1^{+1}	128.1075	128.1075	14.0	MeLeu
b_2^{+1}	291.1709	291.1677	10.7	MeLeu-Tyr
b_3^{+1}	405.2138	405.2092	11.2	MeLeu-Tyr-Asn
b_4^{+1}	556.274	556.2674	11.8	MeLeu-Tyr-Asn-$^2H_2$Hpg
b_5^{+1}	705.3217	705.3126	12.8	MeLeu-Tyr-Asn-$^2H_2$Hpg-Hpg
b_6^{+1}	869.4246	869.4127	13.6	MeLeu-Tyr-Asn-$^2H_2$Hpg-Hpg-4CD_3Phe
b_7^{+1}	1032.4879	1032.4657	21.5	MeLeu-Tyr-Asn-$^2H_2$Hpg-Hpg-4CD_3Phe-Tyr
y_2^{+1}	223.1436	223.1428	3.5	Tyr-propyl
y_3^{+1}	387.2464	387.2405	15.2	4CD_3Phe-Tyr-propyl
y_4^{+1}	536.2941	536.3021	14.9	Hpg-4CD_3Phe-Tyr-propyl
y_5^{+1}	687.3544	687.3403	20.4	$^2H_2$Hpg-Hpg-4CD_3Phe-Tyr-propyl
y_7^{+1}	964.4606	964.4409	21.2	Asn-$^2H_2$Hpg-Hpg-4CD_3Phe-Tyr-propyl

*HR-MS/MS for product **38***

Charge State	Calculated m/z	Observed m/z	Δppm	Sequence
b_2^{+1}	291.1709	291.1657	17.5	MeLeu-Tyr
b_3^{+1}	405.2138	405.2051	21.3	MeLeu-Tyr-Asn
y_6^{+1}	798.3754	798.3901	18.4	Asn-$^2H_2$Hpg$_m$-Hpg-4CD_3Tyr$_m$-Tyr-propyl

Table S36. HR-MS/MS data for starting material AA2 = 4-Me-L-Phe and AA4 = D-PhGly (**39**) and -2 Da product upon reaction with OxyB (**40**).

*HR-MS/MS for starting material **39** (AA2 =4-Me-L-Phe and AA4 = D-PhGly)*

Charge State	Calculated m/z	Observed m/z	Δppm	Sequence
b_1^{+1}	128.1075	128.107	3.9	MeLeu
b_2^{+1}	291.1709	291.171	0.3	MeLeu-Tyr
b_3^{+1}	405.2138	405.2141	0.7	MeLeu-Tyr-Asn
b_4^{+1}	538.2666	538.2674	1.4	MeLeu-Tyr-Asn-PhGly
b_5^{+1}	687.2142	687.3147	0.7	MeLeu-Tyr-Asn-PhGly-Hpg
b_6^{+1}	848.3983	848.3987	0.5	MeLeu-Tyr-Asn-PhGly-Hpg-4MePhe
b_7^{+1}	1011.4616	1011.4618	0.2	MeLeu-Tyr-Asn-PhGly-Hpg-4MePhe-Tyr
y_2^{+1}	223.1436	223.1445	4.0	Tyr-propyl
y_3^{+1}	384.2276	384.2287	2.8	4MePhe-Tyr-propyl
y_4^{+1}	533.2753	533.2766	2.4	Hpg-4MePhe-Tyr-propyl
y_5^{+1}	666.3281	666.3303	3.3	PhGly-Hpg-4MePhe-Tyr-propyl
y_6^{+1}	780.371	780.3753	5.5	Asn-PhGly-Hpg-4MePhe-Tyr-propyl
y_7^{+1}	943.4343	943.4359	1.7	Tyr-Asn-PhGly-Hpg-4MePhe-Tyr-propyl

*HR-MS/MS for starting material **40** (AA2 =4-Me-L-Phe and AA4 = D-PhGly)*

Charge State	Calculated m/z	Observed m/z	Δppm	Sequence
b_2^{+1}	291.1709	291.1703	2.0	MeLeu-Tyr
b_3^{+1}	405.2138	405.2137	0.2	MeLeu-Tyr-Asn
b_4^{+1}	538.2666	538.2666	1.6	MeLeu-Tyr-Asn-PhGly
b_6^{+1}	846.3827	846.3804	2.7	MeLeu-Tyr-Asn-PhGly-Hpg$_m$-4MePhe$_m$
b_7^{+1}	1009.446	1009.4438	2.1	MeLeu-Tyr-Asn-PhGly-Hpg$_m$-4MePhe$_m$-Tyr
y_4^{+1}	531.2596	531.2564	6.0	Hpg$_m$-4MePhe$_m$-Tyr-propyl
y_5^{+1}	664.3124	664.3142	2.7	PhGly-Hpg$_m$-4MePhe$_m$-Tyr-propyl
y_6^{+1}	778.3553	778.3545	1.0	Asn-PhGly-Hpg$_m$-4MePhe$_m$-Tyr-propyl
y_7^{+1}	941.4187	941.4202	1.5	Tyr-Asn-PhGly-Hpg$_m$-4MePhe$_m$-Tyr-propyl

Table S37. HR-MS/MS data for starting material with AA2 = 4-CD_3-L-Phe and AA4 = D-PhGly and -2 Da product upon reaction with OxyB (**41**).

HR-MS/MS for starting material AA2 =4-CD_3-L-Phe and AA4 = D-PhGly

Charge State	Calculated m/z	Observed m/z	Δppm	Sequence
b_1^{+1}	128.1075	128.1053	17.0	MeLeu
b_2^{+1}	291.1709	291.1676	11.0	MeLeu-Tyr
b_3^{+1}	405.2138	405.2088	12.1	MeLeu-Tyr-Asn
b_4^{+1}	538.2666	538.2594	13.2	MeLeu-Tyr-Asn-PhGly
b_5^{+1}	687.2142	687.3068	10.7	MeLeu-Tyr-Asn-PhGly-Hpg
b_6^{+1}	851.4171	851.4063	12.6	MeLeu-Tyr-Asn-PhGly-Hpg-4CD_3Phe
b_7^{+1}	1014.4805	1014.4535	26.5	MeLeu-Tyr-Asn-PhGly-Hpg-4CD_3Phe-Tyr
y_2^{+1}	223.1436	223.1436	5.6	Tyr-propyl
y_3^{+1}	387.2464	387.2419	11.3	4CD_3Phe-Tyr-propyl
y_4^{+1}	536.2941	536.2917	4.3	Hpg-4CD_3Phe-Tyr-propyl
y_5^{+1}	669.3469	669.3436	4.8	PhGly-Hpg-4CD_3PheTyr-propyl
y_6^{+1}	783.3898	783.3969	9.1	Asn-PhGly-Hpg-4CD_3Phe-Tyr-propyl
y_7^{+1}	946.4531	946.4325	21.7	4MePhe-Asn-PhGly-Hpg-4CD_3Phe-Tyr-propyl

*HR-MS/MS for product **41***

Charge State	Calculated m/z	Observed m/z	Δppm	Sequence
b_2^{+1}	291.1709	291.1635	25.1	MeLeu-Tyr
b_3^{+1}	405.2138	405.2138	13.8	MeLeu-Tyr-Asn

Table S38. HR-MS/MS data for starting material containing 4-Me-L-Phe2, *ortho*-$^{2}H_2$-D-Hpg3, D-PhGly4 and -3 Da product upon reaction with OxyB (**42**).

HR-MS/MS for starting material AA2 =4-Me-L-Phe; AA3 = ortho-$^{2}H_2$-D-Hpg; AA4 = D-PhGly

Charge State	Calculated m/z	Observed m/z	Δppm	Sequence
b_2^{+1}	291.1709	291.1740	10.8	MeLeu-Tyr
b_3^{+1}	405.2138	405.2138	5.5	MeLeu-Tyr-Asn
b_4^{+1}	538.2666	538.2666	7.0	MeLeu-Tyr-Asn-PhGly
b_5^{+1}	689.3317	689.3268	7.1	MeLeu-Tyr-Asn-PhGly-Hpg
b_6^{+1}	850.4109	850.4152	5.0	MeLeu-Tyr-Asn-PhGly-Hpg-4MePhe
b_7^{+1}	1013.4742	1013.4642	9.8	MeLeu-Tyr-Asn-PhGly-Hpg-4MePhe-Tyr
y_2^{+1}	223.1436	223.1460	11.1	Tyr-propyl
y_3^{+1}	384.2276	384.2316	10.5	4MePhe-Tyr-propyl
y_4^{+1}	533.2753	533.2766	2.4	Hpg-4MePhe-Tyr-propyl
y_7^{+1}	945.4469	945.4468	0.0	Tyr-Asn-PhGly-Hpg-4MePhe-Tyr-propyl

*HR-MS/MS for product **42***

Charge State	Calculated m/z	Observed m/z	Δppm	Sequence
b_2^{+1}	291.1709	291.1724	5.2	MeLeu-Tyr
b_3^{+1}	405.2138	405.2166	7.0	MeLeu-Tyr-Asn
b_4^{+1}	538.2666	538.2683	3.1	MeLeu-Tyr-Asn-PhGly
b_6^{+1}	847.3889	847.3803	10.0	MeLeu-Tyr-Asn-PhGly-Hpg$_m$-4MePhe$_m$
b_7^{+1}	1010.4523	1010.4431	9.1	MeLeu-Tyr-Asn-PhGly-Hpg$_m$-4MePhe$_m$-Tyr
y_2^{+1}	223.1436	223.1456	9.1	Tyr-propyl
y_5^{+1}	665.3187	665.3192	0.8	PhGly-Hpg$_m$-4MePhe$_m$-Tyr-propyl

Table S39. HR-MS/MS data for starting material AA2 = 4-NH_2-L-Phe and AA4 = D-Hpg (**43**) and -2 Da product upon reaction with OxyB (**44**).

*HR-MS/MS for starting material AA2 =4-NH_2-L-Phe and AA4 = D-Hpg **43***

Charge State	Calculated m/z	Observed m/z	Δppm	Sequence
b_2^{+1}	291.1709	291.1674	12	MeLeu-Tyr
b_3^{+1}	405.2138	405.216	5.5	MeLeu-Tyr-Asn
b_4^{+1}	554.2644	554.2615	5.3	MeLeu-Tyr-Asn-Hpg
b_5^{+1}	703.3092	703.306	4.5	MeLeu-Tyr-Asn-Hpg-Hpg
b_6^{+1}	865.3885	865.3865	2.2	MeLeu-Tyr-Asn-Hpg-Hpg-Asn
b_7^{+1}	1028.4518	1028.4454	6.1	MeLeu-Tyr-Asn-Hpg-Hpg-4NH_2Phe-Tyr
y_3^{+1}	385.2229	385.2215	3.4	4NH_2Phe-Tyr-propyl
y_4^{+1}	534.2705	534.2761	10.5	Hpg-4NH_2Phe-Tyr-propyl
y_5^{+1}	683.3182	683.3166	2.3	Hpg-Hpg-4NH_2Phe-Tyr-propyl
y_7^{+1}	960.4245	960.4114	13.5	Tyr-Asn-Hpg-Hpg-4NH_2Phe-Tyr-propyl

*HR-MS/MS for product **44***

Charge State	Calculated m/z	Observed m/z	Δppm	Sequence
b_2^{+1}	291.1709	291.1693	5.3	MeLeu-Tyr
b_3^{+1}	405.2138	405.2159	5.3	MeLeu-Tyr-Asn
b_6^{+1}	863.3728	863.3725	0.2	MeLeu-Tyr-Asn-Hpg$_m$-Hpg-4NH_2Phe$_m$
b_7^{+1}	1026.4361	1026.4337	2.3	MeLeu-Tyr-Asn-Hpg$_m$-Hpg-4NH_2Phe$_m$-Tyr
y_6^{+1}	795.3455	795.3484	3.7	Asn-Hpg$_m$-Hpg-4NH_2Phe$_m$-Tyr-propyl
y_7^{+1}	958.4088	958.401	8	Tyr-Asn-Hpg$_m$-Hpg-4NH_2Phe$_m$-Tyr-propyl

Table S40. HR-MS/MS data for starting material AA2 = 4-NH_2-L-Phe and AA4 = *ortho*-$^2H_2$-D-Hpg and -3 Da product upon reaction with OxyB (**45**).

HR-MS/MS for starting material AA2 =4-NH_2-L-Phe and AA4 = ortho-$^2H_2$-D-Hpg

Charge State	Calculated m/z	Observed m/z	Δppm	Sequence
b_2^{+1}	291.1709	291.1635	25.1	MeLeu-Tyr
b_3^{+1}	405.2138	405.2126	2.7	MeLeu-Tyr-Asn
b_4^{+1}	556.274	556.2704	6.4	MeLeu-Tyr-Asn-$^2H_2$Hpg
b_5^{+1}	705.3217	705.3158	8.3	MeLeu-Tyr-Asn-$^2H_2$Hpg-Hpg
b_7^{+1}	1030.4642	1030.4546	9.2	MeLeu-Tyr-Asn-$^2H_2$Hpg-Hpg-4NH_2Phe-Tyr
y_3^{+1}	385.2229	385.2205	6.2	4NH_2Phe-Tyr-propyl
y_4^{+1}	534.2705	534.2688	3.1	Hpg-4NH_2Phe-Tyr-propyl
y_5^{+1}	685.3308	685.3296	1.6	$^2H_2$Hpg-Hpg-4NH_2Phe-Tyr-propyl
y_7^{+1}	962.437	962.4326	4.5	Tyr-Asn-^{2}H2Hpg-Hpg-4NH_2Phe-Tyr-propyl

*HR-MS/MS for product **45***

Charge State	Calculated m/z	Observed m/z	Δppm	Sequence
b_2^{+1}	291.1709	291.166	16.7	MeLeu-Tyr
b_3^{+1}	405.2138	405.2109	7	MeLeu-Tyr-Asn
b_6^{+1}	864.3791	864.3741	5.6	MeLeu-Tyr-Asn-$^2H_2Hpg_m$-Hpg-4NH_2Phe_m
b_7^{+1}	1027.4424	1027.4359	6.3	MeLeu-Tyr-Asn-$^2H_2Hpg_m$-Hpg-4NH_2Phe_m-Tyr
y_6^{+1}	796.3518	796.3467	6.3	Asn-$^2H_2Hpg_m$-Hpg-4NH_2Phe_m-Tyr-propyl
y_7^{+1}	959.4151	959.4101	5.1	Tyr-Asn-$^2H_2Hpg_m$-Hpg-4NH_2Phe_m-Tyr-propyl

Table S41. HR-MS/MS data for starting material AA2 = 4-NH_2-L-Phe and AA4 = D-PhGly (**46**) and -2 Da product upon reaction with OxyB (**47**).

*HR-MS/MS for starting material AA2 =4-NH_2-L-Phe and AA4 = D-PhGly **46***

Charge State	Calculated m/z	Observed m/z	Δppm	Sequence
b_2^{+1}	291.1709	291.1674	12	MeLeu-Tyr
b_3^{+1}	405.2138	405.2137	0.2	MeLeu-Tyr-Asn
b_4^{+1}	538.2666	538.2656	1.8	MeLeu-Tyr-Asn-PhGly
b_5^{+1}	687.3142	687.3092	7.2	MeLeu-Tyr-Asn-PhGly-Hpg
b_6^{+1}	849.3836	849.3869	3.9	MeLeu-Tyr-Asn-PhGly-Hpg-4NH2Phe
b_7^{+1}	1012.4569	1012.4497	7.1	MeLeu-Tyr-Asn-PhGly-Hpg-4NH2Phe-Tyr
y_3^{+1}	385.2229	385.2215	9.3	4NH2Phe-Tyr-propyl
y_4^{+1}	534.2705	534.2694	2	Hpg-4NH2Phe-Tyr-propyl
y_5^{+1}	667.3233	667.3137	14.2	PhGly-Hpg-4NH2Phe-Tyr-propyl
y_6^{+1}	781.3663	781.3621	5.2	Asn-PhGly-Hpg-4NH2Phe-Tyr-propyl
y_7^{+1}	944.4296	944.4274	2.3	4MePhe-Asn-PhGly-Hpg-4NH2Phe-Tyr-propyl

*HR-MS/MS for product **47***

Charge State	Calculated m/z	Observed m/z	Δppm	Sequence
b_2^{+1}	291.1709	291.1691	6	MeLeu-Tyr
b_3^{+1}	405.2138	405.2162	5.9	MeLeu-Tyr-Asn
b_4^{+1}	538.2666	538.2682	3	MeLeu-Tyr-Asn-PhGly
b_6^{+1}	847.3779	847.3812	4	MeLeu-Tyr-Asn-PhGly-Hpg_m-4NH_2Phe_m
y_5^{+1}	665.3077	665.3038	5.8	Asn-PhGly-Hpg_m-4NH_2Phe_m-Tyr-propyl

Table S42. HR-MS data for substrates and products of OxyB, OxyA and OxyC enzymatic reactions. Sequence of peptides shown is (D/L-Dpg)-AA2-(D-Hpg)-AA4-(L-Ans5)-(D-Tyr6)-(*N*-Me-D-Leu7).

Compound	AA1	AA2	AA4	Charge State	Calculated mass	Observed mass	Δppm
48	Dpg	L-HomoTyr	D-Hpg	$[M+H]^+$	1138.4647	1138.463	1.4
-2 pdt of 48	Dpg	L-HomoTyr	D-Hpg	$[M+H]^+$	1136.4491	1136.44933	0.2
49	Dpg	L-HomoTyr	D-Hpg	$[M+H]^+$	1134.4334	1134.43179	1.4
50	Dpg	3-Cl-HomoTyr	D-Hpg	$[M+H+3Na]^+$	1238.3715	1238.3535	14.5
-2 pdt of **50**	Dpg	3-Cl-HomoTyr	D-Hpg	$[M+H+3Na]^+$	1236.35591	1236.34339	10.1
-4 pdt of **50**	Dpg	3-Cl-HomoTyr	D-Hpg	$[M+H+3Na]^+$	1234.3402	1234.34881	6.9
51	Dpg	3-Cl-HomoTyr	D-Hpg	$[M+H+3Na]^+$	1232.32461	1232.33977	12.3

References

(1) Forneris, C. C.; Ozturk, S.; Gibson, M. I.; Sorensen, E. J.; Seyedsayamdost, M. R. In Vitro Reconstitution of OxyA Enzymatic Activity Clarifies Late Steps in Vancomycin Biosynthesis. *ACS Chem. Biol.* **2017**, *12*, 2248–2253.

(2) Forneris, C. C.; Seyedsayamdost, M. R. In Vitro Reconstitution of OxyC Activity Enables Total Chemoenzymatic Syntheses of Vancomycin Aglycone Variants. *Angew. Chemie Int. Ed.* **2018**, *57*, 8048–8052.

(3) Haslinger, K.; Maximowitsch, E.; Brieke, C.; Koch, A.; Cryle, M. J. Cytochrome P450 OxyBtei Catalyzes the First Phenolic Coupling Step in Teicoplanin Biosynthesis. *ChemBioChem* **2014**, *15*, 2719–2728.

(4) Brieke, C.; Kratzig, V.; Peschke, M.; Cryle, M. J. Facile Synthetic Access to Glycopeptide Antibiotic Precursor Peptides for the Investigation of Cytochrome P450 Action in Glycopeptide Antibiotic Biosynthesis. In *Nonribosomal Peptide and Polyketide Biosynthesis: Methods and Protocols*; Evans, B. S., Ed.; Springer New York: New York, NY, 2016; pp 85–102.

(5) Woithe, K.; Geib, N.; Zerbe, K.; Dong, B. L.; Heck, M.; Fournier-Rousset, S.; Meyer, O.; Vitali, F.; Matoba, N.; Abou-Hadeed, K.; Robinson, J. A. Oxidative Phenol Coupling Reactions Catalyzed by OxyB: A Cytochrome P450 from the Vancomycin Producing Organism. Implications for Vancomycin Biosynthesis. *J. Am. Chem. Soc.* **2007**, *129*, 6887–6895.

(6) Geib, N.; Weber, T.; Wörtz, T.; Zerbe, K.; Wohlleben, W.; Robinson, J. A. Genome Mining in Amycolatopsis Balhimycina for Ferredoxins Capable of Supporting Cytochrome P450 Enzymes Involved in Glycopeptide Antibiotic Biosynthesis. *FEMS Microbiol. Lett.* **2010**, *306*, 45–53.

(7) Pearce, C. M.; Williams, D. H. Complete Assignment of the 13C NMR Spectrum of Vancomycin. *J. Chem. Soc. Perkin Trans 2* **1995**, 153–157.

(8) Cochrane, J. R.; White, J. M.; Wille, U.; Hutton, C. A. Total Synthesis of Mycocyclosin. *Org. Lett.* **2012**, *14*, 2402–2405.

(9) Kulanthaivel, P.; Kreuzman, A. J.; Strege, M. A.; Belvo, M. D.; Smitka, T. A.; Clemens, M.; Swartling, J. R.; Minton, K. L.; Zheng, F.; Angleton, E. L.; Mullen, D.; Jungheim, L. N.; Klimkowski, V. J.; Nicas, T. I.; Thompson, R. C.; Peng, S. Novel Lipoglycopeptides as Inhibitors of Bacterial Signal Peptidase I. *J. Biol. Chem.* **2004**, *279*, 36250–36258.